



Mathematical analysis on the transmission dynamics of delta and omicron variants of COVID-19 in the United States

Benjamin Idoko Omede¹ · Sayooj Aby Jose^{2,3} · J. Anuwat³ · Taesung Park^{2,4}

Received: 12 June 2024 / Accepted: 6 July 2024

© The Author(s), under exclusive licence to Springer Nature Switzerland AG 2024

Abstract

The COVID-19 pandemic has undergone significant changes due to the emergence of new variants. The Delta and Omicron variants, in particular, have posed unique challenges because of their increased transmissibility and potential for vaccine escape. Understanding the transmission dynamics of these variants is crucial for public health planning and response. Consequently, this paper introduces a new deterministic mathematical model to understand the transmission dynamics of the Delta and Omicron variants of COVID-19, considering re-infection and imperfect vaccination. The analysis begins with the computation of the basic reproduction number for the Delta and Omicron variants and the examination of the local stability of the disease-free equilibrium using the Routh–Hurwitz criterion. An in-depth analysis of the COVID-19 model highlights that both variants demonstrate a phenomenon called backward bifurcation, which is characterized by the co-existence of a stable disease-free equilibrium and a stable endemic equilibrium when their basic reproduction number falls below one. This property poses challenges in effectively controlling COVID-19 within the population. However, assuming flawless vaccine efficacy and zero re-infection, these variants have a globally asymptotically stable disease-free equilibrium. We conducted a sensitivity analysis on the basic parameters of the Delta and Omicron reproduction numbers to identify influential factors contributing to the transmission of these variants. Additionally, we calculated the Omicron invasion reproduction number and developed analytical expressions to determine the necessary percentage of vaccinated individuals required for COVID-19 eradication, even with an imperfect vaccine. The model was validated by fitting it with the daily confirmed cases of COVID-19 in the United States during the period coinciding with the emergence of the Omicron variant. It was determined that with a COVID-19 vaccine offering 60% protection against the Omicron variant, a vaccination rate of at least 97.67% among the susceptible population is required to attain the herd immunity threshold. Numerical simulations indicate that increasing both the vaccination rate and the efficacy of the vaccine against the Delta and Omicron variants significantly reduces the number of hospitalized individuals.

Keywords Delta and Omicron variants · COVID-19 · Basic reproduction number · Stability · Invasion reproduction number · Herd immunity threshold · Bifurcation

Mathematics Subject Classification 92B05 · 92D30 · 92-10 · 34D20

✉ Sayooj Aby Jose
sayooj@snu.ac.kr

¹ Department of Mathematical Sciences, Prince Abubakar Audu (Formerly Kogi State) University, Anyigba, Nigeria

² Department of Statistics, Seoul National University, Seoul 08826, Republic of Korea

³ Department of Mathematics, Faculty of Education, Phuket Rajabhat University, Phuket, Thailand

⁴ Interdisciplinary Program of Bioinformatics, Seoul National University, Seoul 08826, Republic of Korea

Introduction

In December 2019, Wuhan, China, became the initial epicenter of an outbreak involving a newly identified and highly infectious virus referred to as severe acute respiratory syndrome coronavirus 2 (SARS-CoV-2), resulting in the emergence of the illness known as coronavirus disease 2019 (COVID-19). This outbreak swiftly disseminated across the globe, evolving into a significant and worldwide public health crisis (Nadim and Chattopadhyay 2020; Gilbert et al. 2020). The primary mode of transmission for SARS-CoV-2

is through respiratory droplets, which are transferred from person to person in close proximity, often through activities like coughing or sneezing. It can also be transmitted through the air, by touching contaminated surfaces (fomite transmission), and through various other means, including contact with biological materials such as urine and feces (Chan et al. 2020). People of all age groups, including newborns and pregnant women, can become infected with the virus. The most frequently observed symptoms of the infection typically include fever, fatigue, and a dry cough. Additional upper respiratory symptoms may manifest as a sore throat, headaches, and muscle pain. There is a documented case report mentioning patients, particularly children and adolescents, who exhibited gastrointestinal symptoms like abdominal pain and diarrhea (Centers for Disease 2021). Similar to other RNA (ribonucleic acid) viruses, SARS-CoV-2 has undergone multiple changes that have affected its ability to spread and infect individuals, posing significant challenges to the global population (Chakraborty et al. 2022). Certainly, since the emergence of the COVID-19 pandemic in December 2019, a multitude of variants of the SARS-CoV-2 virus have indeed emerged (Chakraborty et al. 2022). As of January 25, 2022, the World Health Organization (WHO) has officially recognized five variants of concern (Alpha, Beta, Gamma, Delta, and Omicron), two variants of interest (Lambda and Mu), and is actively monitoring three other variants (Chakraborty et al. 2022). The WHO identifies variants of concern (VOC) as SARS-CoV-2 mutations that heighten transmissibility, severity of illness, or potency, or diminish the efficacy of public health measures, diagnostics, treatments, or vaccines. Variants of interest (VOI) encompass genetic alterations expected to increase the virus's transmissibility, identified in various countries causing community spread and potentially posing a global public health risk. Variants under monitoring entail genetic changes suspected to impact virus traits, with currently uncertain effects on characteristics or spread, both phenotypically and epidemiologically. Variants under monitoring usually remain unnamed until they advance to the status of a variant of interest or concern (Chakraborty et al. 2022).

By April 2022, there were at least two notable variants of the SARS-CoV-2 virus in circulation: the Delta (B.1.617.2) and Omicron (B.1.1.529) variants. The Delta variant was first identified in late 2020 in Maharashtra, India, and by May 2, 2021, it was responsible for around 70% of cases in the Indian subcontinent according to various medical reports (Chakraborty et al. 2022). Due to its significant transmission rates, the Centers for Disease Control and Prevention (CDC) elevated it from a variant of interest (VOI) to a variant of concern (VOC). The Delta variant quickly spread to 50 other countries by August 2021, affecting a total of 163 countries worldwide. Among various VOCs, the Delta variant, according to the

World Health Organization (WHO), was deemed the most rapid and adaptable strain up to that point (Chakraborty et al. 2022). On November 26, 2021, the World Health Organization's Technical Advisory Group on SARS-CoV-2 Virus Evolution designated the B.1.1.529 variant, initially discovered in Gauteng province, South Africa, as the Omicron variant of concern (South African 2021). This classification was based on a sharp rise in confirmed cases of SARS-CoV-2 infection in South Africa, coinciding with increased detection of the Omicron variant, the presence of troubling mutations, and early indications of heightened reinfection risk among recently recovered individuals. The Omicron variant harbors numerous mutations, notably within the spike protein's receptor-binding domain, which have been linked to enhanced transmissibility and the ability to evade immunity post-infection or vaccination (European Centre 2021). In December 2021, the Omicron variant surpassed the Delta variant in Gauteng, South Africa, being responsible for 98.4% of newly sequenced cases in the region. Notably, the fourth wave of COVID-19 occurred amidst the rollout of COVID-19 vaccination, which began in South Africa on May 17, 2021 (Madhi et al. 2022).

When a new variant of a virus, such as the Omicron variant of COVID-19, becomes dominant and supersedes the prevalence of a previous variant like the Delta variant, it's often referred to as "viral displacement" or "competitive replacement". This describes the process where one variant becomes more prevalent in a population, often due to factors such as increased transmissibility or immune evasion, leading to a decline in the prevalence of the earlier variant. New findings from actual situations suggest that the Omicron variant might be less severe compared to the earlier variants. However, even though Omicron tends to cause milder symptoms, the large number of infections could still lead to increased hospitalizations and fatalities among individuals who are more susceptible to the virus (Young et al. 2022). Omicron variant shows broad but incomplete ability to evade immunity from both natural infection and vaccines. When compared to the Delta variant, Omicron requires about a 10-fold higher level of antibodies to be neutralized after receiving vaccines like ChAdOx1 nCoV-19 (Oxford-AstraZeneca) and BNT162b2 (Pfizer-BioNTech) (European Centre 2021; South African 2021; Young et al. 2022). The global urgency caused by the COVID-19 pandemic led to a swift worldwide quest to find safe and efficient vaccines for the SARS-CoV-2 virus. By January 25, 2022, there were 194 vaccines in pre-clinical stages and 140 in clinical development. Many studies have investigated the efficacy of approved vaccines, but considerable differences in their effectiveness have been documented. These variations likely stem from diverse factors within the studies, such as the country, data collection methods, study populations

and the presence of different SARS-CoV-2 variants during the research period (Young et al. 2022).

Mathematical modeling is crucial for grasping the dynamics of infectious diseases, with numerous models specifically crafted to explore how COVID-19 transmits and its dynamic transmission patterns (see Abioye et al. 2021; Paul et al. 2023; Mohamadou et al. 2020; Kouidere et al. 2023; Ando et al. 2023; Hassan et al. 2023; Logeswari et al. 2024; Khajanchi et al. 2021; Mohamadou et al. 2020; Ghosh and Ghosh 2023; Ndairou et al. 2020; Bugalia et al. 2020). For instance, Gumel et al. (2021), introduced a primer for formulating, analysing and simulating mathematical models to understand COVID-19 dynamics. This included basic epidemic models and an endemic model to evaluate a hypothetical COVID-19 vaccine's potential impact on the population-level outcomes. Okuonghae and Omame (2020), developed a mathematical model examining how different non-pharmaceutical control measures influence COVID-19 transmission in Lagos, Nigeria. According to their study, if around 55% of the population adheres to social distancing and approximately 55% consistently wear face masks in public, the disease is projected to eventually diminish within the population. Omede et al. (2023), introduced a deterministic mathematical model to analyze the transmission patterns of the third wave of COVID-19 in Nigeria, incorporating optimal control strategies. Their findings indicated that implementing two control measures (vaccination and the sensitization on the danger of self-medication) resulted in a substantial decrease in the spread of COVID-19. Samui et al. (2020), developed a compartmental deterministic model to forecast and manage the transmission patterns of the COVID-19 pandemic in India, utilizing epidemic data until April 30, 2020. Their model predicted a higher peak for COVID-19 in India around 60 days from the given data, followed by a plateau in the curve. However, despite this plateau, the virus is expected to persist for an extended period. Iboi et al. (2020) devised a mathematical model aimed at assessing the impact of a theoretical imperfect anti-COVID-19 vaccine on containing the spread of the virus within the United States. According to their research, if a vaccine with an assumed efficacy of 80% were to be utilized, about 82% of the susceptible population in the US would need to be vaccinated to achieve the threshold required for herd immunity. Hellewell et al. (2020) introduced a stochastic model to evaluate the effectiveness of contact tracing and isolation in controlling the disease. According to their study, if these two control measures are highly effective, COVID-19 spread could be effectively contained within a span of 3 months. Khan and Atangana (2022) proposed a novel mathematical model to understand the dynamics of the Omicron variant of COVID-19. Their study included a second-order differential epidemic model to explore the

potential existence of multiple layers or waves within the spread of the virus.

Goswami et al. (2022) developed and analyzed a novel deterministic mathematical model to assess the impact of media awareness programs on the spread of COVID-19. They introduced three time-dependent controls: personal protection, diagnosis, and treatment measures. The optimal control analysis showed that implementing these controls significantly reduces the spread of COVID-19 compared to a model without such controls. Alaje and Olayiwola (2023) proposed a fractional-order mathematical model to study the spatiotemporal spread of COVID-19 in the context of vaccine distribution. Their analysis of homogeneous fractional-order vaccine distribution revealed that an optimal vaccination strategy is crucial. Higher-order vaccine implementation can substantially reduce disease transmission and help achieve herd immunity. Sepulveda et al. (2023) formulated a mathematical model to investigate the effects of transmission rates, vaccination, and time delays on the dynamics of the COVID-19 pandemic. Riyapan and Shuaib (2021) proposed and analyzed a new mathematical model to understand the transmission dynamics of the COVID-19 pandemic in Bangkok, Thailand. The outcome of their model analysis and numerical results demonstrate that the consistent use of face masks significantly reduces the spread of COVID-19. Masandawa et al. (2021) formulated a mathematical model for the transmission dynamics of COVID-19 between healthcare workers and the community. They incorporated public control measures as a parameter and healthcare workers as an independent compartment. Their results indicated that the protection of healthcare workers can be achieved through the effective use of personal protective equipment and minimizing the transmission of COVID-19 in the general public through the implementation of control measures.

Few mathematical models have been designed to understand the dynamics of COVID-19 variants. Saha and Saha (2023) formulated a new mathematical model considering the wild strain and its two variants, Delta and Omicron, to understand the dynamics of COVID-19 transmission. The aim of their study was to assess the impact of the original strain and its two variants on developing new infections, hospitalizations, and deaths. The results from their numerical simulation revealed that the emergence of new variants of concern increases COVID-19 infections and related deaths. Furthermore, the combination of non-pharmaceutical interventions with vaccination programs using new, more effective vaccines should be continued to control the disease outbreak. León et al. (2022) designed a mathematical model to depict the dynamics of the two-strain model under one vaccination regime, showing the impact of multiple variants and their response to the vaccine. Liozzi et al. (2023) developed a compartmental mathematical model to analyze

the transmission dynamics of the Delta and Omicron variants of SARS-CoV-2 in Greece. They considered the proportion of the vaccinated population, individuals with natural immunity, the secondary attack rate, and parameters related to population behavior, such as the use of masks and social distancing.

One of the limitations in the work of Saha and Saha (2023), León et al. (2022) and Lioffi et al. (2023) is their omission of the potential re-infection of individuals who recovered from the Delta variant with the Omicron variant of COVID-19. In response, this study presents a comprehensive and sophisticated deterministic mathematical model designed to explore the intricate transmission dynamics of both the Delta and Omicron variants. By thoroughly accounting for factors such as the re-infection of Delta variant recovered individuals with Omicron and the imperfections in vaccination, it aims to elucidate the complex interactions between these variants. The research aims to decode pivotal aspects influencing their competitive advantages, encompassing factors like transmissibility, immune evasion, and the efficacy of vaccines. Ultimately, the study aspires to furnish actionable insights that can inform precise and effective strategies for managing and controlling the ongoing pandemic. The subsequent sections of the paper are organized as follows: the next section elucidates the method, including model formulation and its basic properties. Following section delves into the model analysis. The next section presents the results. Following section is the Discussion, and the last section provides concluding remarks.

Methods

This section presents the development of the COVID-19 model, model assumptions, the model flow diagram, basic properties of the COVID-19 model, and the model analysis.

Model formulation

We propose a deterministic mathematical model on the transmission dynamics of COVID-19 in a population where the Delta and Omicron variants of COVID-19 are co-circulating. At time t , the overall population, labeled as $N(t)$, is divided into ten distinct compartments, each representing mutually exclusive groups of susceptible individuals denoted by $S(t)$, vaccinated individuals $V(t)$, exposed individuals to Delta variant of COVID-19 $E_d(t)$, exposed individuals to Omicron variant of COVID-19 $E_o(t)$, quarantined individuals $Q(t)$, infected individuals with Delta variant of COVID-19 $I_d(t)$, infected individuals with Omicron variant of COVID-19 $I_o(t)$, detected and hospitalized individuals $I_h(t)$, recovered individuals from Delta variant of COVID-19

$R_d(t)$, and recovered individuals from Omicron variant of COVID-19 $R_o(t)$, so that

$$N(t) = S(t) + V(t) + E_d(t) + E_o(t) + Q(t) + I_d(t) + I_o(t) + I_h(t) + R_d(t) + R_o(t).$$

The susceptible population expands through the influx of individuals into the community, facilitated by either birth or migration, occurring at a consistent rate denoted by Π , and reduces by the natural death rate μ (the natural death rate is the same in all the epidemiological compartments). Susceptible individuals acquire COVID-19 infection upon effective contact with infected individuals carrying either the Delta or Omicron variant of COVID-19. This acquisition occurs at rates represented by λ_d and λ_o , respectively, given by:

$$\lambda_d = \frac{(1 - \phi)\alpha_d J_d}{N}, \quad \text{and} \quad \lambda_o = \frac{(1 - \phi)\alpha_o J_o}{N}.$$

where α_d and α_o are the effective contact rate for Delta and Omicron variant of COVID-19 respectively, and ϕ is the compliance rate to COVID-19 safety protocols. The population of the vaccinated individuals is generated by susceptible individuals that got vaccinated at the rate ψ . The vaccinated individuals acquires COVID-19 infection following an effective contact with infected individuals with Delta or Omicron variant of COVID-19 at the rate $(1 - \tau_d)\lambda_d$ or $(1 - \tau_o)\lambda_o$, where τ_d and τ_o are the efficacy rates of the vaccine to Delta and Omicron variant of COVID-19 respectively. Susceptible individuals in contact with infected individuals with either Delta or Omicron variant of COVID-19 moves to the exposed classes $E_d(t)$ and $E_o(t)$ at the rates λ_d and λ_o respectively. Similarly the Vaccinated individuals in contact with infected individuals with either Delta or Omicron variant of COVID-19 moves to the exposed classes $E_d(t)$ and $E_o(t)$ at the rates $(1 - \tau_d)\lambda_d$ and $(1 - \tau_o)\lambda_o$ respectively. Exposed individuals to Delta or Omicron variant of COVID-19 are quarantined via contact tracing at the rate σ_d and σ_o respectively. Exposed individuals to Delta or Omicron variant of COVID-19 that were not quarantined progressed to the Delta variant infected class $I_d(t)$ at the rate γ_d , and to the Omicron variant infected class $I_o(t)$ at the rate γ_o . Quarantined individuals that progressed to being infected are hospitalized at the rate κ . Furthermore, quarantined individuals that do not developed symptoms of COVID-19 and are uninfected progressed back to the susceptible class at the rate ω . Infected individuals with either Delta or Omicron variant of COVID-19 recovers from COVID-19 due to strong body immune system at the rates η_d and η_o respectively. The rates δ_d and δ_o are the disease-induced death rates for infected individuals with Delta and Omicron variant of COVID-19. Infected individuals with Delta variant of COVID-19 acquires Omicron variant of COVID-19 as secondary infection following an effective contact with infected individuals with Omicron

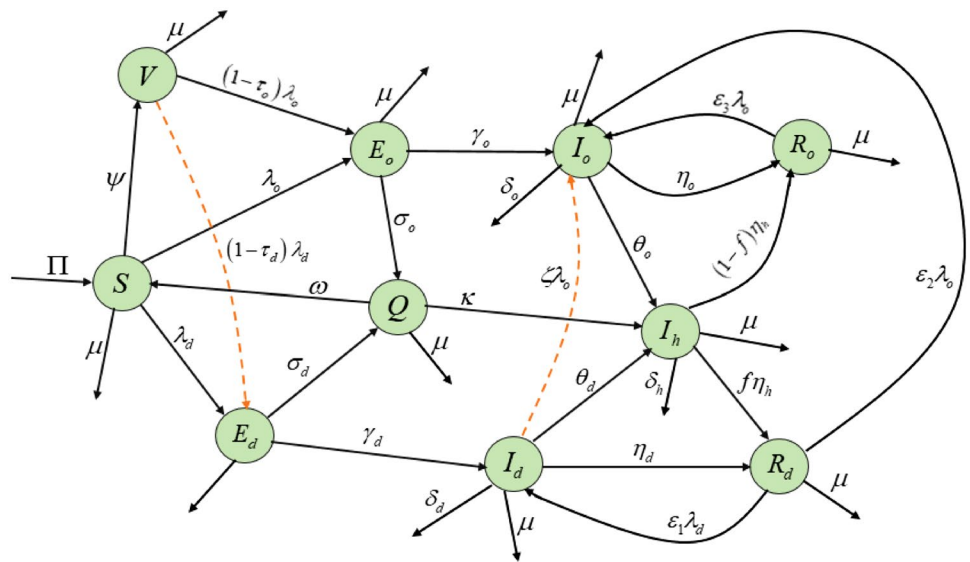
variant of COVID-19 at the rate $\zeta\lambda_o$, where ζ is the secondary infection rate. The infected individuals with either Delta or Omicron variant are detected and hospitalized at the rates θ_d and θ_o respectively. the rate δ_h is the disease-induced death rate of the detected and hospitalized individuals while receiving treatment, and η_h is the recovery rate of detected and hospitalized individuals. A proportion, $0 < f \leq 1$, of the hospitalized individuals recovers from Delta variant, while the remaining proportion, $(1 - f)$, recovers from Omicron variant of COVID-19 (Table 1). The Recovered

individuals from Delta variant are re-infected with Delta variant at the rate $\varepsilon_1\lambda_d$, and re-infected with Omicron variant of COVID-19 at the rate $\varepsilon_2\lambda_o$. Individuals that recovered from Omicron variant are re-infected with Omicron variant of COVID-19 at the rate $\varepsilon_3\lambda_o$. Based on the aforementioned formulations and assumptions (Fig. 1), the dynamics of the COVID-19 model are described by the following set of non-linear differential equations:

Table 1 Description of the model variables and parameters

Variable	Description
S	Susceptible individuals
V	Vaccinated individuals
E_d	Exposed individuals to Delta variant of COVID-19
E_o	Exposed individuals to Omicron variant of COVID-19
Q	Quarantined individuals
I_d	Infected individuals with Delta variant of COVID-19
I_o	Infected individuals with Omicron variant of COVID-19
I_h	Detected and hospitalized individuals
R_d	Recovered individuals from Delta variant of COVID-19
R_o	Recovered individuals from Omicron variant of COVID-19
Parameter	Description
Π	Recruitment rate
α_d	Delta variant effective contact rate
α_o	Omicron variant effective contact rate
ψ	Vaccination rate
τ_d	Efficacy of vaccine to Delta variant of COVID-19
τ_o	Efficacy of vaccine to Omicron variant of COVID-19
ϕ	Compliance rate to COVID-19 safety Protocols
μ	Natural death rate
δ_d	Delta variant disease-induced death rate
δ_o	Omicron variant disease-induced death rate
δ_h	Disease-induced death rate of individuals in I_h class
ω	The rate at which quarantined individuals that do not progressed to being infected progressed back to being susceptible again
η_d	Recovery rate of infected individuals with Delta variant of COVID-19
η_o	Recovery rate of infected individuals with Omicron variant of COVID-19
η_h	Recovery rate of detected and hospitalized individuals
θ_d	Detection rate of infected individuals with Delta variant of COVID-19 via testing and contact tracing
θ_o	Detection rate of infected individuals with Omicron variant of COVID-19 via testing and contact tracing
ζ	Secondary infection rate of Delta variant infected individuals with Omicron variant of COVID-19
ε_1	Re-infection rate of individuals that recovered from Delta variant of COVID-19 with Delta variant of COVID-19
ε_2	Re-infection rate of individuals that recovered from Delta variant of COVID-19 with Omicron variant of COVID-19
ε_3	Re-infection rate of individuals that recovered from Omicron variant of COVID-19 with Omicron variant of COVID-19
σ_d	Quarantine rate of exposed individuals to Delta variant of COVID-19 via contact tracing
σ_o	Quarantine rate of exposed individuals to Omicron variant of COVID-19 via contact tracing
γ_d	Progression rate from E_d compartment to I_d compartment
γ_o	Progression rate from E_o compartment to I_o compartment
f	Fraction of detected and hospitalized individuals that recovered from Delta variant of COVID-19
κ	Progression rate from quarantined compartment to detected and hospitalized compartment

Fig. 1 Flowchart of the COVID-19 model with $\lambda_d = \frac{(1-\phi)\alpha_d I_d}{N}$ and $\lambda_o = \frac{(1-\phi)\alpha_o I_o}{N}$



$$\begin{aligned} \frac{dS}{dt} &= \Pi - \lambda_d S - \lambda_o S - (\psi + \mu)S + \omega Q, \\ \frac{dV}{dt} &= \psi S - (1 - \tau_d)\lambda_d V - (1 - \tau_o)\lambda_o V - \mu V, \\ \frac{dE_d}{dt} &= \lambda_d(S + (1 - \tau_d)V) - (\gamma_d + \sigma_d + \mu)E_d, \\ \frac{dE_o}{dt} &= \lambda_o(S + (1 - \tau_o)V) - (\gamma_o + \sigma_o + \mu)E_o, \\ \frac{dQ}{dt} &= \sigma_d E_d + \sigma_o E_o - (\kappa + \omega + \mu)Q, \\ \frac{dI_d}{dt} &= \gamma_d E_d + \varepsilon_1 \lambda_d R_d - \zeta \lambda_o I_d - (\theta_d + \delta_d + \eta_d + \mu)I_d, \quad (1) \\ \frac{dI_o}{dt} &= \gamma_o E_o + \zeta \lambda_o I_d + \varepsilon_2 \lambda_o R_d + \varepsilon_3 \lambda_o R_o \\ &\quad - (\theta_o + \delta_o + \eta_o + \mu)I_o, \\ \frac{dI_h}{dt} &= \kappa Q + \theta_d I_d + \theta_o I_o - (\eta_h + \delta_h + \mu)I_h, \\ \frac{dR_d}{dt} &= \eta_d I_d + f \eta_h I_h - \varepsilon_1 \lambda_d R_d - \varepsilon_2 \lambda_o R_d - \mu R_d, \\ \frac{dR_o}{dt} &= \eta_o I_o + (1 - f) \eta_h I_h - \varepsilon_3 \lambda_o R_o - \mu R_o. \end{aligned}$$

where

$$\lambda_d = \frac{(1 - \phi)\alpha_d I_d}{N}, \quad \text{and} \quad \lambda_o = \frac{(1 - \phi)\alpha_o I_o}{N}.$$

Basic properties of the model

Positivity of solution

The biological validity of the COVID-19 model (1) depends on the solution of the system to being positive for all values of time *t*. Therefore, it is crucial to demonstrate

that all the state variables of the COVID-19 Model (1) remain non-negative for all time *t* > 0.

Theorem 1 *Let the initial data for the COVID-19 model (1) be S(0) > 0, V(0) > 0, E_d(0) > 0, E_o(0) > 0, Q(0) > 0, I_d(0) > 0, I_o(0) > 0, I_h(0) > 0, R_d(0) > 0, and R_o(0) > 0. Then the solution (S, V, E_d, E_o, Q, I_d, I_o, I_h, R_d, R_o) of the COVID-19 model (1) are non-negative for all time t > 0.*

Proof Let $t_f = \sup \{t > 0 : (S > 0, V > 0, E_d > 0, E_o > 0, Q > 0, I_d > 0, I_o > 0, I_h > 0, R_d > 0, R_o > 0) \in [0, t]\}$. Thus, $t_f > 0$.

From the first equation of the COVID-19 model system (1), we have

$$\frac{dS}{dt} = \Pi - \lambda_d S - \lambda_o S - (\psi + \mu)S + \omega Q \quad (2)$$

After solving the aforementioned equation, we derived the following result:

$$\begin{aligned} \frac{d}{dt} \left\{ S(t) \left[\exp \left(\int_0^t \lambda_d(z) dz + \lambda_o(z) dz + (\psi + \mu)t \right) \right] \right\} \\ = (\Pi + \omega Q) \exp \left(\int_0^t \lambda_d(z) dz + \lambda_o(z) dz + (\psi + \mu)t \right) \end{aligned} \quad (3)$$

Upon integrating the above equation over the interval [0, *t_f*], we obtain:

$$\begin{aligned} \left\{ S(t) \exp \left[\int_0^{t_f} \lambda_d(z) dz + \lambda_o(z) dz + (\psi + \mu)t_f \right] \right\} \\ - S(0) = (\Pi + \omega Q) \\ \times \int_0^{t_f} \exp \left[\int_0^x \lambda_d(z) dz + \lambda_o(z) dz + (\psi + \mu)x \right] dx \end{aligned} \quad (4)$$

So that

$$\begin{aligned}
 S(t) = & S(0) \exp \left[- \left(\int_0^{t_f} \lambda_d(z) dz + \lambda_o(z) dz + (\psi + \mu) t_f \right) \right] \\
 & + \exp \left[- \left(\int_0^{t_f} \lambda_d(z) dz + \lambda_o(z) dz + (\psi + \mu) t_f \right) \right] \\
 & \times (\Pi + \omega Q) \int_0^{t_f} \exp \left[\int_0^x (\lambda_d(z) dz + \lambda_o(z) dz \right. \\
 & \left. + (\psi + \mu)x \right] dx > 0.
 \end{aligned}
 \tag{5}$$

Likewise, it can be demonstrated that $V > 0, E_d > 0, E_o > 0, Q > 0, I_d > 0, I_o > 0, I_h > 0, R_d > 0, R_o > 0$.

□

Invariant Region

Lemma 1 *The region*

$$\begin{aligned}
 \mathcal{D} = & \left\{ (S, V, E_d, E_o, Q, I_d, I_o, I_h, R_d, R_o) \in \mathfrak{R}_+^{10} : S + V \right. \\
 & \left. + E_d + E_o + Q + I_d + I_o + I_h + R_d + R_o \leq \frac{\Pi}{\mu} \right\}
 \end{aligned}$$

is positively-invariant and attracts all solution in \mathfrak{R}_+^{10} (Omede et al. 2023).

Proof By summing the equations of the COVID-19 model system (1), we find the rate of change of the total population to be:

$$\frac{dN}{dt} = \Pi - \mu N - \delta_d I_d - \delta_o I_o - \delta_h I_h.
 \tag{6}$$

from Eq. (3), we have that

$$\Pi - (\mu + 3\delta)N \leq \frac{dN}{dt} \leq \Pi - \mu N,
 \tag{7}$$

where $\delta = \min \{ \delta_d, \delta_o, \delta_h \}$.

Thus, since it follows that the right hand side of the inequality (4) is bounded by $\Pi - \mu N$, it can be shown using a standard comparison theorem from (Lakshmikantham et al. 1989) that

$$N(t) \leq N(0)e^{-\mu t} + \frac{\Pi}{\mu} (1 - e^{-\mu t})
 \tag{8}$$

Hence, it follows that $N(t) \leq \frac{\Pi}{\mu}$, if $N(0) \leq \frac{\Pi}{\mu}$. Thus, the closed region \mathcal{D} is positively invariant and attracts all the solution in \mathfrak{R}_+^{10} . Furthermore, whenever $N > \frac{\Pi}{\mu}$, then $\frac{dN}{dt} < 0$. Consequently, the COVID-19 model (1) is both mathematically and biologically well-posed within the region \mathcal{D} . Thus, it is adequate to analyze the dynamics of the COVID-19

model solely within this region, as established in prior studies (Hethcote 2000). □

Model analysis

In this section, we embark on a qualitative exploration of the COVID-19 model (1). Our inquiry spans several critical dimensions. We commence by computing the basic reproduction number and then delve into examining the presence and stability of equilibrium points for both the Delta and Omicron variants of COVID-19. Additionally, we ascertain the invasion reproduction number for the Omicron variant, pinpoint the threshold for herd immunity, and meticulously analyze the primary parameters shaping the reproduction numbers.

Disease-free equilibrium point

The disease-free equilibrium denotes a stable condition characterized by the absence of COVID-19 infection in the population. To attain this state in the model, we set all disease-related compartments to zero (specifically, $E_d = E_o = Q = I_d = I_o = I_h = R_d = R_o = 0$) and equated the right-hand side of the model system (1) equations to zero. Consequently, the expression for the disease-free equilibrium is formulated as follows:

$$\begin{aligned}
 \Delta_0 = & (S^*, V^*, E_d^*, E_o^*, Q^*, I_d^*, I_o^*, I_h^*, R_d^*, R_o^*) \\
 = & \left(\frac{\Pi}{\psi + \mu}, \frac{\Pi\psi}{(\psi + \mu)\mu}, 0, 0, 0, 0, 0, 0, 0, 0 \right)
 \end{aligned}
 \tag{9}$$

Basic reproduction number

The COVID-19 basic reproduction number, denoted by \mathcal{R}_0^v , is defined as the average number of new infections generated when a single infectious individual is introduced into a completely susceptible population (Driessche and Watmough 2002). The basic reproduction number serves as a yardstick for infectious disease, it helps predict the potential for an outbreak. If the basic reproduction is equal to 1, each infected person spreads the disease to one other person on average, maintaining a steady rate of infection. When the basic reproduction number is above 1, each infected person passes the disease to more than one person, causing an outbreak to grow. Conversely, if the basic reproduction number is less than 1, the disease gradually fades away because infected individuals, on average, pass it to fewer than one person.

The computation of the basic reproduction number can be conducted utilizing the next-generation operator

method outlined in Driessche and Watmough (2002). Following the methodology described in Driessche and Watmough (2002), the non-negative matrix \mathcal{F} and the non-singular matrix \mathcal{V} , representing the new infection and the remaining transition terms respectively, at the disease-free equilibrium point, are given by:

$$\mathcal{F} = \begin{bmatrix} 0 & 0 & 0 & \mathcal{X}_1 & 0 & 0 \\ 0 & 0 & 0 & 0 & \mathcal{X}_2 & 0 \\ 0 & 0 & 0 & 0 & 0 & 0 \\ 0 & 0 & 0 & 0 & 0 & 0 \\ 0 & 0 & 0 & 0 & 0 & 0 \\ 0 & 0 & 0 & 0 & 0 & 0 \end{bmatrix},$$

and

$$\mathcal{V} = \begin{bmatrix} K_2 & 0 & 0 & 0 & 0 & 0 \\ 0 & K_3 & 0 & 0 & 0 & 0 \\ -\sigma_d & -\sigma_o & K_4 & 0 & 0 & 0 \\ -\gamma_d & 0 & 0 & K_5 & 0 & 0 \\ 0 & -\gamma_o & 0 & 0 & K_6 & 0 \\ 0 & 0 & -\kappa & -\theta_d & -\theta_o & K_7 \end{bmatrix}$$

where

$$\mathcal{X}_1 = \frac{(1 - \phi)\alpha_d(S^* + (1 - \tau_d)V^*)}{S^* + V^*},$$

$$\mathcal{X}_2 = \frac{(1 - \phi)\alpha_o(S^* + (1 - \tau_o)V^*)}{S^* + V^*},$$

$$K_1 = \psi + \mu, \quad K_2 = \gamma_d + \sigma_d + \mu, \quad K_3 = \gamma_o + \sigma_o + \mu, \\ K_4 = \kappa + \omega + \mu, \quad K_5 = \theta_d + \delta_d + \eta_d + \mu, \\ K_6 = \theta_o + \delta_o + \eta_o + \mu, K_7 = \eta_h + \delta_h + \mu, \text{ and } K_8 = (1 - f)\eta_h$$

It follows that $\mathcal{R}_0^v = \rho(\mathcal{F}\mathcal{V}^{-1})$, where ρ is the dominant eigenvalue of the $(\mathcal{F}\mathcal{V}^{-1})$. Hence, the COVID-19 basic reproduction number is given as

$$\mathcal{R}_0^v = \max\{\mathcal{R}_0^{vd}, \mathcal{R}_0^{vo}\} \tag{10}$$

where

$$\mathcal{R}_0^{vd} = \frac{(1 - \phi)\alpha_d(\mu + (1 - \tau_d)\psi)\gamma_d}{(\psi + \mu)(\gamma_d + \sigma_d + \mu)(\theta_d + \delta_d + \eta_d + \mu)},$$

$$\mathcal{R}_0^{vo} = \frac{(1 - \phi)\alpha_o(\mu + (1 - \tau_o)\psi)\gamma_o}{(\psi + \mu)(\gamma_o + \sigma_o + \mu)(\theta_o + \delta_o + \eta_o + \mu)}.$$

Here, \mathcal{R}_0^{vd} represents the basic reproduction number for Delta variant of COVID-19, while \mathcal{R}_0^{vo} represents the basic reproduction number for Omicron variant of COVID-19.

In the absence of COVID-19 vaccination in the population (i.e. $\psi = 0$), the basic reproduction number is given as

$$\mathcal{R}_0 = \max\{\mathcal{R}_0^d, \mathcal{R}_0^o\} \tag{11}$$

where

$$\mathcal{R}_0^d = \frac{(1 - \phi)\alpha_d\gamma_d}{(\gamma_d + \sigma_d + \mu)(\theta_d + \delta_d + \eta_d + \mu)},$$

$$\mathcal{R}_0^o = \frac{(1 - \phi)\alpha_o\gamma_o}{(\gamma_o + \sigma_o + \mu)(\theta_o + \delta_o + \eta_o + \mu)}.$$

Furthermore, if the COVID-19 vaccines are perfect (i.e. $\tau_d = \tau_o = 1$), then the basic reproduction number is reduced to

$$\mathcal{R}_0^{v*} = \max\{\mathcal{R}_0^{vd*}, \mathcal{R}_0^{vo*}\} \tag{12}$$

where

$$\mathcal{R}_0^{vd*} = \frac{(1 - \phi)\alpha_d\gamma_d\mu}{(\psi + \mu)(\gamma_d + \sigma_d + \mu)(\theta_d + \delta_d + \eta_d + \mu)},$$

$$\mathcal{R}_0^{vo*} = \frac{(1 - \phi)\alpha_o\gamma_o\mu}{(\psi + \mu)(\gamma_o + \sigma_o + \mu)(\theta_o + \delta_o + \eta_o + \mu)}.$$

Local stability of the disease-free equilibrium

Theorem 2 *The disease-free equilibrium (DFE) of the COVID-19 model (1) is locally asymptotically stable (LAS) if $\mathcal{R}_0^v < 1$, and unstable if $\mathcal{R}_0^v > 1$.*

Proof We investigated the local stability of the COVID-19 model by calculating the Jacobian matrix of the model system (1) assessed at the disease-free equilibrium (Δ_0) , as expressed by:

$$J(\Delta_0) = \begin{bmatrix} -K_1 & 0 & 0 & 0 & \omega & d_1 & d_2 & 0 & 0 & 0 \\ \psi & -\mu & 0 & 0 & 0 & d_3 & d_4 & 0 & 0 & 0 \\ 0 & 0 & -K_2 & 0 & 0 & d_5 & 0 & 0 & 0 & 0 \\ 0 & 0 & 0 & -K_3 & 0 & 0 & d_6 & 0 & 0 & 0 \\ 0 & 0 & \sigma_d & \sigma_o & -K_4 & 0 & 0 & 0 & 0 & 0 \\ 0 & 0 & \gamma_d & 0 & 0 & -K_5 & 0 & 0 & 0 & 0 \\ 0 & 0 & 0 & \gamma_o & 0 & 0 & -K_6 & 0 & 0 & 0 \\ 0 & 0 & 0 & 0 & \kappa & \theta_d & \theta_o & -K_7 & 0 & 0 \\ 0 & 0 & 0 & 0 & 0 & \eta_d & 0 & f\eta_h & -\mu & 0 \\ 0 & 0 & 0 & 0 & 0 & 0 & \eta_o & K_8 & 0 & -\mu \end{bmatrix}$$

where $d_1 = -\frac{(1-\phi)\alpha_d\mu}{K_1}$, $d_2 = -\frac{(1-\phi)\alpha_o\mu}{K_1}$, $d_3 = -\frac{(1-\phi)(1-\tau_d)\alpha_d\psi}{K_1}$, $d_4 = -\frac{(1-\phi)(1-\tau_o)\alpha_o\psi}{K_1}$, $d_5 = \frac{(1-\phi)\alpha_d(\mu+(1-\tau_d)\psi)}{K_1}$, $d_6 = \frac{(1-\phi)\alpha_o(\mu+(1-\tau_o)\psi)}{K_1}$, $K_1 = \psi + \mu$, $K_2 = \gamma_d + \sigma_d + \mu$, $K_3 = \gamma_o + \sigma_o + \mu$, $K_4 = \kappa + \omega + \mu$, $K_5 = \theta_d + \delta_d + \eta_d + \mu$, $K_6 = \theta_o + \delta_o + \eta_o + \mu$, $K_7 = \eta_h + \delta_h + \mu$, and $K_8 = (1 - f)\eta_h$.

The eigenvalues of the Jacobian matrix $J(\Delta_0)$ are $\lambda_1 = -\mu, \lambda_2 = -K_1, \lambda_3 = -\mu, \lambda_4 = -\mu$, and the roots of the characteristic polynomial given below

$$g(\lambda) = \lambda^6 + \xi_1 \lambda^5 + \xi_2 \lambda^4 + \xi_3 \lambda^3 + \xi_4 \lambda^2 + \xi_5 \lambda + \xi_6 \quad (13)$$

where

$$\begin{aligned} \xi_1 &= K_2 + K_3 + K_4 + K_5 + K_6 + K_7, \\ \xi_2 &= K_2(K_2 + K_3 + K_4 + K_5 + K_6 + K_7) \\ &\quad + K_3(K_4 + K_5 + K_7) + K_4(K_5 + K_6 + K_7) \\ &\quad + K_5(K_6 + K_7) + K_6 K_7 + K_2 K_5(1 - \mathcal{R}_0^{vd}) \\ &\quad + K_3 K_6(1 - \mathcal{R}_0^{vo}), \\ \xi_3 &= K_3(K_4 K_5 + K_4 K_7 + K_5 K_7) \\ &\quad + K_2 K_5(K_3 + K_4 + K_6 + K_7)(1 - \mathcal{R}_0^{vd}) \\ &\quad + K_4 K_5(K_6 + K_7) + K_2 K_4(K_6 + K_7) \\ &\quad + K_3 K_6(K_2 + K_4 + K_5 + K_7)(1 - \mathcal{R}_0^{vo}) \\ &\quad + K_6 K_7(K_2 + K_4 + K_5), \\ \xi_4 &= K_4 K_7(K_3 + K_6)(K_2 + K_5) \\ &\quad + K_2 K_5(K_4(K_6 + K_7) + K_6 K_7)(1 - \mathcal{R}_0^{vd}) \\ &\quad + K_2 K_3 K_5(K_4 + K_6 + K_7)(1 - \mathcal{R}_0^{vd}) \\ &\quad + K_3 K_6(K_4(K_5 + K_7) + K_5 K_7)(1 - \mathcal{R}_0^{vo}) \\ &\quad + \frac{(1 - \phi)^2(\mu + (1 - \tau_d)\psi)(\mu + (1 - \tau_o)\psi)\alpha_d \alpha_o \gamma_d \gamma_o}{K_1^2} \\ &\quad - \frac{(1 - \phi)(\mu + (1 - \tau_o)\psi)\alpha_o \gamma_o K_2 K_3 K_6(K_4 + K_7)}{K_1}, \\ \xi_5 &= K_3 K_4 K_6 K_7(K_2 + K_5) \\ &\quad + K_2 K_3 K_4 K_5(K_6 + K_7)(1 - \mathcal{R}_0^{vd}) \\ &\quad + K_2 K_5 K_6 K_7(K_3 + K_4)(1 - \mathcal{R}_0^{vd}) \\ &\quad + \frac{(1 - \phi)^2(\mu + (1 - \tau_d)\psi)(\mu + (1 - \tau_o)\psi)\alpha_d \alpha_o \gamma_d \gamma_o K_4}{K_1^2} \\ &\quad + \frac{(1 - \phi)^2(\mu + (1 - \tau_o)\psi)\alpha_d \alpha_o \gamma_d \gamma_o \mu K_7}{K_1^2} \\ &\quad + \frac{(1 - \phi)^2(\mu + (1 - \tau_o)\psi)(1 - \tau_d)\psi \alpha_d \alpha_o \gamma_d \gamma_o K_7}{K_1^2} \\ &\quad - \frac{(1 - \phi)(\mu + (1 - \tau_o)\psi)\alpha_o \gamma_o K_2 K_4(K_5 + K_7)}{K_1} \\ &\quad - \frac{(1 - \phi)(\mu + (1 - \tau_o)\psi)\alpha_o \gamma_o K_5 K_7(K_2 + K_4)}{K_1}, \\ \xi_6 &= K_1^2 K_2 K_3 K_4 K_5 K_6 K_7(1 - \mathcal{R}_0^{vd})(1 - \mathcal{R}_0^{vo}). \end{aligned}$$

Employing the Routh–Hurwitz criterion, as referenced in Hassan et al. (2022), which asserts that for all roots of the characteristic polynomial ($g(\lambda)$) to have negative real parts,

it is necessary that $\xi_1 > 0, \xi_2 > 0, \xi_3 > 0, \xi_4 > 0, \xi_5 > 0, \xi_6 > 0$. It is evident that if $\mathcal{R}_0^v < 1$ (that is, if both $\mathcal{R}_0^{vd} < 1$ and $\mathcal{R}_0^{vo} < 1$), then all conditions are met. Consequently, based on the Routh–Hurwitz Criterion, the disease-free equilibrium of the COVID-19 model (1) exhibits local asymptotic stability if and only if $\mathcal{R}_0^v < 1$. \square

From a biological standpoint, Theorem 2 suggests that a minor introduction of COVID-19 infected individuals into the community will not trigger a COVID-19 outbreak provided that the basic reproduction number (\mathcal{R}_0^v) remains below one (Omede et al. 2023). It’s important to emphasize that this conclusion hinges on the initial proportions of infected individuals within the population.

Existence and stability of boundary equilibria

In this section, we will explore the presence and stability of the equilibria in the COVID-19 model (1) where the infected variables corresponding to the Delta and Omicron variants of COVID-19 are not equal to zero. Consequently, the potential equilibria of the COVID-19 model (1) are outlined as follows:

1. Delta variant dominance equilibrium, $\chi_d = (S^{**}, V^{**}, E_d^{**}, 0, Q^{**}, I_d^{**}, 0, I_h^{**}, R_d^{**}, 0)$ (i.e., no Omicron variant).
2. Omicron variant dominance equilibrium, $\chi_o = (S^{**}, V^{**}, 0, E_o^{**}, Q^{**}, 0, I_o^{**}, I_h^{**}, 0, R_o^{**})$ (i.e., no Delta variant).
3. Co-existence of Delta and Omicron Equilibrium, $\chi_{do} = (S^{**}, V^{**}, E_d^{**}, E_o^{**}, Q^{**}, I_d^{**}, I_o^{**}, I_h^{**}, R_d^{**}, R_o^{**})$

The COVID-19 model (1) is solved at steady state in terms of the forces of infection, given by

$$\lambda_d^{**} = \frac{(1 - \phi)\alpha_d I_d^{**}}{N^{**}}, \quad \text{and} \quad \lambda_o^{**} = \frac{(1 - \phi)\alpha_o I_o^{**}}{N^{**}}, \quad (14)$$

where

$$\begin{aligned} N^{**} &= S^{**} + V^{**} + E_d^{**} + E_o^{**} + Q^{**} + I_d^{**} \\ &\quad + I_o^{**} + I_h^{**} + R_d^{**} + R_o^{**}, \end{aligned} \quad (15)$$

with

$$\begin{aligned}
 S^{**} &= \frac{\Pi((1-\tau_d)\lambda_d^{**} + (1-\tau_o)\lambda_o^{**} + \mu)K_2K_3K_4}{M}, \\
 V^{**} &= \frac{\Pi\psi K_2K_3K_4}{M}, E_d^{**} = \frac{\lambda_d^{**}\Pi K_3K_4A_1}{M}, \\
 E_o^{**} &= \frac{\lambda_o^{**}\Pi K_2K_4A_2}{M}, \\
 Q^{**} &= \frac{\Pi(\lambda_d^{**}\sigma_d K_3A_1 + \lambda_o^{**}\sigma_o K_2A_2)}{M}, \\
 I_d^{**} &= \frac{\lambda_d^{**}\Pi K_3K_4\gamma_d A_1(B_2B_5 - B_3B_6)}{M(\lambda_o^{**}\zeta + K_5)(B_2B_5 - B_3B_6)} \\
 &\quad + \frac{\lambda_d^{**}\varepsilon_1 M(B_4B_5 + B_1)}{M(\lambda_o^{**}\zeta + K_5)(B_2B_5 - B_3B_6)}, \\
 I_o^{**} &= \frac{B_7(B_2B_5 - B_3B_6) + B_{10}(B_4B_5 + B_1)}{K_6M(\lambda_o^{**}\zeta + K_5)(B_2B_5 - B_3B_6)} \\
 &\quad + \frac{M\varepsilon_3(\lambda_o^{**2}\zeta + \lambda_o^{**}K_5)(B_1B_2 + B_3B_4)}{K_6M(\lambda_o^{**}\zeta + K_5)(B_2B_5 - B_3B_6)}, \\
 I_h^{**} &= \frac{B_8(B_2B_5 - B_3B_6) + B_9(B_4B_5 + B_1)}{K_6K_7M(\lambda_o^{**}\zeta + K_5)(B_2B_5 - B_3B_6)} \\
 &\quad + \frac{M\theta_o\varepsilon_3(\lambda_o^{**2}\zeta + \lambda_o^{**}K_5)(B_1B_2 + B_3B_4)}{K_6K_7M(\lambda_o^{**}\zeta + K_5)(B_2B_5 - B_3B_6)}, \\
 R_d^{**} &= \frac{B_4B_5 + B_1}{B_2B_5 - B_3B_6}, R_o^{**} = \frac{B_1B_2 + B_3B_4}{B_2B_5 - B_3B_6}.
 \end{aligned} \tag{16}$$

where $K_1 = \psi + \mu$, $K_2 = \gamma_d + \sigma_d + \mu$, $K_3 = \gamma_o + \sigma_o + \mu$, $K_4 = \kappa + \omega + \mu$, $K_5 = \theta_d + \delta_d + \eta_d + \mu$, $K_6 = \theta_o + \delta_o + \eta_o + \mu$, $K_7 = \eta_h + \delta_h + \mu$, $K_8 = (1-f)\eta_h$,

$$\begin{aligned}
 A_1 &= (1-\tau_d)\lambda_d^{**} + (1-\tau_o)\lambda_o^{**} + \mu + (1-\tau_d)\psi, \\
 A_2 &= (1-\tau_d)\lambda_d^{**} + (1-\tau_o)\lambda_o^{**} + \mu + (1-\tau_o)\psi, \\
 M &= (1-\tau_d)\lambda_d^{**}(\lambda_d^{**} + \lambda_o^{**} + K_1)K_2K_3K_4 \\
 &\quad + ((1-\tau_o)\lambda_o^{**} + \mu)(\lambda_d^{**} + \lambda_o^{**} + K_1)K_2K_3K_4 \\
 &\quad - \omega(\lambda_d^{**}\sigma_d K_3A_1 + \lambda_o^{**}\sigma_o K_2A_2), \\
 B_1 &= \lambda_o^{**2}A_2e_1 + \lambda_d^{**}\lambda_o^{**}A_1e_2 + \lambda_o^{**}A_2e_3 + \lambda_d^{**}A_1e_4, \\
 B_2 &= M(\lambda_o^{**2}e_5 + \lambda_d^{**}\lambda_o^{**}e_6 + \lambda_o^{**}e_7 + \lambda_d^{**}e_8 + e_9), \\
 B_3 &= M(\lambda_o^{**2}e_{10} + \lambda_d^{**}\lambda_o^{**}e_{11} + \lambda_o^{**}e_{12} + \lambda_d^{**}e_{13}), \\
 B_4 &= \lambda_o^{**2}A_2e_{14} + \lambda_d^{**}\lambda_o^{**}A_1e_{15} + \lambda_o^{**}A_2e_{16} \\
 &\quad + \lambda_d^{**}A_1e_{17}, \\
 B_5 &= M(\lambda_o^{**}e_{18} - \lambda_o^{**2}e_{19} + e_{20}), \\
 B_6 &= \lambda_o^{**2}Me_{21} + \lambda_o^{**}e_{22}, \\
 B_7 &= \lambda_o^{**2}\Pi\zeta K_2K_4\gamma_o A_2 + \lambda_d^{**}\lambda_o^{**}\Pi\zeta K_3K_4\gamma_d A_1 \\
 &\quad + \lambda_o^{**}\Pi K_2K_4K_5\gamma_o A_2, \\
 B_8 &= \lambda_o^{**2}A_2e_{24} + \lambda_d^{**}\lambda_o^{**}A_1e_{23} + \lambda_o^{**}A_2e_{26} + \lambda_d^{**}A_1e_{25}, \\
 B_9 &= M(\lambda_o^{**2}\zeta\varepsilon_2\theta_o + \lambda_d^{**}\lambda_o^{**}\zeta\varepsilon_1\theta_o + \lambda_o^{**}\varepsilon_2\theta_o K_5) \\
 &\quad + \lambda_d^{**}\varepsilon_1\theta_d K_6 M, \\
 B_{10} &= M(\lambda_o^{**2}\zeta\varepsilon_2 + \lambda_d^{**}\lambda_o^{**}\zeta\varepsilon_1 + \lambda_o^{**}\varepsilon_2 K_5).
 \end{aligned}$$

With

$$\begin{aligned}
 e_1 &= \Pi\zeta K_2(K_8(\kappa\sigma_o K_6 + \gamma_o\theta_o K_4) + \gamma_o\eta_o K_4 K_7), \\
 e_2 &= \Pi\zeta K_3(K_8(\kappa\sigma_d K_6 + \gamma_d\theta_o K_4) + \gamma_d\eta_o K_4 K_7), \\
 e_3 &= \Pi K_2 K_5(K_8(\kappa\sigma_o K_6 + \gamma_o\theta_o K_4) + \gamma_o\eta_o K_4 K_7), \\
 e_4 &= \Pi K_3 K_6 K_8(\kappa\sigma_d K_5 + \gamma_d\theta_d K_4), \\
 e_5 &= \zeta\varepsilon_2(K_6 K_7 - f\eta_h\theta_o), e_6 = \zeta\varepsilon_1(K_6 K_7 - f\eta_h\theta_o), \\
 e_7 &= K_6 K_7(\zeta\mu + \varepsilon_2 K_5) - \varepsilon_2 f\eta_h\theta_o K_5, \\
 e_8 &= \varepsilon_1 K_6(K_5 K_7 - (\eta_d K_7 + f\eta_h\eta_d)), e_9 = \mu K_5 K_6 K_7, \\
 e_{10} &= \zeta\varepsilon_2(\eta_o K_7 + \theta_o K_8), e_{11} = \zeta\varepsilon_1(\eta_o K_7 + \theta_o K_8), \\
 e_{12} &= \varepsilon_2 K_5(\eta_o K_7 + \theta_o K_8), e_{13} = \varepsilon_1\theta_d K_6 K_8, \\
 e_{14} &= \Pi\zeta f\eta_h K_2(\kappa\sigma_o K_6 + \gamma_o\theta_o K_4), \\
 e_{15} &= \Pi\zeta f\eta_h K_3(\kappa\sigma_d K_6 + \gamma_d\theta_o K_4), \\
 e_{16} &= \Pi f\eta_h K_2 K_5(\kappa\sigma_o K_6 + \gamma_o\theta_o K_4), \\
 e_{17} &= \Pi K_3 K_6((\kappa\sigma_d K_5 + \gamma_d\theta_d K_4)f\eta_h + \gamma_d\eta_d K_4 K_7), \\
 e_{18} &= \zeta K_6 K_7 - \varepsilon_2 K_5(\eta_o K_7 + K_8), \\
 e_{19} &= \zeta\varepsilon_3(\eta_o K_7 + K_8), e_{20} = K_5 K_6 K_7, e_{21} = \zeta\varepsilon_3 f\eta_h\theta_o \\
 e_{22} &= \varepsilon_3 f\eta_h\theta_o K_5, e_{23} = \Pi\zeta K_3(\kappa\sigma_d K_6 + \gamma_d\theta_o K_4), \\
 e_{24} &= \Pi\zeta K_2(\kappa\sigma_o K_6 + \gamma_o\theta_o K_4), \\
 e_{25} &= \Pi K_3 K_6(\kappa\sigma_d K_5 + \gamma_d\theta_d K_4), \\
 e_{26} &= \Pi K_3 K_5(\kappa\sigma_o K_6 + \gamma_o\theta_o K_4), e_{27} = \Pi\zeta K_2 K_4 \gamma_o, \\
 e_{28} &= \Pi\zeta K_3 K_4 \gamma_d, e_{29} = \Pi K_2 K_4 K_5 \gamma_o, e_{30} = \Pi K_3 K_4 \gamma_d.
 \end{aligned} \tag{17}$$

The equilibrium states of the COVID-19 model (1) can be derived by inserting the components of the steady-state equilibrium into the equations in Eq. (14), and then identifying the fixed points of the system, as outlined in Omede et al. (2023) as follows:

$$u = \chi(u) = \begin{pmatrix} \chi_1(\lambda_d^{**}, \lambda_o^{**}) \\ \chi_2(\lambda_d^{**}, \lambda_o^{**}) \end{pmatrix}, \text{ where } u = \begin{pmatrix} \lambda_d^{**} \\ \lambda_o^{**} \end{pmatrix} \tag{18}$$

Additionally, χ_1 and χ_2 represent the right-hand sides of the equations governing λ_d^{**} and λ_o^{**} in Eq. (14), respectively.

Delta variant dominance equilibrium

The Delta variant dominance equilibrium, denoted by χ_d , is given by

$$\chi_d = (S^{**}, V^{**}, E_d^{**}, 0, Q^{**}, I_d^{**}, 0, I_h^{**}, R_d^{**}, 0) \tag{19}$$

With

$$\begin{aligned}
 S^{**} &= \frac{\Pi M_2 K_2 K_4}{(\lambda_d^{**} + K_1) M_2 K_2 K_4 - \lambda_d^{**} \sigma_d \omega M_1}, \\
 V^{**} &= \frac{\Pi \psi K_2 K_4}{(\lambda_d^{**} + K_1) M_2 K_2 K_4 - \lambda_d^{**} \sigma_d \omega M_1}, \\
 E_d^{**} &= \frac{\lambda_d^{**} \Pi M_1 K_4}{(\lambda_d^{**} + K_1) M_2 K_2 K_4 - \lambda_d^{**} \sigma_d \omega M_1}, \\
 Q^{**} &= \frac{\lambda_d^{**} \Pi \sigma_d M_1}{(\lambda_d^{**} + K_1) M_2 K_2 K_4 - \lambda_d^{**} \sigma_d \omega M_1}, \\
 I_d^{**} &= \frac{\lambda_d^{**} \Pi M_1 \gamma_d K_4 K_7 (\varepsilon_1 \lambda_d^{**} + \mu)}{((\lambda_d^{**} + K_1) M_2 K_2 K_4 - \lambda_d^{**} \sigma_d \omega M_1) Z_1} \\
 &\quad + \frac{\lambda_d^{**2} \Pi M_1 \varepsilon_1 f \eta_h \sigma_d \kappa}{((\lambda_d^{**} + K_1) M_2 K_2 K_4 - \lambda_d^{**} \sigma_d \omega M_1) Z_1}, \\
 I_h^{**} &= \frac{\lambda_d^{**} \Pi M_1 \sigma_d \kappa ((\varepsilon_1 \lambda_d^{**} + \mu) K_5 - \lambda_d^{**} \varepsilon_1 \eta_d)}{((\lambda_d^{**} + K_1) M_2 K_2 K_4 - \lambda_d^{**} \sigma_d \omega M_1) Z_1} \\
 &\quad + \frac{\lambda_d^{**} \Pi M_1 \theta_d \gamma_d K_4 (\varepsilon_1 \lambda_d^{**} + \mu)}{((\lambda_d^{**} + K_1) M_2 K_2 K_4 - \lambda_d^{**} \sigma_d \omega M_1) Z_1}, \\
 R_d^{**} &= \frac{\lambda_d^{**} \Pi M_1 \eta_d \gamma_d K_4 K_7}{((\lambda_d^{**} + K_1) M_2 K_2 K_4 - \lambda_d^{**} \sigma_d \omega M_1) Z_1} \\
 &\quad + \frac{\lambda_d^{**} \Pi M_1 f \eta_h (\sigma_d \kappa K_5 + \theta_d \gamma_d K_4)}{((\lambda_d^{**} + K_1) M_2 K_2 K_4 - \lambda_d^{**} \sigma_d \omega M_1) Z_1}.
 \end{aligned}
 \tag{20}$$

where

$$\begin{aligned}
 M_1 &= (1 - \tau_d) \lambda_d^{**} + \mu + (1 - \tau_d) \psi, \\
 M_2 &= (1 - \tau_d) \lambda_d^{**} + \mu, \\
 Z_1 &= (\varepsilon_1 \lambda_d^{**} + \mu) K_5 K_7 - \lambda_d^{**} \varepsilon_1 (\eta_d K_7 + \theta_d f \eta_h).
 \end{aligned}$$

The equilibrium corresponding to the dominance of the Delta variant can be identified by solving the fixed-point problem $\chi_1(\lambda_d^{**}, 0) = \lambda_d^{**}$. Upon solving this fixed-point problem with respect to λ_d^{**} , we derived the polynomial:

$$P(\lambda_d^{**}) = C_1 \lambda_d^{**3} + C_2 \lambda_d^{**2} + C_3 \lambda_d^{**} + C_4 \tag{21}$$

where

$$\begin{aligned}
 C_1 &= \Pi \varepsilon_1 (1 - \tau_d) (\sigma_d + K_4) (K_5 K_7 + \eta_d K_7 + f \eta_h \theta_d) \\
 &\quad + \Pi \varepsilon_1 (1 - \tau_d) \gamma_d K_4 (\theta_d + K_7) \\
 &\quad + \Pi \varepsilon_1 (1 - \tau_d) \sigma_d \kappa (K_5 + \eta_d + f \eta_h), \\
 C_2 &= \Pi \varepsilon_1 (1 - \tau_d) (K_2 K_4 (K_7 (K_5 - \eta_d) + f \eta_h \theta_d)) \\
 &\quad + \Pi \varepsilon_1 K_4 (\mu + (1 - \tau_d) \psi) (\eta_d K_7 + f \eta_h \theta_d) \\
 &\quad + \Pi \varepsilon_1 K_4 (\mu + (1 - \tau_d) \psi) (K_5 K_7 + \gamma_d (\theta_d + K_7)) \\
 &\quad + \Pi \varepsilon_1 \sigma_d \kappa (\mu + (1 - \tau_d) \psi) (K_5 + \eta_d + f \eta_h) \\
 &\quad + \Pi \varepsilon_1 \sigma_d (\mu + (1 - \tau_d) \psi) (K_5 K_7 - (\eta_d K_7 + f \eta_h \theta_d)) \\
 &\quad + \Pi \gamma_d K_4 K_7 (1 - \tau_d) (\mu + \eta_d) \\
 &\quad + \Pi (1 - \tau_d) (\mu + f \eta_h) (\sigma_d \kappa K_5 + \theta_d \gamma_d K_4) \\
 &\quad + \Pi \mu K_5 K_7 (1 - \tau_d) (\sigma_d + K_4) \\
 &\quad - \Pi \varepsilon_1 \alpha_d (1 - \phi) (1 - \tau_d) (\gamma_d K_4 K_7 + f \eta_h \sigma_d \kappa), \\
 C_3 &= \Pi (\mu + (1 - \tau_d) \psi) (\mu + f \eta_h) (\sigma_d \kappa K_5 + \theta_d \gamma_d K_4) \\
 &\quad + \Pi \gamma_d K_4 K_7 (\mu + (1 - \tau_d) \psi) (\eta_d + \mu) \\
 &\quad + \Pi \mu K_5 K_7 (\mu + (1 - \tau_d) \psi) (\sigma_d + K_4) \\
 &\quad + \Pi \varepsilon_1 K_1 K_2 K_4 (K_5 K_7 - (\eta_d K_7 + f \eta_h \theta_d)) \\
 &\quad + \Pi \mu K_2 K_4 K_5 K_7 (1 - \tau_d) \\
 &\quad - \Pi \alpha_d (1 - \phi) \mu \gamma_d K_4 K_7 (1 - \tau_d) \\
 &\quad - \Pi \alpha_d (1 - \phi) (\mu + (1 - \tau_d) \psi) \varepsilon_1 \gamma_d K_4 K_7 \\
 &\quad - \Pi \alpha_d (1 - \phi) (\mu + (1 - \tau_d) \psi) \varepsilon_1 f \eta_h \sigma_d \kappa, \\
 C_4 &= \Pi \mu K_1 K_2 K_4 K_5 K_7 (1 - \mathcal{R}_0^{nd}).
 \end{aligned}$$

Clearly, in the polynomial (21) $C_1 > 0$ (since all the model parameters are positive) and $C_4 > 0$ whenever $\mathcal{R}_0^{nd} < 1$. Therefore, the number of possible positive real roots of the polynomial (21) can be determined depending on the signs of C_2 , and C_3 . Utilizing Descartes' rule of signs (Gumel et al. 2018) on the polynomial $P(\lambda_d^{**}) = C_1 \lambda_d^{**3} + C_2 \lambda_d^{**2} + C_3 \lambda_d^{**} + C_4$, the conclusions presented in Table 2 below are established.

The delta variant dominance equilibrium has a unique endemic equilibrium if $\mathcal{R}_0^{nd} > 1$ and cases 1–3 in Table 2

Table 2 Number of possible positive real roots of $P(\lambda_d^{**})$ for $\mathcal{R}_0^{nd} > 1$ and $\mathcal{R}_0^{nd} < 1$

Cases	C_1	C_2	C_3	C_4	\mathcal{R}_0^{nd}	Number of sign change	Number of positive real roots
1	+	+	+	+	$\mathcal{R}_0^{nd} < 1$	0	0
	+	+	+	-	$\mathcal{R}_0^{nd} > 1$	1	1
2	+	+	-	+	$\mathcal{R}_0^{nd} < 1$	2	0,2
	+	+	-	-	$\mathcal{R}_0^{nd} > 1$	1	1
3	+	-	-	+	$\mathcal{R}_0^{nd} < 1$	2	0,2
	+	-	-	-	$\mathcal{R}_0^{nd} > 1$	1	1
4	+	-	+	+	$\mathcal{R}_0^{nd} < 1$	2	0,2
	+	-	+	-	$\mathcal{R}_0^{nd} > 1$	3	1,3

are satisfied. It could have more than one endemic equilibrium if $\mathcal{R}_0^{nd} > 1$ and case 4 is satisfied. Additionally, it could have two endemic equilibria if $\mathcal{R}_0^{nd} < 1$ and cases 2–4 are satisfied.

From cases 2–4 outlined in Table 2, it's evident that multiple endemic equilibria emerge when the reproduction number (\mathcal{R}_0^{nd}) is below one, indicating a characteristic of backward bifurcation. Backward bifurcation refers to the coexistence of a stable disease-free equilibrium and a stable endemic equilibrium when the basic reproduction number of the model falls below unity, a phenomenon observed in various epidemiological models, as documented in studies such as Gumel (2012); Gumel et al. (2018), Omame et al. (2018, 2020). Biologically, the implication of backward bifurcation is that the requisite condition for effectively controlling the Delta variant of COVID-19 within the population, when the basic reproduction number is less than one ($\mathcal{R}_0^{nd} < 1$), is no longer adequate (Gumel et al. 2018).

Omicron variant dominance equilibrium

Omicron variant dominance equilibrium, denoted by χ_o , is given by

$$\chi_o = (S^{**}, V^{**}, 0, E_o^{**}, Q^{**}, 0, I_o^{**}, I_h^{**}, 0, R_o^*) \quad (22)$$

Putting $\lambda_d^{**} = 0$ in Eq. (14), we obtained:

$$\begin{aligned} S^{**} &= \frac{\Pi M_4 K_3 K_4}{(\lambda_o^{**} + K_1) M_4 K_3 K_4 - \lambda_o^{**} \sigma_o \omega M_3}, \\ V^{**} &= \frac{\Pi \psi K_3 K_4}{(\lambda_o^{**} + K_1) M_4 K_3 K_4 - \lambda_o^{**} \sigma_o \omega M_3}, \\ E_o^{**} &= \frac{\lambda_o^{**} \Pi K_4 M_3}{(\lambda_o^{**} + K_1) M_4 K_3 K_4 - \lambda_o^{**} \sigma_o \omega M_3}, \\ Q^{**} &= \frac{\lambda_o^{**} \Pi \sigma_o M_3}{(\lambda_o^{**} + K_1) M_4 K_3 K_4 - \lambda_o^{**} \sigma_o \omega M_3}, \\ I_o^{**} &= \frac{\lambda_o^{**} \Pi M_3 \gamma_o K_4 K_7 (\varepsilon_3 \lambda_o^{**} + \mu)}{((\lambda_o^{**} + K_1) M_4 K_3 K_4 - \lambda_o^{**} \sigma_o \omega M_3) Z_2} \\ &\quad + \frac{\lambda_o^{**2} \Pi M_3 \varepsilon_3 \sigma_o \kappa K_8}{((\lambda_o^{**} + K_1) M_4 K_3 K_4 - \lambda_o^{**} \sigma_o \omega M_3) Z_2}, \\ I_h^{**} &= \frac{\lambda_o \Pi M_3 Z_3}{((\lambda_o^{**} + K_1) M_4 K_3 K_4 - \lambda_o^{**} \sigma_o \omega M_3) Z_2}, \\ R_o^{**} &= \frac{\lambda_o \Pi M_3 Z_4}{((\lambda_o^{**} + K_1) M_4 K_3 K_4 - \lambda_o^{**} \sigma_o \omega M_4) Z_2}. \end{aligned} \quad (23)$$

where

$$\begin{aligned} M_3 &= ((1 - \tau_o) \lambda_o^{**} + \mu + (1 - \tau_o) \psi), \\ M_4 &= (1 - \tau_o) \lambda_o^{**} + \mu, \\ Z_2 &= (\varepsilon_3 \lambda_o^{**} + \mu) K_6 K_7 - \lambda_o^{**} \varepsilon_3 (\eta_o K_7 + \theta_o K_8), \\ Z_3 &= \sigma_o \kappa ((\varepsilon_3 \lambda_o^{**} + \mu) K_6 - \lambda_o^{**} \varepsilon_3 \eta_o) \\ &\quad + \theta_o \gamma_o K_4 (\varepsilon_3 \lambda_o^{**} + \mu), \\ Z_4 &= (\eta_o \gamma_o K_4 K_7 + K_8 (\sigma_o \kappa K_6 + \theta_o \gamma_o K_4)). \end{aligned}$$

By substituting the expressions from Eq. (23) into the expression for λ_o^{**} in Eq. (14), and subsequently simplifying, we derived the polynomial:

$$P(\lambda_o^{**}) = H_1 \lambda_o^{**3} + H_2 \lambda_o^{**2} + H_3 \lambda_o^{**} + H_4 \quad (24)$$

where

$$\begin{aligned} H_1 &= \Pi \varepsilon_3 (1 - \tau_o) (\sigma_o + K_4) (K_7 (\eta_o + K_6) + \theta_o K_8) \\ &\quad + \Pi \varepsilon_3 (1 - \tau_o) (\theta_o + K_7) \gamma_o K_4 \\ &\quad + \Pi \varepsilon_3 (1 - \tau_o) (K_6 + \eta_o + K_8) \sigma_o \kappa, \\ H_2 &= \Pi \varepsilon_3 (1 - \tau_o) (K_3 K_4 (K_7 (K_6 - \eta_o) + \theta_o K_8)) \\ &\quad + \Pi \varepsilon_3 K_4 (\mu + (1 - \tau_o) \psi) (\eta_o K_7 + \theta_o K_8) \\ &\quad + \Pi \varepsilon_3 K_4 (\mu + (1 - \tau_o) \psi) (K_6 K_7 + \gamma_o (\theta_o + K_7)) \\ &\quad + \Pi \varepsilon_3 \sigma_o \kappa (\mu + (1 - \tau_o) \psi) (K_6 + \eta_o + K_8) \\ &\quad + \Pi \varepsilon_3 \sigma_o (\mu + (1 - \tau_o) \psi) (K_6 K_7 - (\eta_o K_7 + \theta_o K_8)) \\ &\quad + \Pi \gamma_o K_4 K_7 (1 - \tau_o) (\mu + \eta_o) \\ &\quad + \Pi (1 - \tau_o) (\mu + K_8) (\sigma_o \kappa K_6 + \theta_o \gamma_o K_4) \\ &\quad + \Pi \mu K_6 K_7 (1 - \tau_o) (\sigma_o + K_4) \\ &\quad - \Pi \varepsilon_3 \alpha_o (1 - \phi) (1 - \tau_o) (\gamma_o K_4 K_7 + \sigma_o \kappa K_8), \\ H_3 &= \Pi \varepsilon_3 K_1 K_3 K_4 (K_6 K_7 - (\eta_o K_7 + \theta_o K_8)) \\ &\quad + \Pi \gamma_o K_4 K_7 (\mu + (1 - \tau_o) \psi) (\eta_o + \mu) \\ &\quad + \Pi \mu K_6 K_7 (\mu + (1 - \tau_o) \psi) (\sigma_o + K_4) \\ &\quad + \Pi \mu K_3 K_4 K_6 K_7 (1 - \tau_o) \\ &\quad + \Pi (\mu + (1 - \tau_o) \psi) (\mu + K_8) (\sigma_o \kappa K_6 + \theta_o \gamma_o K_4) \\ &\quad - \Pi \alpha_o (1 - \phi) (1 - \tau_o) \mu \gamma_o K_4 K_7 \\ &\quad - \Pi \alpha_o (1 - \phi) \varepsilon_3 (\mu + (1 - \tau_o) \psi) \gamma_o K_4 K_7 \\ &\quad - \Pi \alpha_o (1 - \phi) \varepsilon_3 (\mu + (1 - \tau_o) \psi) \sigma_o \kappa K_8, \\ H_4 &= \Pi \mu K_1 K_3 K_4 K_6 K_7 (1 - \mathcal{R}_0^{no}). \end{aligned}$$

Examining the polynomial presented in Eq. (24), it becomes apparent that the coefficient H_1 consistently maintains a positive value, and H_4 is positive (or negative) when $\mathcal{R}_0^{no} < 1$ (or $\mathcal{R}_0^{no} > 1$). The form of the polynomial in Eq. (24) strongly indicates the presence of backward bifurcation.

Co-existence of Delta and Omicron equilibrium

The analysis of the co-existence of Delta and Omicron equilibrium, denoted by χ_{do} , given by

$$\chi_{do} = (S^{**}, V^{**}, E_d^{**}, E_o^{**}, Q^{**}, I_d^{**}, I_o^{**}, I_h^{**}, R_d^{**}, R_o^{**}) \quad (25)$$

From (14) we have that

$$\begin{aligned} N^{**} \lambda_d^{**} &= (1 - \phi) \alpha_d I_d^{**} \\ N^{**} \lambda_o^{**} &= (1 - \phi) \alpha_o I_o^{**} \end{aligned} \quad (26)$$

So that

$$\begin{aligned} N^{**} &= \frac{(1 - \phi) \alpha_d I_d^{**}}{\lambda_d^{**}} \\ N^{**} &= \frac{(1 - \phi) \alpha_o I_o^{**}}{\lambda_o^{**}} \end{aligned} \quad (27)$$

Subtracting the second expression from the first expression in equation (27), we obtained

$$0 = \frac{(1 - \phi) \alpha_d I_d^{**}}{\lambda_d^{**}} - \frac{(1 - \phi) \alpha_o I_o^{**}}{\lambda_o^{**}}. \quad (28)$$

We have that

$$\frac{(1 - \phi) \alpha_o I_o}{\lambda_o^{**}} = \frac{(1 - \phi) \alpha_d I_d}{\lambda_d^{**}} \quad (29)$$

Substituting the values of I_d and I_o in Eq. (16) into Eq. (29), The substitution is in the appendix section

Omicron invasion reproduction number

The invasion reproduction number, denoted by $\mathcal{R}_0^{o:d}$, is a concept used in epidemiology to estimate the potential of a new variant or strain of a pathogen to spread and establish itself within a population that has little to no immunity against it (Martcheva 2015; Mitchell and Kribs 2019). This number represents the average number of secondary infections generated by an index case (a single infected individual) in a completely susceptible population, typically at the beginning of an outbreak or introduction of a new variant. It helps in understanding the potential of a new pathogen or variant to spread rapidly and cause an outbreak. If the invasion reproduction number is greater than 1, it suggests that the new variant has the potential to cause sustained transmission and become established in

the population. Estimating the invasion reproduction number can help public health officials and researchers understand the threat level posed by a new pathogen or variant.

Similarly, just like the case of the basic reproduction number, the Omicron invasion reproduction number can be computed using the next generation operator method as described in Martcheva (2015). Following the approach in Martcheva (2015), the non-negative matrix \mathcal{F} and the non-singular matrix \mathcal{V} for the new Omicron infection and the remaining transition terms respectively, evaluated at the delta variant dominance equilibrium is given by

$$\mathcal{F} = \begin{bmatrix} \frac{(1-\phi)\alpha_o I_o (S^{**} + (1-\tau_o)V^{**})}{N^{**}} & 0 \\ \frac{(1-\phi)\xi\alpha_o I_o I_d^{**}}{N^{**}} + \frac{(1-\phi)\varepsilon_2\alpha_o I_o R_d^{**}}{N^{**}} & 0 \end{bmatrix}, \text{ and}$$

$$\mathcal{V} = \begin{bmatrix} (\gamma_o + \sigma_o + \mu)E_o & \\ -\sigma_o E_o + (\kappa + \omega + \mu)Q & \\ -\gamma_o E_o + (\theta_o + \delta_o + \eta_o + \mu)I_o & \\ -\kappa Q - \theta_o I_o + (\eta_h + \delta_h + \mu)I_h & \end{bmatrix}$$

$$\mathcal{F} = \begin{bmatrix} 0 & 0 & \frac{(1-\phi)\alpha_o (S^{**} + (1-\tau_o)V^{**})}{N^{**}} & 0 \\ 0 & 0 & 0 & 0 \\ 0 & 0 & \frac{(1-\phi)\alpha_o (\xi I_d^{**} + \varepsilon_2 R_d^{**})}{N^{**}} & 0 \\ 0 & 0 & 0 & 0 \end{bmatrix}$$

$$\mathcal{V} = \begin{bmatrix} K_3 & 0 & 0 & 0 \\ -\sigma_o & K_4 & 0 & 0 \\ -\gamma_o & 0 & K_6 & 0 \\ 0 & -\kappa & -\theta_o & K_7 \end{bmatrix}$$

where $K_3 = \gamma_o + \sigma_o + \mu$, $K_4 = \kappa + \omega + \mu$, $K_6 = \theta_o + \delta_o + \eta_o + \mu$, and $K_7 = \eta_h + \delta_h + \mu$.

It follows that $\mathcal{R}_0^{o:d} = \rho(\mathcal{F}\mathcal{V}^{-1})$, where ρ is the dominant eigenvalue of the $(\mathcal{F}\mathcal{V}^{-1})$. Hence, the Omicron invasion reproduction number is given as

$$\begin{aligned} \mathcal{R}_0^{o:d} &= \frac{(1 - \phi) \alpha_o (S^{**} + (1 - \tau_o) V^{**}) \gamma_o}{N^{**} K_3 K_6} \\ &+ \frac{(1 - \phi) \alpha_o (\xi I_d^{**} + \varepsilon_2 R_d^{**})}{N^{**} K_6}. \end{aligned} \quad (30)$$

Where S^{**} , V^{**} , I_d^{**} , R_d^{**} , and N^{**} are values of the delta variant dominance equilibrium.

Possibility of the existence of backward bifurcation

The existence of the backward bifurcation is explored through the application of the center manifold theory, a method popularized by Castillo-Chavez and Song (2004).

Castillo–Chavez and Song theorem

Theorem 3 *Considering a general system of ordinary differential equations with a parameter ∇ ;*

$$\frac{du}{dt} = f(u, \nabla), f : \mathbb{R}^n \times \mathbb{R} \rightarrow \mathbb{R}^n, f \in \mathbf{C}^2(\mathbb{R}^n \times \mathbb{R}) \quad (31)$$

where $u = 0$ is an equilibrium point for the system in Eq. (31). That is, $f(0, \nabla) \equiv 0 \forall \nabla$.

Consider the following assumptions:

\mathcal{G}_1 : $A = D_u f(0, 0) = \left[\frac{\partial f}{\partial u}(0, 0) \right]$ represents the linearization matrix of the system described by Eq. (31) around the equilibrium 0, with ∇ evaluated at 0. Zero is a simple eigenvalue of A , and all other eigenvalues of A possess negative real parts.

\mathcal{G}_2 : The matrix A possesses a non-negative right eigenvector w and a left eigenvector v corresponding to the zero eigenvalue.

Let f_k be the k th component of f and

$$\begin{aligned} a &= \sum_{k,i,j=1}^n v_k w_i w_j \frac{\partial^2 f_k}{\partial u_i \partial u_j}(0, 0), \\ b &= \sum_{k,i=1}^n v_k w_i \frac{\partial^2 f_k}{\partial u_i \partial \nabla}(0, 0). \end{aligned} \quad (32)$$

The local dynamics of Eq. (31) around the equilibrium point 0 are entirely dictated by the signs of a and b .

1. In the scenario where $a > 0$ and $b > 0$:
 - When $\nabla < 0$ with $|\nabla| \ll 1$, the equilibrium at 0 is locally asymptotically stable, and there exists a positive unstable equilibrium.

- When $0 < \nabla \ll 1$, the equilibrium at 0 is unstable, and there exists a negative, locally asymptotically stable equilibrium.
2. If $a < 0$ and $b < 0$:
 - When $\nabla < 0$ with $|\nabla| \ll 1$, the equilibrium at 0 is unstable.
 - When $0 < \nabla \ll 1$, the equilibrium at 0 is a locally asymptotically stable equilibrium, and there exists a positive unstable equilibrium.
 3. If $a > 0$ and $b < 0$:
 - When $\nabla < 0$ with $|\nabla| \ll 1$, the equilibrium at 0 is unstable, and there exists a locally asymptotically stable negative equilibrium.
 - When $0 < \nabla \ll 1$, the equilibrium at 0 is stable, and a positive unstable equilibrium emerges.
 4. In the case where $a < 0$ and $b > 0$:
 - When ∇ transitions from negative to positive, the stability of the equilibrium at 0 shifts from stable to unstable. Consequently, a negative unstable equilibrium transforms into a positive, locally asymptotically stable equilibrium.

Specifically, if $a < 0$ and $b > 0$, the bifurcation is forward; whereas if $a > 0$ and $b > 0$, the bifurcation is backward. Utilizing this method, we can derive the following result.

Theorem 4 *The model of system (1) exhibits backward bifurcation at $\mathcal{R}_0^v = 1$.*

Proof To analyze the nature of the bifurcation, we employ center manifold theory (Agwu et al. 2023; Castillo-Chavez and Song 2004). For effective application of this theory, it is essential to introduce the following change of variables: Let $S = u_1$, $V = u_2$, $E_d = u_3$, $E_o = u_4$, $Q = u_5$, $I_d = u_6$, $I_o = u_7$, $I_h = u_8$, $R_d = u_9$, $R_o = u_{10}$. So that

$$N = \sum_{i=1}^7 u_i \quad (33)$$

Moreover, employing vector notation $u = (u_1, u_2, u_3, \dots, u_{10})^T$ and $\frac{du}{dt} = F(u)$, where

$F = (f_1, f_2, f_3, \dots, f_{10})^T$, the COVID-19 model (1) can be expressed as follows:

$$\begin{aligned}
 \frac{du_1}{dt} &\equiv f_1 = \Pi - \frac{(1-\phi)\alpha_d u_6 u_1}{N} - \frac{(1-\phi)\alpha_o u_7 u_1}{N} - (\psi + \mu)u_1 + \omega u_5 \\
 \frac{du_2}{dt} &\equiv f_2 = \psi u_1 - \frac{(1-\phi)(1-\tau_d)\alpha_d u_6 u_2}{N} - \frac{(1-\phi)(1-\tau_o)\alpha_o u_7 u_2}{N} - \mu u_2 \\
 \frac{du_3}{dt} &\equiv f_3 = \frac{(1-\phi)\alpha_d u_6 (u_1 + (1-\tau_d)u_2)}{N} - (\gamma_d + \sigma_d + \mu)u_3 \\
 \frac{du_4}{dt} &\equiv f_4 = \frac{(1-\phi)\alpha_o u_7 (u_1 + (1-\tau_o)u_2)}{N} - (\gamma_o + \sigma_o + \mu)u_4 \\
 \frac{du_5}{dt} &\equiv f_5 = \sigma_d u_3 + \sigma_o u_4 - (\kappa + \omega + \mu)u_5 \\
 \frac{du_6}{dt} &\equiv f_6 = \gamma_d u_3 + \frac{(1-\phi)\varepsilon_1 \alpha_d u_6 u_9}{N} - \frac{(1-\phi)\zeta \alpha_o u_7 u_6}{N} - (\theta_d + \delta_d + \eta_d + \mu)u_6 \\
 \frac{du_7}{dt} &\equiv f_7 = \gamma_o u_4 + \frac{(1-\phi)\zeta \alpha_o u_7 u_6}{N} + \frac{(1-\phi)\varepsilon_2 \alpha_o u_7 u_9}{N} + \frac{(1-\phi)\varepsilon_3 \alpha_o u_7 u_{10}}{N} - (\theta_o + \delta_o + \eta_o + \mu)u_7 \\
 \frac{du_8}{dt} &\equiv f_8 = \kappa u_5 + \theta_d u_6 + \theta_o u_7 - (\eta_h + \delta_h + \mu)u_8 \\
 \frac{du_9}{dt} &\equiv f_9 = \eta_d u_6 + f \eta_h u_8 - \frac{(1-\phi)\varepsilon_1 \alpha_d u_6 u_9}{N} - \frac{(1-\phi)\varepsilon_2 \alpha_o u_7 u_9}{N} - \mu u_9 \\
 \frac{du_{10}}{dt} &\equiv f_{10} = \eta_o u_7 + (1-f)\eta_h u_8 - \frac{(1-\phi)\varepsilon_3 \alpha_o u_7 u_{10}}{N} - \mu u_{10}
 \end{aligned}
 \tag{34}$$

where

$$N = u_1 + u_2 + u_3 + u_4 + u_5 + u_6 + u_7 + u_8 + u_9 + u_{10}$$

Let's consider the Delta variant effective contact rate α_d as the bifurcation parameter. Solving for $\alpha_d = \alpha_d^*$ from $\mathcal{R}_0^d = 1$ yields:

$$\alpha_d^* = \frac{(\psi + \mu)(\gamma_d + \sigma_d + \mu)(\theta_d + \delta_d + \eta_d + \mu)}{(1-\phi)(\mu + (1-\tau_d)\psi)\gamma_d}
 \tag{35}$$

The Jacobian matrix of the transformed system (34) at the disease-free equilibrium (DFE) (Δ_0) with $\alpha_d = \alpha_d^*$ is determined as follows:

$$J(\Delta_0)|_{\alpha_d=\alpha_d^*} = \begin{bmatrix} -K_1 & 0 & 0 & 0 & \omega & d_1 & d_2 & 0 & 0 & 0 \\ \psi & -\mu & 0 & 0 & 0 & d_3 & d_4 & 0 & 0 & 0 \\ 0 & 0 & -K_2 & 0 & 0 & d_5 & 0 & 0 & 0 & 0 \\ 0 & 0 & 0 & -K_3 & 0 & 0 & d_6 & 0 & 0 & 0 \\ 0 & 0 & \sigma_d & \sigma_o & -K_4 & 0 & 0 & 0 & 0 & 0 \\ 0 & 0 & \gamma_d & 0 & 0 & -K_5 & 0 & 0 & 0 & 0 \\ 0 & 0 & 0 & \gamma_o & 0 & 0 & -K_6 & 0 & 0 & 0 \\ 0 & 0 & 0 & 0 & \kappa & \theta_d & \theta_o & -K_7 & 0 & 0 \\ 0 & 0 & 0 & 0 & 0 & \eta_d & 0 & f\eta_h & -\mu & 0 \\ 0 & 0 & 0 & 0 & 0 & 0 & \eta_o & K_8 & 0 & -\mu \end{bmatrix}$$

where $d_1 = -\frac{(1-\phi)\alpha_d^* \mu}{K_1}$, $d_2 = -\frac{(1-\phi)\alpha_o \mu}{K_1}$, $d_3 = -\frac{(1-\phi)(1-\tau_d)\alpha_d^* \psi}{K_1}$, $d_4 = -\frac{(1-\phi)(1-\tau_o)\alpha_o \psi}{K_1}$, $d_5 = \frac{(1-\phi)\alpha_d^* (\mu + (1-\tau_d)\psi)}{K_1}$, $d_6 = \frac{(1-\phi)\alpha_o (\mu + (1-\tau_o)\psi)}{K_1}$, $K_1 = \psi + \mu$, $K_2 = \gamma_d + \sigma_d + \mu$, $K_3 = \gamma_o + \sigma_o + \mu$, $K_4 = \kappa + \omega + \mu$, $K_5 = \theta_d + \delta_d + \eta_d + \mu$, $K_6 = \theta_o + \delta_o + \eta_o + \mu$, $K_7 = \eta_h + \delta_h + \mu$, and $K_8 = (1-f)\eta_h$.

The right eigenvector, $w = (w_1, w_2, w_3, w_4, w_5, w_6, w_7, w_8, w_9, w_{10})^T$, associated with the simple zero eigenvalue can be obtained from $J(\Delta_0)|_{\alpha_d=\alpha_d^*} w = 0$, given by

$$\begin{aligned}
 -K_1 w_1 + \omega w_5 - \frac{(1-\phi)\alpha_d^* \mu}{K_1} w_6 - \frac{(1-\phi)\alpha_o \mu}{K_1} w_7 &= 0, \\
 \psi w_1 - \mu w_2 - \frac{(1-\phi)(1-\tau_d)\alpha_d^* \psi}{K_1} w_6 - \frac{(1-\phi)(1-\tau_o)\alpha_o \psi}{K_1} w_7 &= 0, \\
 -K_2 w_3 + \frac{(1-\phi)\alpha_d^* y_1}{K_1} w_6 - \frac{(1-\phi)\alpha_o y_2}{K_1} w_7 &= 0, \\
 \sigma_d w_3 + \sigma_o w_4 - K_4 w_5 &= 0, \\
 \gamma_d w_3 - K_5 w_6 &= 0, \\
 \gamma_o w_4 - K_6 w_7 &= 0, \\
 \kappa w_5 + \theta_d w_6 + \theta_o w_7 - K_7 w_8 &= 0, \\
 \eta_d w_6 + f \eta_h w_8 - \mu w_9 &= 0, \\
 \eta_o w_7 + K_8 w_8 - \mu w_{10} &= 0.
 \end{aligned}
 \tag{36}$$

Where $y_1 = \mu + (1-\tau_d)\psi$, and $y_2 = \mu + (1-\tau_o)\psi$.

From the equation (36), we obtained

$$\begin{aligned}
 w_1 &= \frac{((1-\phi)\alpha_d^*y_1 - K_1K_5)\omega\sigma_d w_6}{(K_2 - \gamma_d)K_1^2 K_4} - \frac{(1-\phi)\alpha_d^* \mu w_6}{K_1^2} \\
 &+ \frac{((1-\phi)\alpha_o y_2 - K_1K_6)\omega\sigma_o w_7}{(K_3 - \gamma_o)K_1^2 K_4} - \frac{(1-\phi)\alpha_o \mu w_7}{K_1^2}, \\
 w_2 &= \frac{((1-\phi)\alpha_d^*y_1 - K_1K_5)\omega\sigma_d - \psi w_6}{(K_2 - \gamma_d)\mu K_1^2 K_4} \\
 &- \frac{((1-\phi)\alpha_d^*(\mu + (1-\tau_d)K_1)\psi w_6)}{\mu K_1^2} \\
 &+ \frac{((1-\phi)\alpha_o y_2 - K_1K_6)\omega\sigma_o \psi w_7}{(K_3 - \gamma_o)\mu K_1^2 K_4} \\
 &- \frac{(1-\phi)\alpha_o(\mu + (1-\tau_o)K_1)\psi w_7}{\mu K_1^2}, \\
 w_3 &= \frac{((1-\phi)\alpha_d^*y_1 - K_1K_5)w_6}{(K_2 - \gamma_d)K_1}, \\
 w_4 &= \frac{((1-\phi)\alpha_o y_2 - K_1K_6)w_7}{(K_3 - \gamma_o)K_1}, \\
 w_5 &= \frac{((1-\phi)\alpha_d^*y_1 - K_1K_5)\sigma_d w_6}{(K_2 - \gamma_d)K_1 K_4} + \\
 &\frac{((1-\phi)\alpha_o y_2 - K_1K_6)\sigma_o w_7}{(K_3 - \gamma_o)K_1 K_4}, \\
 w_6 &= w_6 > 0, w_7 = w_7 > 0, \\
 w_8 &= \frac{((1-\phi)\alpha_d^*y_1 - K_1K_5)\kappa\sigma_d w_6}{(K_2 - \gamma_d)K_1 K_4 K_7} + \frac{\theta_d w_6}{K_7} \\
 &+ \frac{((1-\phi)\alpha_o y_2 - K_1K_6)\kappa\sigma_o w_7}{(K_3 - \gamma_o)K_1 K_4 K_7} + \frac{\theta_o w_7}{K_7}, \\
 w_9 &= \frac{((1-\phi)\alpha_d^*y_1 - K_1K_5)\kappa\sigma_d f \eta_h w_6}{(K_2 - \gamma_d)\mu K_1 K_4 K_7} \\
 &+ \frac{(\theta_d f \eta_h + \eta_d K_7)w_6}{\mu K_7} \\
 &+ \frac{((1-\phi)\alpha_o y_2 - K_1K_6)\kappa\sigma_o f \eta_h w_7}{(K_3 - \gamma_o)\mu K_1 K_4 K_7} + \frac{\theta_o \eta_h w_7}{\mu K_7}, \\
 w_{10} &= \frac{((1-\phi)\alpha_d^*y_1 - K_1K_5)\kappa\sigma_d K_8 w_6}{(K_2 - \gamma_d)\mu K_1 K_4 K_7} + \frac{\theta_d K_8 w_6}{\mu K_7} \\
 &+ \frac{((1-\phi)\alpha_o y_2 - K_1K_6)\kappa\sigma_o K_8 + w_7}{(K_3 - \gamma_o)\mu K_1 K_4 K_7} \\
 &+ \frac{(\theta_o K_8 + \eta_o K_7)w_7}{\mu K_7}.
 \end{aligned}
 \tag{37}$$

Likewise, the left eigenvector, $v=(v_1, v_2, v_3, v_4, v_5, v_6, v_7, v_8, v_9, v_{10})$, satisfying $v \cdot w = 1$, associated with the simple zero eigenvalue, can be derived from $vJ(\Delta_0)|_{\alpha_d=\alpha_d^*} = 0$. This is given by:

$$\begin{aligned}
 -K_1 v_1 + \psi v_2 &= 0, \\
 -\mu v_2 &= 0, \\
 -K_2 v_3 + \sigma_d v_5 + \gamma_d v_6 &= 0, \\
 -K_3 v_4 + \sigma_o v_5 + \gamma_o v_7 &= 0, \\
 \omega v_1 - K_4 v_5 + \kappa v_8 &= 0, \\
 -\frac{(1-\phi)\alpha_d^* \mu v_1}{K_1} - \frac{(1-\phi)(1-\tau_d)\alpha_d^* \psi v_2}{K_1} \\
 + \frac{(1-\phi)\alpha_d^* y_1 v_3}{K_1} - K_5 v_6 + \theta_d v_8 + \eta_d v_9 &= 0, \\
 -\frac{(1-\phi)\alpha_o \mu v_1}{K_1} - \frac{(1-\phi)(1-\tau_o)\alpha_o \psi v_2}{K_1} \\
 + \frac{(1-\phi)\alpha_o y_2 v_4}{K_1} - K_6 v_7 + \theta_o v_8 + \eta_o v_{10} &= 0, \\
 -K_7 v_8 + f \eta_h v_9 + K_8 v_{10} &= 0, \\
 -\mu v_9 &= 0, \\
 -\mu v_{10} &= 0.
 \end{aligned}
 \tag{38}$$

We obtained

$$\begin{aligned}
 v_1 = v_2 = v_5 = v_8 = v_9 = v_{10} &= 0, v_3 = v_3 > 0, \\
 v_4 = v_4 > 0, v_6 &= \frac{((1-\phi)\alpha_d^*y_1 - K_1K_2)v_3}{(K_5 - \gamma_d)K_1}, \\
 \text{and } v_7 &= \frac{((1-\phi)\alpha_o y_2 - K_1K_3)v_4}{(K_6 - \gamma_o)K_1}.
 \end{aligned}
 \tag{39}$$

Computation of a and b

Since $v_1 = v_2 = v_5 = v_8 = v_9 = v_{10} = 0$ for $k = 1, 2, 3, \dots, 10$, the only non-zero partial derivatives are

$$\begin{aligned}
 \frac{\partial^2 f_3}{\partial u_1 \partial u_6} &= \frac{\partial^2 f_3}{\partial u_6 \partial u_1} = \frac{(1 - \phi) \alpha_d^* \mu (K_1 - y_1)}{\Pi K_1}, \\
 \frac{\partial^2 f_3}{\partial u_2 \partial u_6} &= \frac{\partial^2 f_3}{\partial u_6 \partial u_2} = \frac{(1 - \phi) \alpha_d^* \mu (K_1 (1 - \tau_d) - y_1)}{\Pi K_1}, \\
 \frac{\partial^2 f_3}{\partial u_3 \partial u_6} &= \frac{\partial^2 f_3}{\partial u_6 \partial u_3} = \frac{\partial^2 f_3}{\partial u_4 \partial u_6} = \frac{\partial^2 f_3}{\partial u_6 \partial u_4} \\
 &= \frac{\partial^2 f_3}{\partial u_5 \partial u_6} = \frac{\partial^2 f_3}{\partial u_6 \partial u_5} = -\frac{(1 - \phi) \alpha_d^* y_1 \mu}{\Pi K_1}, \\
 \frac{\partial^2 f_3}{\partial u_6 \partial u_7} &= \frac{\partial^2 f_3}{\partial u_7 \partial u_6} = \frac{\partial^2 f_3}{\partial u_6 \partial u_8} = \frac{\partial^2 f_3}{\partial u_8 \partial u_6} \\
 &= \frac{\partial^2 f_3}{\partial u_6 \partial u_9} = \frac{\partial^2 f_3}{\partial u_9 \partial u_6} = -\frac{(1 - \phi) \alpha_d^* y_1 \mu}{\Pi K_1}, \\
 \frac{\partial^2 f_3}{\partial u_6 \partial u_{10}} &= \frac{\partial^2 f_3}{\partial u_{10} \partial u_6} = -\frac{(1 - \phi) \alpha_d^* y_1 \mu}{\Pi K_1}, \\
 \frac{\partial^2 f_3}{\partial u_6^2} &= -\frac{2(1 - \phi) \alpha_d^* y_1 \mu}{\Pi K_1}, \quad \frac{\partial^2 f_3}{\partial u_6 \partial \alpha_d^*} = \frac{(1 - \phi) y_1}{K_1} \\
 \frac{\partial^2 f_4}{\partial u_1 \partial u_7} &= \frac{\partial^2 f_4}{\partial u_7 \partial u_1} = \frac{(1 - \phi) \alpha_o \mu (K_1 - y_2)}{\Pi K_1}, \\
 \frac{\partial^2 f_4}{\partial u_2 \partial u_7} &= \frac{\partial^2 f_4}{\partial u_7 \partial u_2} = \frac{(1 - \phi) \alpha_o \mu (K_1 (1 - \tau_o) - y_2)}{\Pi K_1}, \\
 \frac{\partial^2 f_4}{\partial u_3 \partial u_7} &= \frac{\partial^2 f_4}{\partial u_7 \partial u_3} = \frac{\partial^2 f_4}{\partial u_4 \partial u_7} = \frac{\partial^2 f_4}{\partial u_7 \partial u_4} \\
 &= \frac{\partial^2 f_4}{\partial u_5 \partial u_7} = \frac{\partial^2 f_4}{\partial u_7 \partial u_5} = -\frac{(1 - \phi) \alpha_o y_2 \mu}{\Pi K_1}, \\
 \frac{\partial^2 f_4}{\partial u_6 \partial u_7} &= \frac{\partial^2 f_4}{\partial u_7 \partial u_6} = \frac{\partial^2 f_4}{\partial u_7 \partial u_8} = \frac{\partial^2 f_4}{\partial u_8 \partial u_7} \\
 &= \frac{\partial^2 f_4}{\partial u_7 \partial u_9} = \frac{\partial^2 f_4}{\partial u_9 \partial u_7} = -\frac{(1 - \phi) \alpha_o y_2 \mu}{\Pi K_1}, \\
 \frac{\partial^2 f_4}{\partial u_7 \partial u_{10}} &= \frac{\partial^2 f_4}{\partial u_{10} \partial u_7} = -\frac{(1 - \phi) \alpha_o y_2 \mu}{\Pi K_1}, \\
 \frac{\partial^2 f_4}{\partial u_7^2} &= -\frac{2(1 - \phi) \alpha_o y_2 \mu}{\Pi K_1}, \\
 \frac{\partial^2 f_6}{\partial u_6 \partial u_7} &= \frac{\partial^2 f_6}{\partial u_7 \partial u_6} = -\frac{(1 - \phi) \zeta \alpha_o \mu}{\Pi}, \\
 \frac{\partial^2 f_6}{\partial u_6 \partial u_9} &= \frac{\partial^2 f_6}{\partial u_9 \partial u_6} = \frac{(1 - \phi) \epsilon_1 \alpha_d^* \mu}{\Pi}, \\
 \frac{\partial^2 f_7}{\partial u_6 \partial u_7} &= \frac{\partial^2 f_7}{\partial u_7 \partial u_6} = \frac{(1 - \phi) \zeta \alpha_o \mu}{\Pi}, \\
 \frac{\partial^2 f_7}{\partial u_7 \partial u_9} &= \frac{\partial^2 f_7}{\partial u_9 \partial u_7} = \frac{(1 - \phi) \epsilon_2 \alpha_o \mu}{\Pi}, \\
 \frac{\partial^2 f_7}{\partial u_7 \partial u_{10}} &= \frac{\partial^2 f_7}{\partial u_{10} \partial u_7} = \frac{(1 - \phi) \epsilon_3 \alpha_o \mu}{\Pi}.
 \end{aligned}
 \tag{40}$$

But

$$\begin{aligned}
 a &= \sum_{k,i,j=1}^n v_k w_i w_j \frac{\partial^2 f_k}{\partial u_i \partial u_j} (\Delta_0) \\
 a &= \frac{2v_3 w_6 (1 - \phi) \alpha_d^* \mu (K_1 - y_1)}{\Pi K_1^3 K_4} (\chi_1 w_6 + \chi_2 w_7) \\
 &+ \frac{2v_3 w_6^2 (1 - \phi) \alpha_d^* \mu (K_1 (1 - \tau_d) - y_1) \psi \chi_3}{\Pi \mu G_3 K_1^3} \\
 &+ \frac{2v_3 w_6 w_7 (1 - \phi) \alpha_d^* \mu (K_1 (1 - \tau_d) - y_1) \psi \chi_4}{\Pi \mu G_3 K_1^3} \\
 &- \frac{2v_3 w_6 (1 - \phi) \alpha_d^* y_1 \mu}{\Pi K_1^2} (\chi_5 w_6 + \chi_6 w_7) \\
 &- \frac{2v_3 w_6^2 (1 - \phi) \alpha_d^* y_1 \mu}{\Pi K_1} - \frac{2v_3 w_6 w_7 (1 - \phi) \alpha_d^* y_1 \mu}{\Pi K_1} + \\
 &\frac{2v_4 w_6 w_7 (1 - \phi) \zeta \alpha_o \mu G_6}{\Pi (K_6 - \gamma_d) K_1} - \\
 &\frac{2v_3 w_6 (1 - \phi) \alpha_d^* y_1 \mu}{\Pi K_1^2 K_7} (\chi_7 w_6 + \chi_8 w_7) \\
 &- \frac{2v_3 w_6 (1 - \phi) \alpha_d^* y_1 \mu}{\Pi \mu K_1^2 K_7} (\chi_9 w_6 + \chi_{10} w_7) \\
 &- \frac{2v_3 w_6 (1 - \phi) \alpha_d^* y_1 \mu}{\Pi \mu K_1^2 K_7} (\chi_7 K_8 w_6 + \chi_{11} w_7) \\
 &+ \frac{2v_4 w_7 (1 - \phi) \alpha_o \mu (K_1 - y_2)}{\Pi K_1^2 K_4} (\chi_1 w_6 + \chi_2 w_7) \\
 &+ \frac{2v_4 w_6 w_7 (1 - \phi) \alpha_o \mu (K_1 (1 - \tau_o) - y_2) \psi \chi_3}{\Pi \mu G_3 K_1^3} \\
 &+ \frac{2v_4 w_7^2 (1 - \phi) \alpha_o \mu (K_1 (1 - \tau_o) - y_2) \psi \chi_4}{\Pi \mu G_3 K_1^3} - \\
 &- \frac{2v_4 w_7 (1 - \phi) \alpha_o y_2 \mu}{\Pi K_1^2} (\chi_5 w_6 + \chi_6 w_7) \\
 &- \frac{2v_4 w_6 w_7 (1 - \phi) \alpha_o y_2 \mu}{\Pi K_1} - \frac{2v_4 w_7^2 (1 - \phi) \alpha_o y_2 \mu}{\Pi K_1} - \\
 &\frac{2v_3 w_6 w_7 (1 - \phi) \zeta \alpha_o \mu G_5}{\Pi (K_5 - \gamma_d) K_1} - \\
 &\frac{2v_4 w_7 (1 - \phi) \alpha_o y_2 \mu}{\Pi K_1^2 K_7} (\chi_7 w_6 + \chi_2 w_8) \\
 &- \frac{2v_4 w_7 (1 - \phi) \alpha_o y_2 \mu}{\Pi \mu K_1^2 K_7} (\chi_9 w_6 + \chi_{10} w_7) \\
 &- \frac{2v_4 w_7 (1 - \phi) \alpha_o y_2 \mu}{\Pi \mu K_1^2 K_7} (\chi_7 K_8 w_6 + \chi_{11} w_7) \\
 &+ \frac{2v_3 w_6 (1 - \phi) \epsilon_1 \alpha_d^* \mu G_5}{\Pi (K_5 - \gamma_d) \mu K_1^2 K_7} (\chi_9 w_6 + \chi_9 w_7) \\
 &+ \frac{2v_4 w_7 (1 - \phi) \epsilon_2 \alpha_o \mu G_6}{\Pi (K_6 - \gamma_d) \mu K_1^2 K_7} (\chi_9 w_6 + \chi_{10} w_7) \\
 &+ \frac{2v_4 w_7 (1 - \phi) \epsilon_2 \alpha_o \mu G_6}{\Pi (K_6 - \gamma_d) \mu K_1^2 K_7} (\chi_7 K_8 w_6 + \chi_{11} w_7).
 \end{aligned}
 \tag{41}$$

$$\begin{aligned}\chi_1 &= \frac{G_1 \omega \sigma_d - (1 - \phi) \alpha_d^* \mu G_3}{K_2 - \gamma_d}, \\ \chi_2 &= \frac{G_2 \omega \sigma_o - (1 - \phi) \alpha_o \mu G_4}{K_3 - \gamma_o}, \\ \chi_3 &= (G_1 \omega \sigma_d - (1 - \phi) \alpha_d^* \mu G_3) \\ &\quad - (1 - \phi) (1 - \tau_d) \alpha_d^* G_3 K_1, \\ \chi_4 &= (G_2 \omega \sigma_o - (1 - \phi) \alpha_o \mu G_4) \\ &\quad - (1 - \phi) (1 - \tau_o) \alpha_o G_4 K_1, \\ \chi_5 &= \frac{(G_3 + (K_2 - \gamma_d) \sigma_d) G_1 w_6}{(K_2 - \gamma_d) G_3}, \\ \chi_6 &= \frac{(G_4 + (K_3 - \gamma_o) \sigma_o) G_2}{(K_3 - \gamma_o) G_4}, \\ \chi_7 &= \frac{G_1 \kappa \sigma_d + G_3 \theta_d K_1}{G_3}, \\ \chi_8 &= \frac{G_2 \kappa \sigma_o + G_4 \theta_o K_1}{G_4}, \\ \chi_9 &= \frac{(G_1 \kappa \sigma_d + G_3 \theta_d K_1) f \eta_h + \eta_d G_3 K_1 K_7}{G_3}, \\ \chi_{10} &= \frac{(G_2 \kappa \sigma_o + G_4 \theta_o K_1) f \eta_h}{G_4}, \\ \chi_{11} &= \frac{(G_2 \kappa \sigma_o + G_4 \theta_o K_1) K_8 + \eta_o G_4 K_1 K_7}{G_4}.\end{aligned}$$

where

$$\begin{aligned}G_1 &= (1 - \phi) \alpha_d^* y_1 - K_1 K_5, & G_2 &= (1 - \phi) \alpha_o y_2 - K_1 K_6, \\ G_3 &= (K_2 - \gamma_d) K_4, & G_4 &= (K_3 - \gamma_o) K_4, \\ G_5 &= (1 - \phi) \alpha_d^* y_1 - K_1 K_2, & \text{and } G_6 &= (1 - \phi) \alpha_o y_2 - K_1 K_3.\end{aligned}$$

$$b = \sum_{k,i=1}^n v_k w_i \frac{\partial^2 f_k}{\partial u_i \partial \alpha_d^*} (\Delta_0)$$

$$b = \frac{v_3 w_6 (1 - \phi) y_1}{K_1} > 0 \quad (42)$$

Therefore, based on Theorem 5 in Castillo-Chavez and Song (2004), with a positive bifurcation coefficient b and a positive coefficient for a , the COVID-19 model demonstrates a backward bifurcation occurring at $\mathcal{R}_0^{vd} = 1$ whenever $a > 0$ (Figs. 2, 3). \square

Global stability of the disease-free equilibrium: special case

Several factors known to contribute to backward bifurcation in epidemiological models include imperfect vaccines,

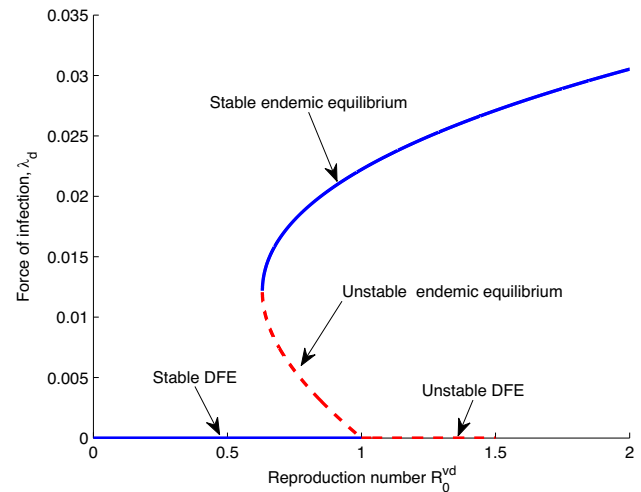


Fig. 2 Bifurcation diagram of the Delta variant dominance equilibrium, parameter values used are $\tau_d = 0.05$, $\alpha_d = 0.75$, $\gamma_d = 0.7$, $\varepsilon_1 = 0.7$ and other parameters are as in Table 3

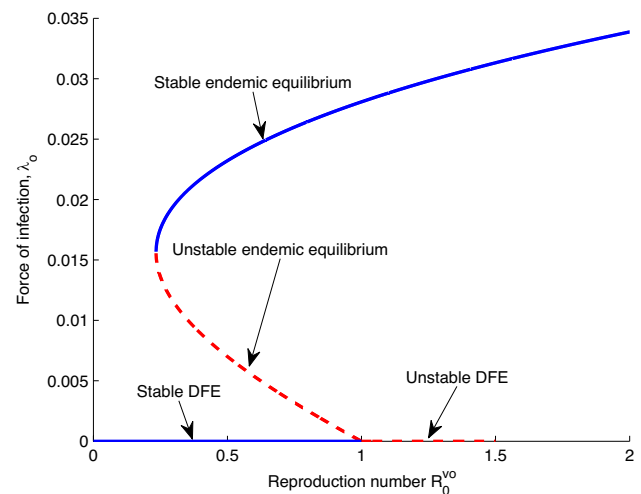


Fig. 3 Bifurcation diagram of the Omicron variant dominance equilibrium, parameter values used are $\tau_o = 0.1$, $\theta_o = 0.1$, $\varepsilon_3 = 0.8$ and other parameters are as in Table 3

secondary infections, and re-infections (as discussed in, for example, Omede et al. 2023; Gumel et al. 2018; Gumel 2012; Omame et al. 2018; Anguelov et al. 2014; Yaagoub 2024; Naim et al. 2024; Feng et al. 2014). Thus, we aim to explore conditions under which the backward bifurcation property can be eliminated from the COVID-19 model (1). Consequently, we examine a specific scenario in which the COVID-19 model (1) is simplified by assuming perfect vaccines and the absence of secondary infections and reinfections (i.e., $\tau_d = \tau_o = 1$, and $\varepsilon_1 = \varepsilon_2 = \varepsilon_3 = \zeta = 0$). The following results are proposed:

Theorem 5 *Considering the special case of the COVID-19 model (1) with $\tau_d = \tau_o = 1$, and $\varepsilon_1 = \varepsilon_2 = \varepsilon_3 = \zeta = 0$. The disease-free equilibrium (Δ_0) of the COVID-19 model (1) is globally asymptotically stable in \mathcal{D} whenever $\mathcal{R}_0^{vd*} \leq 1$ (i.e., $\mathcal{R}_0^{vd*} \leq 1$ and $\mathcal{R}_0^{vo*} \leq 1$)*

Proof We examine the following Lyapunov function:

$$\mathcal{C} = \gamma_d E_d + \gamma_o E_o + K_2 I_d + K_3 I_o. \tag{43}$$

where $K_1 = \psi + \mu$, $K_2 = \gamma_d + \sigma_d + \mu$, $K_3 = \gamma_o + \sigma_o + \mu$, $K_4 = \kappa + \omega + \mu$, $K_5 = \theta_d + \delta_d + \eta_d + \mu$, $K_6 = \theta_o + \delta_o + \eta_o + \mu$, $K_7 = \eta_h + \delta_h + \mu$, and $K_8 = (1 - f)\eta_p$ with Lyapunov derivatives (where a dot denotes differentiation with respect to time)

$$\begin{aligned} \dot{\mathcal{C}} &= \gamma_d \dot{E}_d + \gamma_o \dot{E}_o + K_2 \dot{I}_d + K_3 \dot{I}_o, \\ \dot{\mathcal{C}} &= \gamma_d \left(\frac{(1 - \phi)\alpha_d I_d S}{N} - K_2 E_d \right) \\ &\quad + \gamma_o \left(\frac{(1 - \phi)\alpha_o I_o S}{N} - K_3 E_o \right) \\ &\quad + K_2 (\gamma_d E_d - K_5 I_d) + K_3 (\gamma_o E_o - K_6 I_o), \\ \dot{\mathcal{C}} &= \frac{(1 - \phi)\alpha_d \gamma_d I_d S}{N} + \frac{(1 - \phi)\alpha_o \gamma_o I_o S}{N} \\ &\quad - K_2 K_5 I_d - K_3 K_6 I_o. \end{aligned} \tag{44}$$

It's important to note that $S(t) \leq N(t)$ holds within the feasible region \mathcal{D} for all $t > 0$,

$$\begin{aligned} \dot{\mathcal{C}} &\leq I_d \left(\frac{(1 - \phi)\alpha_d \gamma_d \mu}{\psi + \mu} - K_2 K_5 \right) + \\ &\quad I_o \left(\frac{(1 - \phi)\alpha_o \gamma_o \mu}{\psi + \mu} - K_3 K_6 \right), \\ \dot{\mathcal{C}} &\leq K_2 K_5 I_d \left(\frac{(1 - \phi)\alpha_d \gamma_d \mu}{(\psi + \mu) K_2 K_5} - 1 \right) + \\ &\quad K_3 K_6 I_o \left(\frac{(1 - \phi)\alpha_o \gamma_o \mu}{(\psi + \mu) K_3 K_6} - 1 \right) \\ \dot{\mathcal{C}} &= K_2 K_5 I_d (\mathcal{R}_0^{vd*} - 1) + K_3 K_6 I_o (\mathcal{R}_0^{vo*} - 1) \leq 0 \end{aligned} \tag{45}$$

Hence, since all the COVID-19 model parameters are non-negative, it follows that $\dot{\mathcal{C}} \leq 0$ for $\mathcal{R}_0^{vd*} \leq 1$ (i.e., $\mathcal{R}_0^{vd*} \leq 1$ and $\mathcal{R}_0^{vo*} \leq 1$) with $\dot{\mathcal{C}} = 0$ if and only if $I_d = I_o = 0$. Therefore, \mathcal{C} serves as a Lyapunov function on \mathcal{D} . Hence, according to LaSalle's invariance principle (La 1976), every solution to the COVID-19 model (1), starting from initial conditions within \mathcal{D} , converges to the COVID-19 disease-free equilibrium point (Δ_0) as $t \rightarrow \infty$. \square

Therefore, the significance of the aforementioned findings in epidemiology lies in the fact that $\mathcal{R}_0^{vd*} \leq 1$ serves as both a necessary and sufficient condition for eradicating

COVID-19 infection from the population. This means that any slight perturbation within the system not only leads to a temporary return to the disease-free state (local stability) but also ensures that the entire system trajectory ultimately converges to the disease-free equilibrium over time, regardless of the initial conditions. Furthermore, achieving global asymptotic stability indicates robust and sustainable disease control, offering the possibility of long-term eradication without the threat of recurrent outbreaks.

Results

Herd immunity threshold

Herd immunity, a fundamental concept in public health, indicates that when a substantial portion of a population becomes immune to a particular disease, such as coronavirus, it provides collective protection to the entire community, preventing widespread outbreaks. This immunity can arise through vaccination or prior infection, leading to the development of protective antibodies that reduce the risk of future infections. Essentially, it's like creating a protective shield around the community by ensuring enough people are immune, making it difficult for the disease to spread rampantly (Gumel et al. 2021; Iboi et al. 2020; Patel et al. 2022). Herd immunity might not effectively hold against new or mutated variants of the original virus. These new strains can sometimes evade the immune system's defenses established through prior infection or vaccination. When the virus mutates significantly, it can potentially render the existing immunity less effective, leading to breakthrough infections or re-infections among individuals who were previously immune to the earlier strain.

Given that vaccinated individuals can still get infected, it's important to determine the essential percentage (known as the critical proportion) of vaccinated individuals needed to eliminate COVID-19 when the vaccine is consistently used despite its imperfections.

Recall that the COVID-19 basic reproduction number for the Delta and Omicron variants of COVID-19 in the presence of vaccination is given as

$$\begin{aligned} \mathcal{R}_0^{vd} &= \frac{(1 - \phi)\alpha_d (\mu + (1 - \tau_d)\psi)\gamma_d}{(\psi + \mu)(\gamma_d + \sigma_d + \mu)(\theta_d + \delta_d + \eta_d + \mu)}, \text{ and} \\ \mathcal{R}_0^{vo} &= \frac{(1 - \phi)\alpha_o (\mu + (1 - \tau_o)\psi)\gamma_o}{(\psi + \mu)(\gamma_o + \sigma_o + \mu)(\theta_o + \delta_o + \eta_o + \mu)}. \end{aligned}$$

It's noticeable that the basic reproduction numbers decline as the vaccination rate (ψ) increases. Therefore, higher vaccination rates lead to smaller reproduction numbers.

We have that

$$\begin{aligned} \lim_{\psi \rightarrow \infty} \mathcal{R}_0^{vd}(\psi) &= (1 - \tau_d)\mathcal{R}_0^d, \text{ and} \\ \lim_{\psi \rightarrow \infty} \mathcal{R}_0^{vo}(\psi) &= (1 - \tau_o)\mathcal{R}_0^o \end{aligned} \tag{46}$$

The proportion of vaccinated individuals in the population at the disease-free equilibrium (Δ_0) is given by

$$\mathcal{P}_v = \frac{V^*}{N^*} = \frac{\psi}{\psi + \mu} \tag{47}$$

The herd immunity threshold is determined by solving for \mathcal{P}_v in $\mathcal{R}_0^{vd} = 1$ and $\mathcal{R}_0^{vo} = 1$. Thus, we have that

$$\mathcal{P}_v^d = \frac{1}{\tau_d} \left(1 - \frac{1}{\mathcal{R}_0^d} \right), \text{ and } \mathcal{P}_v^o = \frac{1}{\tau_o} \left(1 - \frac{1}{\mathcal{R}_0^o} \right) \tag{48}$$

The formulas \mathcal{P}_v^d and \mathcal{P}_v^o mentioned above extends the critical vaccination threshold to account for imperfect vaccines. When the vaccine is flawless (that is, when $\tau_d = \tau_o = 1$), it results in the usual formula for critical vaccination threshold applicable to flawless vaccines (Martcheva 2015).

To project the herd immunity threshold for the United States, we calculated the Omicron variant basic reproduction number (\mathcal{R}_0^o) using Eq. (11) with the parameters outlined in Table 3. This computation yielded $\mathcal{R}_0^o = 2.4136$. By substituting this value into Eq. (48), we determined that the herd immunity threshold for the United States stands at approximately 97.67%. Biologically, this implies that to eradicate COVID-19 within the population, assuming a COVID-19 vaccine provides 60% protection against the Omicron variant, a vaccination rate of at least 97.67% among the susceptible population in the United States is necessary to achieve the herd immunity threshold. It's worth emphasizing that our calculation specifically targeted the herd immunity threshold for the Omicron variant due to our model's data fitting occurring during the emergence of Omicron in the United States, where it surpassed the Delta variant to become the dominant variant.

Sensitivity analysis

In this section, we'll perform a sensitivity analysis on the key parameters contributing to the basic reproduction number for both the Delta and Omicron variants of the COVID-19 model. The aim of this analysis is to assess the impact of each parameter on the transmission dynamics of these variants. To achieve this, we'll adopt the methodology delineated in Oguntolu et al. (2024). Following the procedure

outlined in Oguntolu et al. (2024), we'll employ the normalized forward sensitivity index for a variable, represented by 'u', which variably depends on the parameter, denoted as 'x'. This sensitivity index is defined as:

$$\mathcal{F}_x^u = \frac{\partial u}{\partial x} \times \frac{x}{u}. \tag{49}$$

Therefore, the sensitivity index of the basic reproduction number for the Delta and Omicron variants with respect to the parameter 'x' is expressed as:

$$\begin{aligned} \mathcal{F}_x^{\mathcal{R}_0^{vd}} &= \frac{\partial \mathcal{R}_0^{vd}}{\partial x} \times \frac{x}{\mathcal{R}_0^{vd}}, \text{ and} \\ \mathcal{F}_x^{\mathcal{R}_0^{vo}} &= \frac{\partial \mathcal{R}_0^{vo}}{\partial x} \times \frac{x}{\mathcal{R}_0^{vo}}. \end{aligned} \tag{50}$$

We initiate by computing the sensitivity indices of the basic parameters for the Delta variant, utilizing the parameter values detailed in Table 3.

$$\begin{aligned} \mathcal{F}_{\alpha_d}^{\mathcal{R}_0^{vd}} &= \frac{(1 - \phi)(\mu + (1 - \tau_d)\psi)\gamma_d}{(\psi + \mu)(\gamma_d + \sigma_d + \mu)(\theta_d + \delta_d + \eta_d + \mu)} \\ &\quad \times \frac{\alpha_d(\psi + \mu)(\gamma_d + \sigma_d + \mu)(\theta_d + \delta_d + \eta_d + \mu)}{(1 - \phi)\alpha_d(\mu + (1 - \tau_d)\psi)\gamma_d}. \\ \mathcal{F}_{\alpha_d}^{\mathcal{R}_0^{vd}} &= 1, \\ \mathcal{F}_{\phi}^{\mathcal{R}_0^{vd}} &= -\frac{\phi}{1 - \phi} = -0.4286, \\ \mathcal{F}_{\tau_d}^{\mathcal{R}_0^{vd}} &= -\frac{\tau_d\psi}{\mu + (1 - \tau_d)\psi} = -1.8324, \\ \mathcal{F}_{\psi}^{\mathcal{R}_0^{vd}} &= -\frac{\mu\psi\tau_d}{(\psi + \mu)(\mu + (1 - \tau_d)\psi)} = -0.4853, \\ \mathcal{F}_{\gamma_d}^{\mathcal{R}_0^{vd}} &= \frac{\sigma_d + \mu}{\gamma_d + \sigma_d + \mu} = 0.3907 \\ \mathcal{F}_{\sigma_d}^{\mathcal{R}_0^{vd}} &= -\frac{\sigma_d}{\gamma_d + \sigma_d + \mu} = -0.3676, \\ \mathcal{F}_{\theta_d}^{\mathcal{R}_0^{vd}} &= -\frac{\theta_d}{\theta_d + \delta_d + \eta_d + \mu} = -0.3771, \\ \mathcal{F}_{\delta_d}^{\mathcal{R}_0^{vd}} &= -\frac{\delta_d}{\theta_d + \delta_d + \eta_d + \mu} = -0.0566, \\ \mathcal{F}_{\eta_d}^{\mathcal{R}_0^{vd}} &= -\frac{\eta_d}{\theta_d + \delta_d + \eta_d + \mu} = -0.5387, \\ \mathcal{F}_{\mu}^{\mathcal{R}_0^{vd}} &= \frac{\mu}{\mu + (1 - \tau_d)\psi} - \frac{\mu}{\psi + \mu} \\ &\quad - \frac{\mu}{\gamma_d + \sigma_d + \mu} - \frac{\mu}{\theta_d + \delta_d + \eta_d + \mu} = 0.4345. \end{aligned} \tag{51}$$

Since the basic reproduction number for the Delta variant is symmetrical to the Omicron variant, we have that

$$\begin{aligned}
 \mathcal{F}_{\alpha_o}^{oo} &= 1, \\
 \mathcal{F}_{\phi}^{oo} &= -\frac{\phi}{1-\phi} = -0.4286, \\
 \mathcal{F}_{\tau_o}^{oo} &= -\frac{\tau_o\psi}{\mu + (1-\tau_o)\psi} = -1.1897, \\
 \mathcal{F}_{\psi}^{oo} &= -\frac{\mu\psi\tau_o}{(\psi + \mu)(\mu + (1-\tau_o)\psi)} = -0.3151, \\
 \mathcal{F}_{\gamma_o}^{oo} &= \frac{\sigma_o + \mu}{\gamma_o + \sigma_o + \mu} = 0.1941, \\
 \mathcal{F}_{\sigma_o}^{oo} &= -\frac{\sigma_o}{\gamma_o + \sigma_o + \mu} = -0.1826, \\
 \mathcal{F}_{\theta_o}^{oo} &= -\frac{\theta_o}{\theta_o + \delta_o + \eta_o + \mu} = -0.7338, \\
 \mathcal{F}_{\delta_o}^{oo} &= -\frac{\delta_o}{\theta_o + \delta_o + \eta_o + \mu} = -0.0037, \\
 \mathcal{F}_{\eta_o}^{oo} &= -\frac{\eta_o}{\theta_o + \delta_o + \eta_o + \mu} = -0.2446, \\
 \mathcal{F}_{\mu}^{oo} &= \frac{\mu}{\mu + (1-\tau_o)\psi} - \frac{\mu}{\psi + \mu} \\
 &\quad - \frac{\mu}{\gamma_o + \sigma_o + \mu} - \frac{\mu}{\theta_o + \delta_o + \eta_o + \mu} = 0.42.
 \end{aligned}
 \tag{52}$$

Interpretation of the sensitivity indices

The bar charts illustrating the sensitivity indices for the basic reproduction numbers of the Delta and Omicron variants of COVID-19 are presented in Figs. 4 and 5, respectively. Parameters with positive indices in these charts exert a significant impact on accelerating the spread of the diseases. An elevation in the values of these parameters, while keeping others

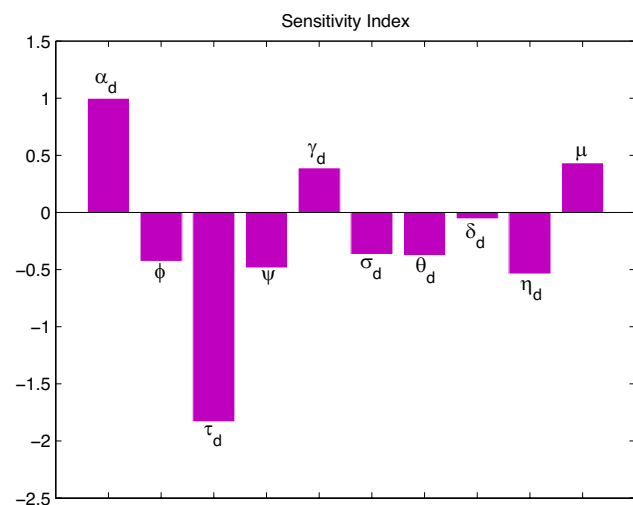


Fig. 4 Sensitivity index of the basic reproduction number of the Delta variant of COVID-19

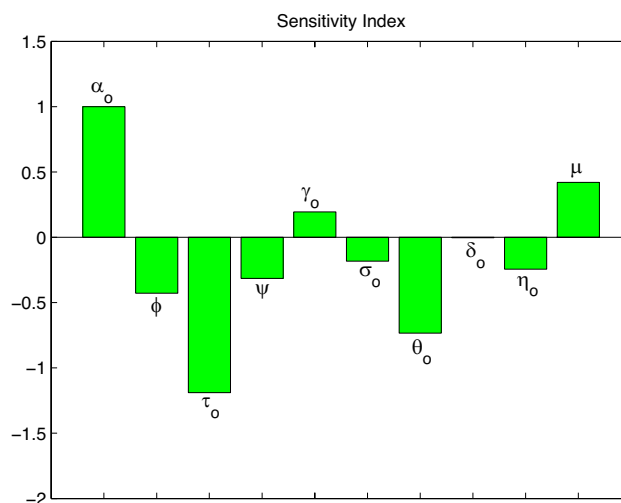


Fig. 5 Sensitivity index of the basic reproduction number of the Omicron variant of COVID-19

Table 3 Parameter values for the COVID-19 model (1)

Parameter	Value	Source
Π	0.056	Hamilton et al. (2024)
α_d	0.3	Fitted
α_o	0.68	Fitted
ψ	0.0203	Iboi et al. (2020)
τ_d	0.88	Estimated from Lauring et al. (2022)
τ_o	0.6	Estimated from Lauring et al. (2022)
ϕ	0.3	Estimated from Okuonghae and Oname (2020)
μ	0.007313	Estimated from Murphy et al. (2020)
δ_d	0.015	Okuonghae and Oname (2020)
δ_o	0.0015	Fitted
δ_h	0.001041	Fitted
ω	$\frac{1}{14}$	Ngonghala et al. (2020)
η_d	$\frac{1}{7}$	Omede et al. (2023)
η_o	$\frac{1}{10}$	Fitted
η_h	0.03	Fitted
θ_d	0.1	Fitted
θ_o	0.05	Fitted
ζ	0.51	Fitted
ϵ_1	0.05	Fitted
ϵ_2	0.4	Fitted
ϵ_3	0.25	Fitted
σ_d	0.1160	Ngonghala et al. (2020)
σ_o	0.1160	Ngonghala et al. (2020)
γ_d	$\frac{1}{5.2}$	Okuonghae and Oname (2020)
γ_o	0.512	Fitted
f	0.5	Fitted
κ	0.05	Fitted

constant, leads to an increase in the basic reproduction number. Conversely, parameters displaying negative indices contribute to mitigating the disease burdens; thus, an increase in their values results in a decrease in the basic reproduction numbers for both variants.

Numerical simulations

In this section, we carried out the numerical simulations of the COVID-19 model (1) using MATLAB software. The numerical simulations were conducted with the aim of providing a visual representation for some of the theoretical analysis previously discussed.

To validate the COVID-19 model, we fitted the COVID-19 model (1) to the daily confirmed cases of COVID-19 in the United States from December 20, 2021, to January 31, 2022. This time frame was selected to coincide with the emergence of the Omicron variant in the United States, with the goal of capturing the dynamics between the Delta and Omicron variants of COVID-19. The data fitting process was conducted using the fmincon algorithm in MATLAB, and the daily confirmed cases data were obtained from the World Health Organization (WHO) (World Health 2019). The estimated total population of the United States is approximately 336 million individuals. The initial values of the state variables used for data fitting purposes are as follows: $V(0) = 208,517,246$, $E_d(0) = 2,000,000$, $E_o = 1,500,000$, $Q(0) = 1,500$, $I_d(0) = 150,000$, $I_o(0) = 350,000$, $I_h(0) = 67,352$, $R_d(0) = 0$, and $R_o(0) = 0$. Thus,

$$S(0) = N - (V(0) + E_d(0) + E_o(0) + Q(0) + I_d(0) + I_o(0) + I_h(0) + R_d(0) + R_o(0)). \tag{53}$$

$$S(0) = 123413902.$$

It's important to highlight that the initial values used for vaccinated individuals were obtained from CDC (Centers for Disease 2024), reflecting the total number of individuals who completed the primary vaccination series as of December 20, 2021 (Table 4). The fitting of the COVID-19 model to the confirmed cases of COVID-19 in the United States is illustrated in Fig. 6. Additionally, our model forecasts the potential trajectory of COVID-19 cases in the United States for a 200-day period, as depicted in Fig. 7.

Utilizing the parameter values outlined in Table 3, the values of the basic reproduction numbers for the Delta and Omicron variants of COVID-19 are presented in Table 5.

We calculated the Omicron invasion reproduction number using the parameter values specified in Table 3, along with the initial conditions of the state variables employed in data fitting. The computed value for the invasion reproduction

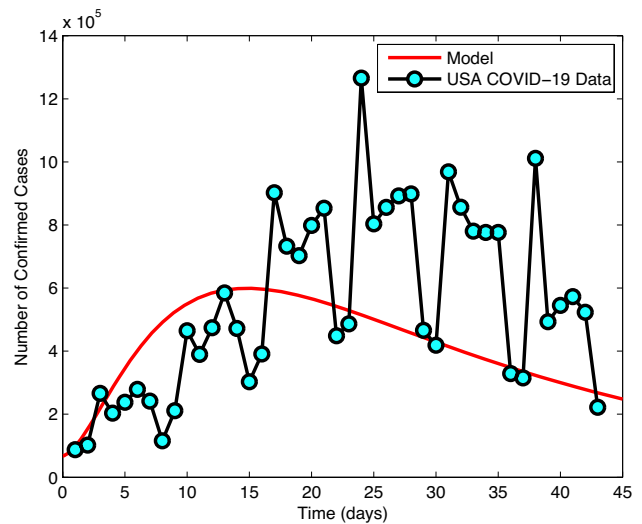


Fig. 6 Confirmed cases of COVID-19 from December 20, 2021 to January 31, 2022

Table 4 The daily confirmed cases of COVID-19 in the United State from December 20, 2021 to January 31, 2022

Day	Confirmed cases						
Dec 20	87,584	Jan 2	471,965	Jan 15	892,303	Jan 28	545,225
Dec 21	102,213	Jan 3	302,957	Jan 16	898,407	Jan 29	572,820
Dec 22	266,159	Jan 4	390,858	Jan 17	465,957	Jan 30	523,326
Dec 23	203,318	Jan 5	902,391	Jan 18	418,737	Jan 31	222,172
Dec 24	237,883	Jan 6	732,514	Jan 19	968,465		
Dec 25	278,812	Jan 7	702,790	Jan 20	856,293		
Dec 26	241,450	Jan 8	798,436	Jan 21	780,466		
Dec 27	115,824	Jan 9	852,951	Jan 22	776,490		
Dec 28	211,284	Jan 10	448,743	Jan 23	776,480		
Dec 29	464,495	Jan 11	486,541	Jan 24	328,564		
Dec 30	389,514	Jan 12	1,265,520	Jan 25	314,947		
Dec 31	474,309	Jan 13	803,539	Jan 26	1,011,148		
Jan 1	584,647	Jan 14	855,880	Jan 27	493,232		

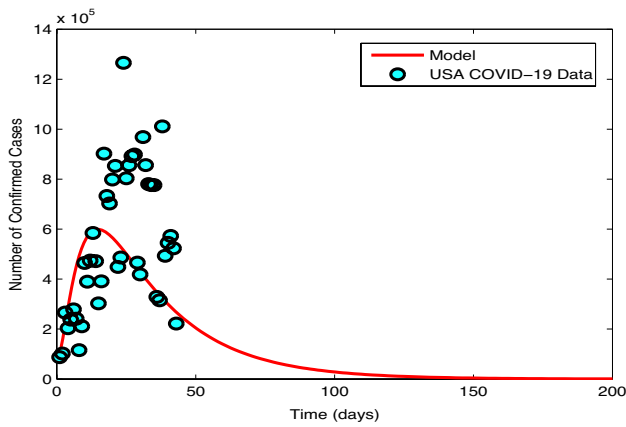


Fig. 7 Projection of the number of confirmed cases of COVID-19

Table 5 Values of the basic reproduction numbers of the Delta and Omicron variants of COVID-19 using parameter values in Table 3

Basic reproduction number	Value
\mathcal{R}_0^{vd}	0.1704
\mathcal{R}_0^d	0.4825
\mathcal{R}_0^{vd*}	0.1278
\mathcal{R}_0^{vo}	1.349
\mathcal{R}_0^o	2.4136
\mathcal{R}_0^{vo*}	0.6392

number is $\mathcal{R}_0^{o:d} = 1.4875$. Additionally, we conducted a study by varying the compliance rate to COVID-19 safety protocols (ϕ) and the efficacy of the vaccine against the Omicron variant (τ_o) to assess their impact on the invasion reproduction number. The resulting values of the invasion reproduction number for different scenarios are summarized in Tables 6 and 7.

Discussion

In this study, a deterministic mathematical model for the transmission dynamics of the Delta and Omicron variants of COVID-19 is presented and rigorously analyzed. We computed the basic reproduction number for both variants

Table 6 The effect of ϕ on Omicron invasion reproduction number

ϕ	0.1	0.3	0.5	0.7	0.9
Invasion reproduction number ($\mathcal{R}_0^{o:d}$)	1.9125	1.4875	1.0625	0.6375	0.2125

Table 7 The effect of τ_o on Omicron invasion reproduction number

τ_o	0.1	0.3	0.5	0.7	0.9
Invasion reproduction number ($\mathcal{R}_0^{o:d}$)	2.2370	1.9372	1.6374	1.3376	1.0378

using the next generation operator method. Our analysis proved that the disease-free equilibrium for the Delta and Omicron variants is locally asymptotically stable when their respective basic reproduction numbers are less than 1. Using center manifold theory, we observed that the COVID-19 model exhibits backward bifurcation, characterized by the coexistence of a stable disease-free equilibrium and a stable endemic equilibrium whenever the reproduction numbers for the Delta and Omicron variants are less than 1. Assuming perfect vaccine efficacy and no reinfection, the disease-free equilibrium for both variants is globally asymptotically stable whenever their basic reproduction numbers are below 1. We also computed the Omicron variant invasion reproduction number to determine how the Omicron variant invades the population and becomes the dominant strain. Sensitivity analysis on the basic reproduction numbers for both variants revealed that the key parameters driving the spread and expansion of these variants are the transmission rates (α_d and α_o), natural death rate (μ), and the progression rates from the exposed to infected compartments (γ_d and γ_o). Additionally, we calculated the necessary percentage of susceptible individuals that need to be vaccinated to achieve herd immunity. It was found that with a vaccine offering 60% protection, 97.67% of the susceptible population would need to be vaccinated against the Omicron variant. We carried out the numerical simulations of our model and fitted it to the daily cumulative cases of COVID-19 in the United States. Figure 8a and b depicts the surface plots of the basic reproduction number for the Delta and Omicron variants of COVID-19 (\mathcal{R}_0^{vd} and \mathcal{R}_0^{od}) as function of the detection rates (θ_d and θ_o) and the efficacy of vaccine against the variants of COVID-19 (τ_d and τ_o), it is observed that an increase in the detection rates (θ_d and θ_o) and the efficacy of vaccine (τ_d and τ_o) will significantly reduce the basic reproduction numbers (\mathcal{R}_0^{vd} and \mathcal{R}_0^{od}). This outcome aligns seamlessly with the results from the sensitivity analysis.

Fig. 9a and b is the surface plots of the Delta and Omicron variants basic reproduction number (\mathcal{R}_0^{vd} and \mathcal{R}_0^{od}) as a function of the compliance rate to COVID-19 Safety protocols (ϕ) and efficacy rate of vaccine to Delta variant (τ_d) and Omicron variant (τ_o) respectively. Figure 9a and b reveals that by enhancing the compliance rate to COVID-19 safety protocols to approximately 50% and achieving perfect efficacy in vaccines against the Delta and Omicron variants, the

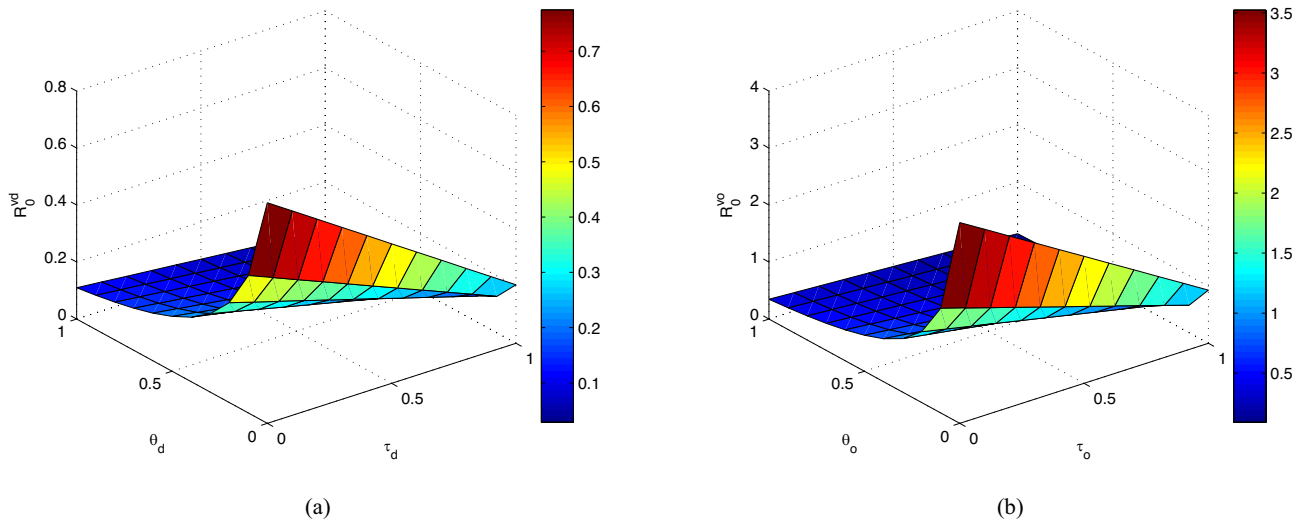


Fig. 8 Surface plots of (a) the Delta variant basic reproduction number as a function of the efficacy rate of vaccine to Delta variant (τ_d) and the detection rate of Delta variant via testing (θ_d). (b) The Omicron variant basic reproduction number as a function of the efficacy rate of vaccine to Omicron variant (τ_o) and the detection rate of Omicron variant via testing (θ_o)

(repeated from above)

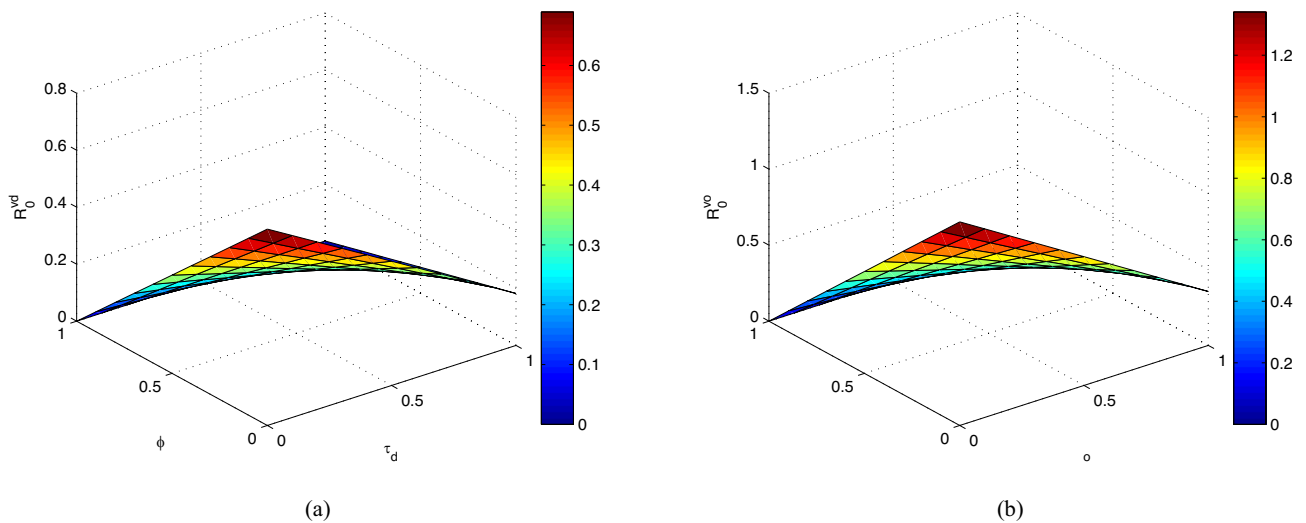


Fig. 9 Surface plots of (a) the Delta variant basic reproduction number as a function of the efficacy rate of vaccine to Delta variant (τ_d) and the compliance rate to COVID-19 safety protocols(ϕ). (b) The Omicron variant basic reproduction number as a function of the efficacy rate of vaccine to Omicron variant (τ_o) and the compliance rate to COVID-19 safety protocols (ϕ)

(repeated from above)

basic reproduction numbers for these variants can be notably reduced, potentially reaching levels below 0.2 and 0.4, respectively. Figure 10a and b depicts the surface plots of the Delta and Omicron variants basic reproduction number (R_0^{vd} and R_0^{vo}) as a function of the vaccination rate (ψ) and the detection rate of the Delta variant (θ_d) and detection rate of Omicron variant (θ_o) via testing respectively. In Fig. 10a and b, it is observed that a decrease in the vaccination rate (ψ) and a reduction in the detection rate of individuals infected with the Delta and Omicron variants (θ_d and θ_o) correspond to an increase in the basic reproduction numbers of both

variants. This observation aligns seamlessly with the conclusions drawn from the sensitivity analysis. Figure 11 is the surface plot of the Omicron variant basic reproduction number (R_0^{vo}) as a function of the vaccination rate (ψ) and the compliance rate to COVID-19 safety protocol (ϕ). Figure 11 illustrates that by elevating both the vaccination rate (ψ) and the compliance rate to COVID-19 safety protocols beyond 50%, the basic reproduction number of the Omicron variant can be reduced to below one.

Figure 12 illustrates the simulations of the effect of the vaccination rate (ψ) on the infected individuals with Delta

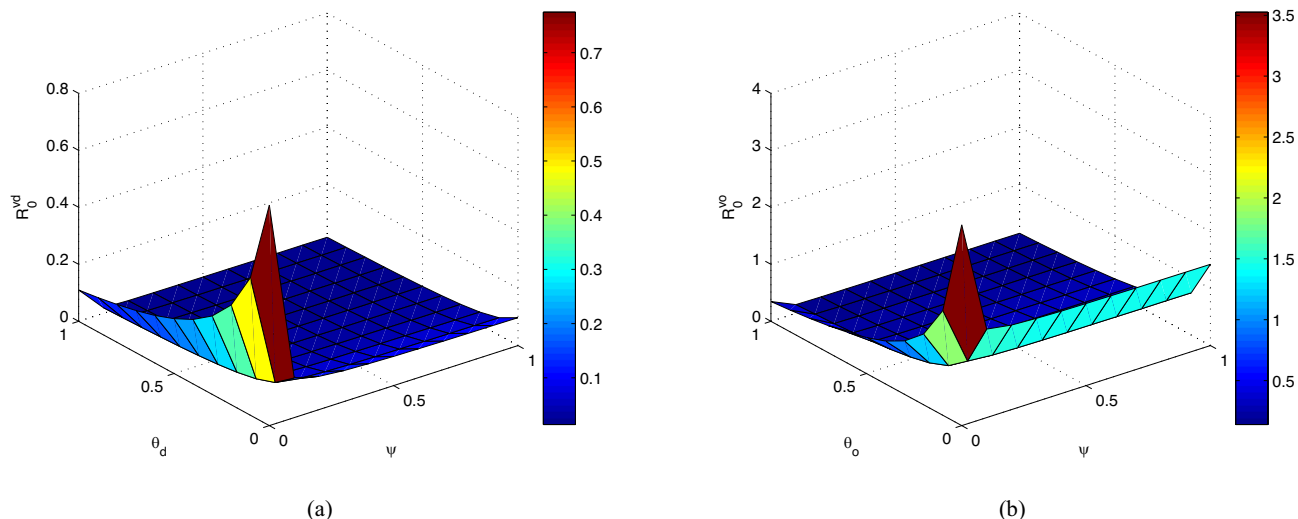


Fig. 10 Surface plots of (a) the Delta variant basic reproduction number as a function of the vaccination rate (ψ) and the detection rate of Delta variant via testing (θ_d). (b) The Omicron variant basic

reproduction number as a function of the vaccination rate (ψ) and the detection rate of Omicron variant via testing (θ_o)

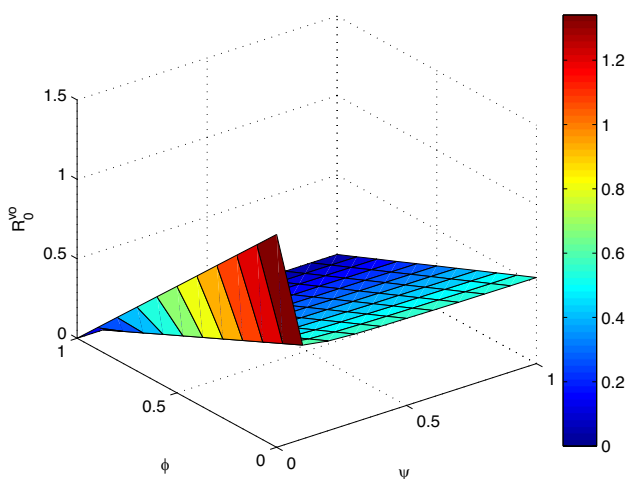


Fig. 11 Surface plot of the Omicron variant basic reproduction number as a function of the vaccination rate (ψ) and the compliance rate to COVID-19 safety protocols (ϕ)

variant of COVID-19, Omicron variant of COVID-19, and hospitalized individuals respectively. In Fig. 12a, it was observed that an increase in the vaccination rate decreases the number of individuals infected with Delta variant of COVID-19, furthermore, it was observed that if the vaccination rate can be stepped up to 70%, the number of infected individuals with Delta variant of COVID-19 can be reduced to be below 100,000 within 15 days. Similar results is observed in Fig. 12b for the infected individuals with Omicron variant of COVID-19. In Fig. 12c, it was observed that when the vaccination rate is stepped up to 70%, the peak

value of the number of hospitalized individuals decreases from 2.8 million to 2 million.

Fig. 13 illustrates the simulations of the effect of the compliance rate to COVID-19 safety protocols (Usage of face mask and hand sanitizer) (ϕ) on the infected individuals with Delta variant of COVID-19, Omicron variant of COVID-19, and hospitalized individuals respectively. In Fig. 13a and b, it is observed that if the compliance rate of COVID-19 safety protocols can be stepped up to about 50%, the number of infected individuals with Delta and Omicron variants of COVID-19 will be reduced below 200,000 individuals within 20 days. In Fig. 13c, if the compliance rate to COVID-19 safety protocols is stepped up to 70%, it is observed that the number of hospitalized individuals will be reduced to below 1 million in 45 days.

Figure 14 is the simulations of the effect of the efficacy rate of vaccine to Omicron variant of COVID-19 (τ_o) on the infected individuals with Omicron variant of COVID-19 and the hospitalized individuals. It is shown that an increase in the efficacy rate of vaccine to Omicron variant (τ_o) significantly reduces the number of individuals infected with the Omicron variant of COVID-19 as well as the hospitalized individuals. Figure 15 illustrates the simulations of the effect of the efficacy rate of vaccine to Delta variant of COVID-19 (τ_d) on the infected individuals with Delta variant of COVID-19 and the hospitalized individuals. Unlike the results in Fig. 14, it was observed that an increase in the efficacy rate of the vaccine to Delta variant of COVID-19 (τ_d) has minimal effect in decreasing the number of infected individuals with delta variant as well as the hospitalized individuals.

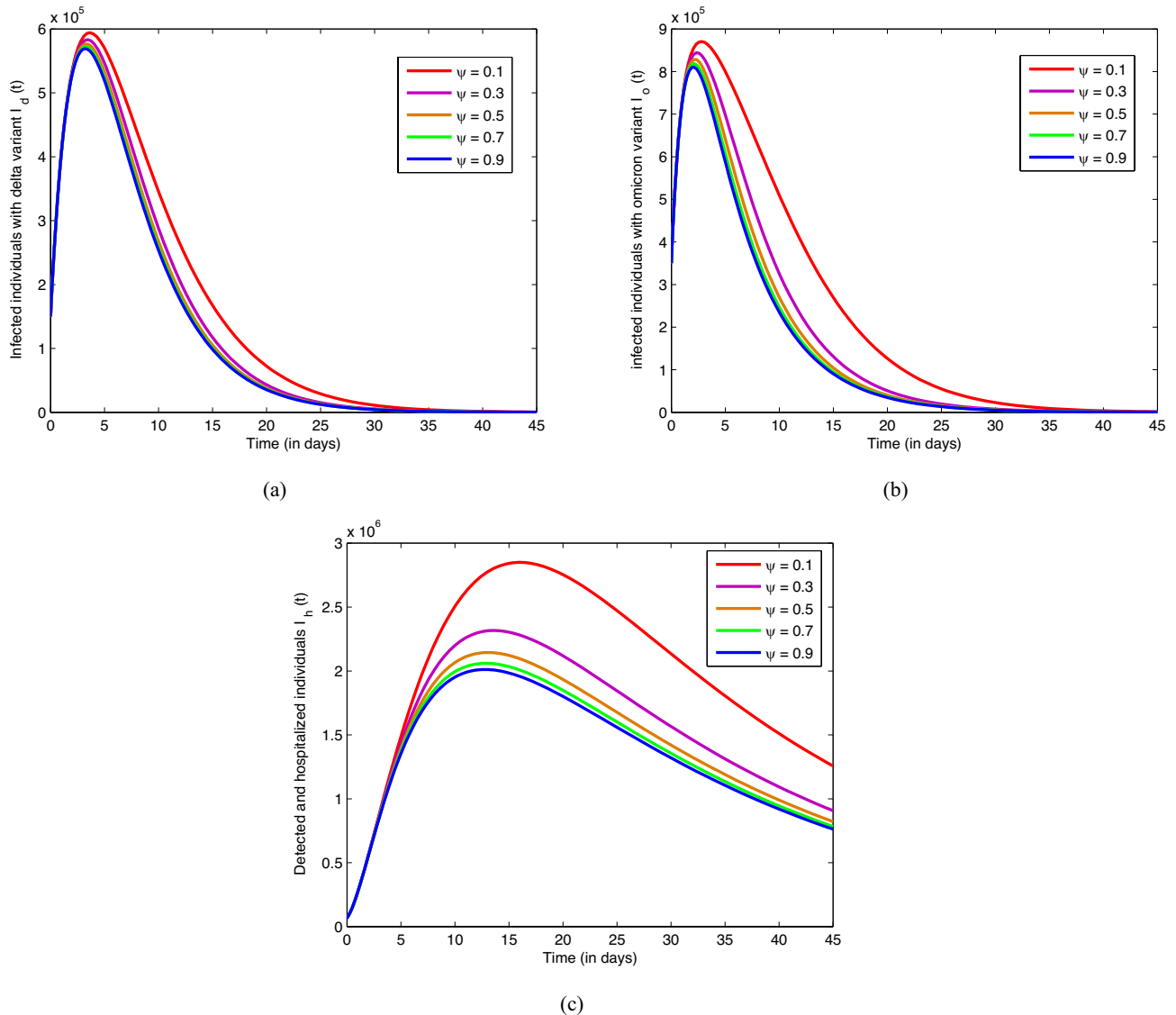


Fig. 12 The effect of the vaccinated rate (ψ) on **(a)** infected individuals with Delta variant of COVID-19 $I_d(t)$, **(b)** infected individuals with Omicron variant of COVID-19 $I_o(t)$, **(c)** detected and hospitalized individuals $I_h(t)$

Figures 16a, b, and 17a demonstrates that in scenarios where vaccination is implemented and the vaccine efficacy against both the Delta and Omicron variants of COVID-19 is perfect, the number of infected individuals drastically decreases in comparison to scenarios without vaccination within the population. Correspondingly, in Figs. 16c and 17b, it is evident that elevating the vaccination rate to approximately 50% and achieving perfect efficacy in vaccines against the Delta and Omicron variants leads to a significant decrease in the number of hospitalized individuals.

Conclusion

This paper presents a deterministic mathematical model designed to explore the transmission dynamics of the Delta and Omicron variants of COVID-19, considering reinfection and imperfect vaccination. The detailed examination of this model reveals that both the Delta and Omicron variants exhibit the "backward bifurcation" phenomenon when their basic reproduction number drops below one. This distinct characteristic poses significant challenges in effectively managing COVID-19 within the population.

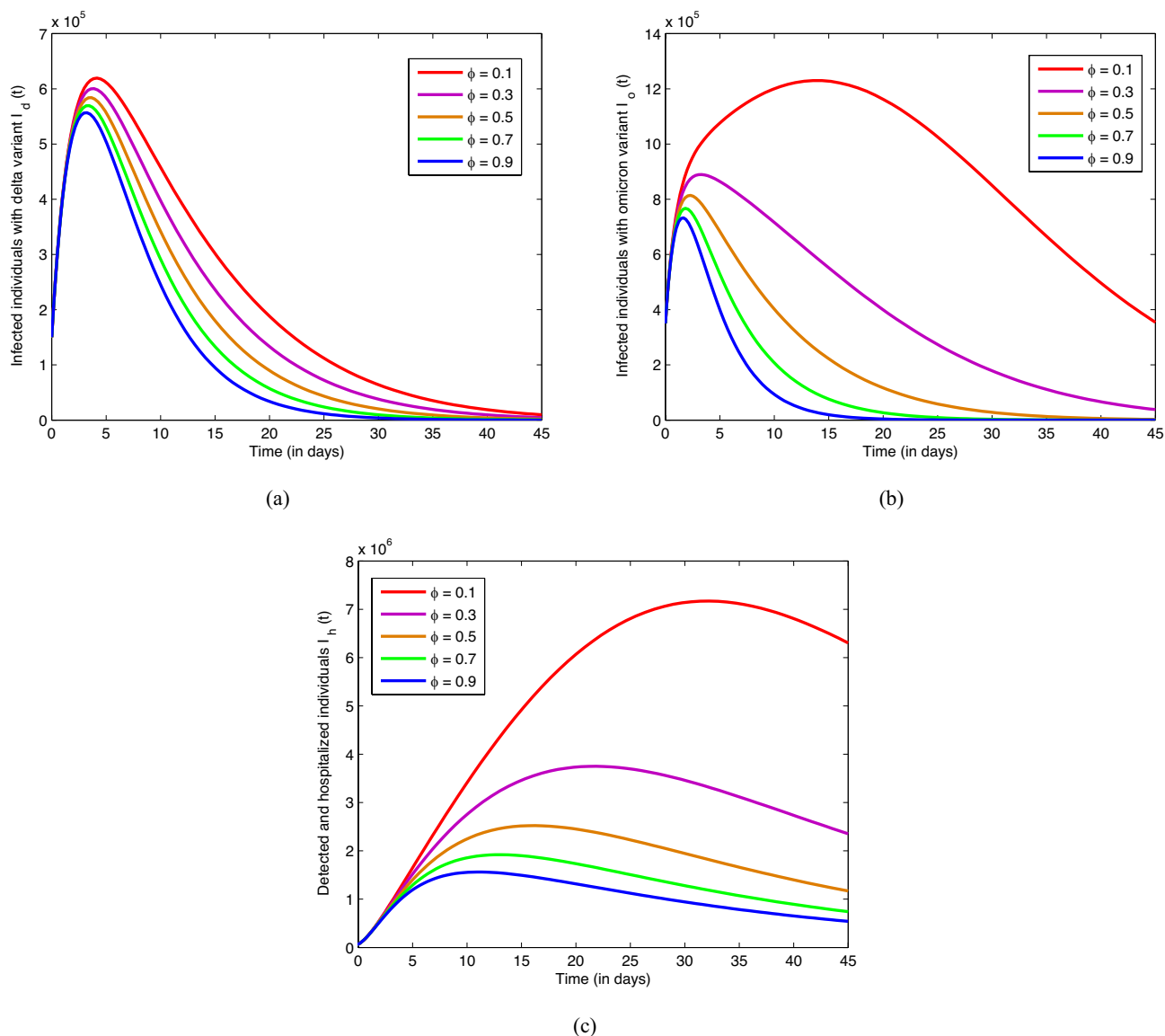


Fig. 13 The effect of the compliance rate to COVID-19 safety protocols (ϕ) on (a) infected individuals with Delta variant of COVID-19 $I_d(t)$, (b) infected individuals with Omicron variant of COVID-19 $I_o(t)$, (c) detected and hospitalized individuals $I_h(t)$

However, under the assumption of perfect vaccine efficacy and no reinfection, these variants have a globally asymptotically stable disease-free equilibrium. To further investigate, a sensitivity analysis was conducted on the basic parameters of the reproduction numbers for both the Delta and Omicron variants, identifying the key factors influencing their transmission. Additionally, the paper calculates the Omicron invasion reproduction number and formulates analytical expressions to determine the required percentage of vaccinated individuals necessary for eradicating COVID-19, even with the consistent use of an imperfect vaccine. The main findings of this study include:

1. Both the Delta and Omicron variants exhibit the phenomenon of backward bifurcation when their basic reproduction number falls below one. This unique property poses challenges in effectively controlling COVID-19 within the population.
2. In a scenario where vaccine efficacy is perfect and there are no instances of re-infection, both the Delta and Omicron variants of COVID-19 attain a globally asymptotically stable disease-free equilibrium.
3. The sensitivity analysis conducted on the reproduction numbers of the Delta and Omicron variants reveals that the most influential parameters affecting the trans-

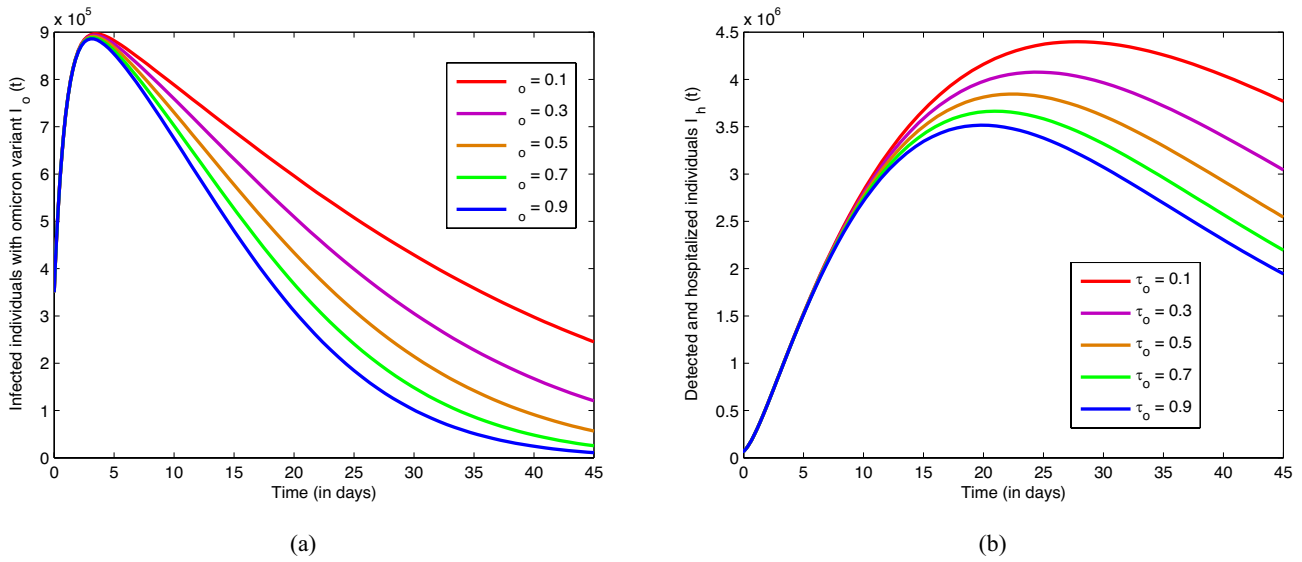


Fig. 14 The effect of the efficacy rate of vaccine to Omicron variant (τ_o) on **(a)** infected individuals with Omicron variant of COVID-19 $I_o(t)$, **(b)** detected and hospitalized individuals $I_h(t)$

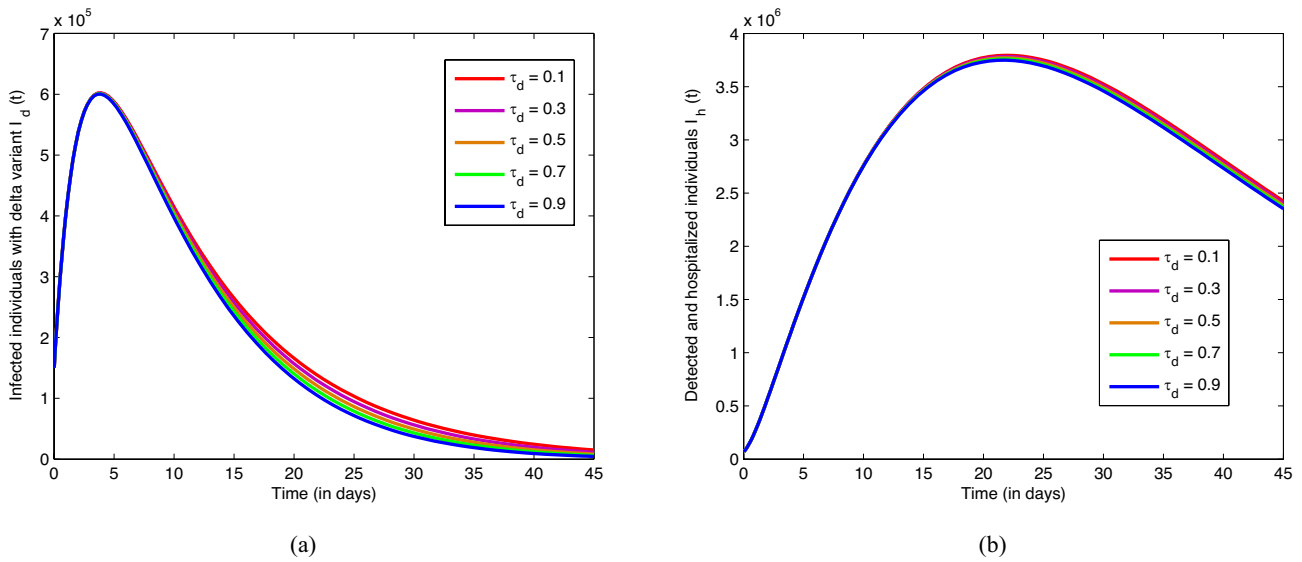


Fig. 15 The effect of the efficacy rate of vaccine to Delta variant (τ_d) on **(a)** infected individuals with Delta variant of COVID-19 $I_d(t)$, **(b)** detected and hospitalized individuals $I_h(t)$

mission of both variants are the effective contact rates (denoted as α_d for the Delta variant and α_o for the Omicron variant) along with the rate of progression from the exposed class to the infectious class (represented as γ_d for the Delta variant and γ_o for the Omicron variant).

4. With a COVID-19 vaccine offering 60% protection against the Omicron variant, a vaccination rate of at least 97.67% among the susceptible population is required to attain the herd immunity threshold.

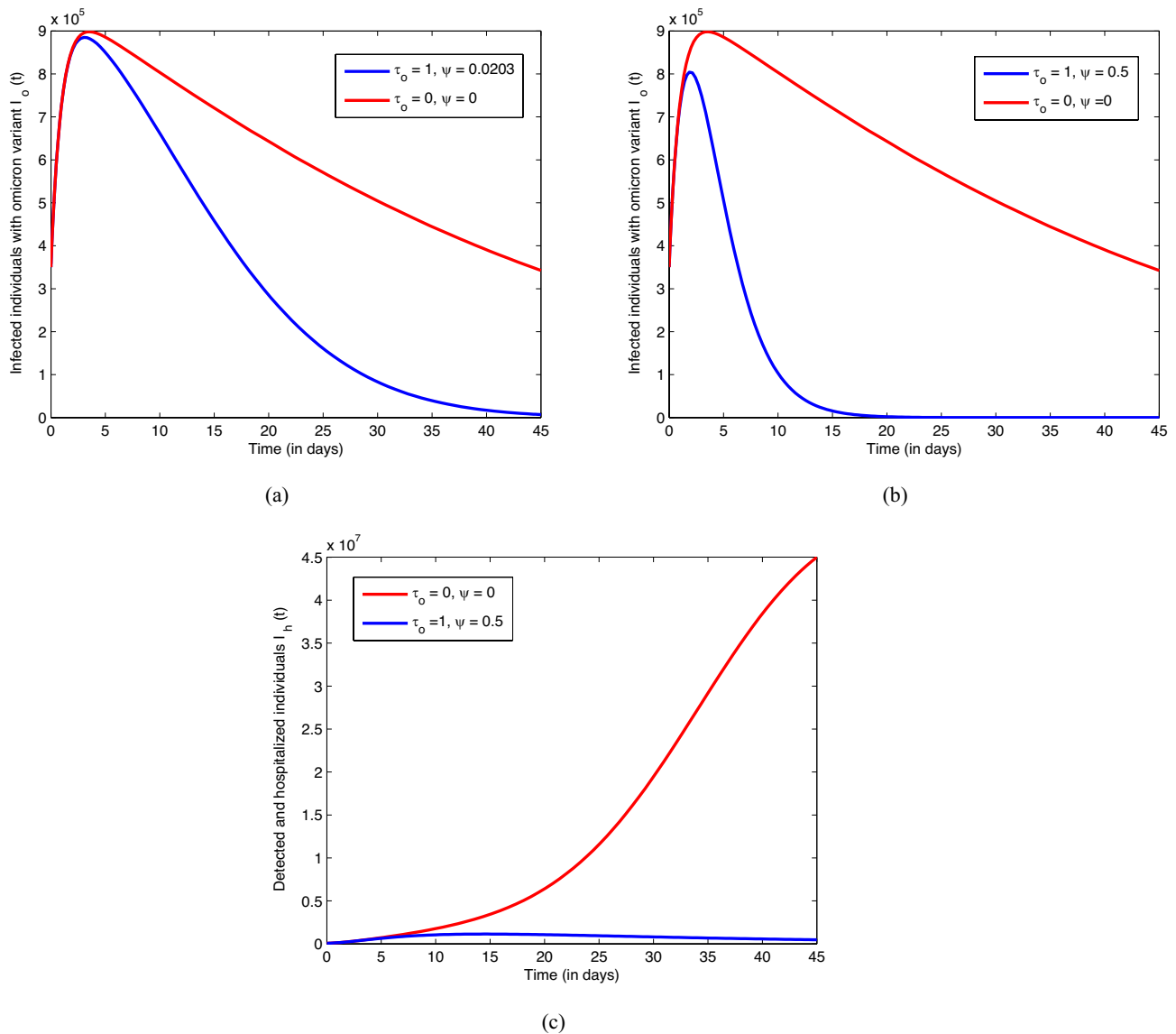


Fig. 16 The effect of the efficacy rate of vaccine to Omicron variant (τ_o) and the vaccination rate (ψ) on (a) infected individuals with Omicron variant of COVID-19 $I_o(t)$, (b) infected individuals with Omicron variant of COVID-19 $I_o(t)$, (c) detected and hospitalized individuals $I_h(t)$

5. The findings from numerical simulations reveal that increasing both the vaccination rate and the effectiveness of the vaccine against the Delta and Omicron variants, alongside higher adherence to COVID-19 safety protocols, leads to a substantial reduction in the number of individuals requiring hospitalization.

Drawing from the outcomes of this study, here are some recommendations for healthcare practitioners and

policymakers aimed at combating and alleviating the impact of COVID-19:

1. Prioritize increasing vaccination rates across all eligible populations, focusing on vaccine effectiveness against prevalent variants like omicron.
2. Encourage strict adherence to COVID-19 safety measures, including mask-wearing, social distancing, and hand hygiene, to curb transmission rates.

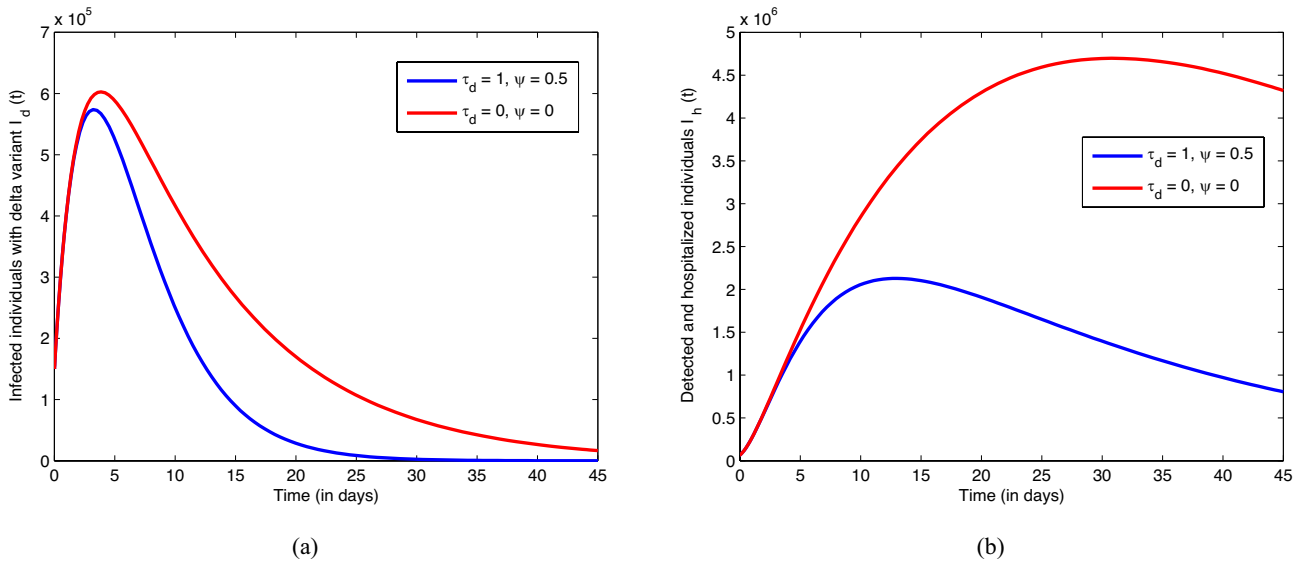


Fig. 17 The effect of the efficacy rate of vaccine to Delta variant (τ_d) and the vaccination rate (ψ) on (a) infected individuals with Delta variant of COVID-19 $I_d(t)$, (b) detected and hospitalized individuals $I_h(t)$

3. Strengthen healthcare facilities by providing adequate resources, equipment, and personnel to manage potential surges in hospitalizations.
4. Educate the public about the significance of vaccinations and adherence to safety protocols through comprehensive awareness campaigns.
5. Foster community engagement and collaboration to ensure the successful implementation of preventive measures and vaccination campaigns.

There are several directions for extending this study:

1. Expanding the scope of this study could involve reformulating the model using Caputo-based or Atangana-Beleanu-based fractional order models. This approach would offer fresh insights into the dynamics of COVID-19 from a different mathematical perspective. Numerically solving these models could provide a more detailed understanding of disease spread and its control mechanisms.
2. Introducing an age-structured model that would allow for a more detailed examination of COVID-19 dynamics within different age groups. This approach could uncover age-specific patterns of transmission, susceptibility, and the impact of interventions, aiding in targeted strategies for disease management and vaccination distribution.

Appendix

Appendix: Continuation of the co-existence of the Delta and Omicron equilibrium

$$\begin{aligned}
 \mathcal{W}(\lambda_d^{**}, \lambda_o^{**}) = & \lambda_o^{**8} \mathcal{L}_1 + \lambda_d^{**} \lambda_o^{**7} \mathcal{L}_2 + \lambda_o^{**7} \mathcal{L}_3 + \lambda_d^{**} \lambda_o^{**6} \mathcal{L}_4 \\
 & + \lambda_d^{**2} \lambda_o^{**6} \mathcal{L}_5 + \lambda_o^{**6} \mathcal{L}_6 + \lambda_d^{**} \lambda_o^{**5} \mathcal{L}_7 + \\
 & \lambda_d^{**2} \lambda_o^{**5} \mathcal{L}_8 + \lambda_d^{**3} \lambda_o^{**5} \mathcal{L}_9 + \lambda_o^{**5} \mathcal{L}_{10} + \\
 & + \lambda_d^{**} \lambda_o^{**4} \mathcal{L}_{11} + \lambda_d^{**2} \lambda_o^{**4} \mathcal{L}_{12} + \lambda_d^{**3} \lambda_o^{**4} \mathcal{L}_{13} + \\
 & \lambda_d^{**4} \lambda_o^{**4} \mathcal{L}_{14} + \lambda_o^{**4} \mathcal{L}_{15} + \lambda_d^{**} \lambda_o^{**3} \mathcal{L}_{16} + \\
 & \lambda_d^{**2} \lambda_o^{**3} \mathcal{L}_{17} + \lambda_d^{**3} \lambda_o^{**3} \mathcal{L}_{18} + \lambda_d^{**4} \lambda_o^{**3} \mathcal{L}_{19} + \\
 & \lambda_d^{**5} \lambda_o^{**3} \mathcal{L}_{20} + \lambda_o^{**3} \mathcal{L}_{21} + \lambda_d^{**} \lambda_o^{**2} \mathcal{L}_{22} \\
 & + \lambda_d^{**2} \lambda_o^{**2} \mathcal{L}_{23} + \lambda_d^{**3} \lambda_o^{**2} \mathcal{L}_{24} + \lambda_d^{**4} \lambda_o^{**2} \mathcal{L}_{25} + \\
 & \lambda_d^{**5} \lambda_o^{**2} \mathcal{L}_{26} + \lambda_o^{**2} \mathcal{L}_{27} + \lambda_d^{**} \lambda_o^{**} \mathcal{L}_{28} + \\
 & \lambda_d^{**2} \lambda_o^{**} \mathcal{L}_{29} + \lambda_d^{**3} \lambda_o^{**} \mathcal{L}_{30} + \lambda_d^{**4} \lambda_o^{**} \mathcal{L}_{31} + \\
 & \lambda_d^{**5} \lambda_o^{**} \mathcal{L}_{32} + \lambda_o^{**} \mathcal{L}_{33} + \lambda_d^{**} \mathcal{L}_{34} + \lambda_d^{**2} \mathcal{L}_{35} + \\
 & \lambda_d^{**3} \mathcal{L}_{36} + \lambda_d^{**4} \mathcal{L}_{37} + \lambda_d^{**5} \mathcal{L}_{38} + \mathcal{L}_{39} = 0,
 \end{aligned}
 \tag{54}$$

where

$$\begin{aligned}
 \mathcal{L}_1 &= (1 - \phi)\alpha_o(1 - \tau_o)b_2n_1, \\
 \mathcal{L}_2 &= (1 - \phi)\alpha_o(1 - \tau_d)b_2 \\
 &\quad + (1 - \phi)\alpha_o(1 - \tau_o)(b_3n_1 + b_2(n_2 + n_3)), \\
 \mathcal{L}_3 &= m_1 + r_1, \mathcal{L}_4 = m_2 + r_2, \\
 \mathcal{L}_5 &= (1 - \phi)\alpha_o(1 - \tau_d)(b_3n_1 + b_2(n_2 + n_3)) \\
 &\quad + (1 - \phi)\alpha_o(1 - \tau_o)(b_1n_1 + b_2n_8 + b_3(n_2 + n_3)), \\
 \mathcal{L}_6 &= m_3 - r_3, \mathcal{L}_7 = m_4 - r_4, \mathcal{L}_8 = m_5 + r_5, \\
 \mathcal{L}_9 &= (1 - \phi)\alpha_o(1 - \tau_d)(b_1n_1 + b_2n_8 + b_3) \\
 &\quad + (1 - \phi)\alpha_o(1 - \tau_o)(b_1(n_2 + n_3) + b_3n_8), \\
 \mathcal{L}_{10} &= m_6 - r_6, \mathcal{L}_{11} = m_7 - r_7, \\
 \mathcal{L}_{12} &= m_8 - r_8, \mathcal{L}_{13} = m_9 + r_9, \\
 \mathcal{L}_{14} &= (1 - \phi)\alpha_o(1 - \tau_d)(b_1(n_2 + n_3) + b_3n_8) \\
 &\quad + (1 - \phi)\alpha_o(1 - \tau_o)b_1n_8, \\
 \mathcal{L}_{15} &= m_{10} - r_{10}, \mathcal{L}_{16} = m_{11} - r_{11}, \mathcal{L}_{17} = m_{12} - r_{12}, \\
 \mathcal{L}_{18} &= m_{13} - r_{13}, \mathcal{L}_{19} = m_{14} + r_{14}, \\
 \mathcal{L}_{20} &= (1 - \phi)\alpha_o(1 - \tau_d)b_1n_8, \mathcal{L}_{21} = m_{15} - r_{15}, \\
 \mathcal{L}_{22} &= m_{16} - r_{16}, \mathcal{L}_{23} = m_{17} - r_{17}, \mathcal{L}_{24} = m_{18} - r_{18}, \\
 \mathcal{L}_{25} &= m_{19} - r_{19}, \mathcal{L}_{26} = (1 - \phi)\alpha_o(1 - \tau_d)b_1n_{17}, \\
 \mathcal{L}_{27} &= m_{20} - r_{20}, \mathcal{L}_{28} = m_{21} - r_{21}, \mathcal{L}_{29} = m_{22} - r_{22}, \\
 \mathcal{L}_{30} &= m_{23} - r_{23}, \mathcal{L}_{31} = m_{24} - r_{24}, \\
 \mathcal{L}_{32} &= (1 - \phi)\alpha_o(1 - \tau_d)b_1n_{25}, \mathcal{L}_{33} = m_{25} - r_{25}, \\
 \mathcal{L}_{34} &= m_{26} - r_{26}, \mathcal{L}_{35} = m_{27} - r_{27}, \mathcal{L}_{36} = m_{28} - r_{28}, \\
 \mathcal{L}_{37} &= m_{29} - r_{29}, \mathcal{L}_{38} = (1 - \phi)\alpha_o(1 - \tau_d)b_1n_{29}, \\
 \mathcal{L}_{39} &= \Pi\mu^2 K_1^2 K_2^2 K_3^2 K_4^2 K_5^3 K_6^3 K_7^3 (\mathcal{R}_0^{vo} - \mathcal{R}_0^{vd}) \\
 &\quad - \Pi K_1 K_2 K_3 K_4 K_5 K_6 e_{10} e_{22} \mathcal{R}_0^{vo}.
 \end{aligned}$$

With

$$\begin{aligned}
 m_1 &= (1 - \phi)\alpha_o((1 - \tau_o)(b_5n_1 + b_2n_4) + b_2y_2n_1), \\
 m_2 &= (1 - \phi)\alpha_o(1 - \tau_d)(b_5n_1 + b_2n_4 + b_3y_2n_1) \\
 &\quad + (1 - \phi)\alpha_o(1 - \tau_o)(b_4n_1 + b_5(n_2 + n_3) + b_3n_4) \\
 &\quad + (1 - \phi)\alpha_o(1 - \tau_o)(b_2(n_6 + n_7) + b_2(y_1n_2 + y_1n_3)), \\
 m_3 &= (1 - \phi)\alpha_o(1 - \tau_o)(b_6n_1 + b_5n_4 + b_2n_9) \\
 &\quad + (1 - \phi)\alpha_o y_2(b_5n_1 + b_2n_4), \\
 m_4 &= (1 - \phi)\alpha_o(1 - \tau_d)(b_6n_1 + b_5n_4 + b_2n_9) \\
 &\quad + (1 - \phi)\alpha_o y_2(b_2n_7 + b_3n_4 + b_4n_1 + b_5n_3) \\
 &\quad + (1 - \phi)\alpha_o y_1(b_2n_6 + b_5n_2) \\
 &\quad + (1 - \phi)\alpha_o(1 - \tau_o)(b_2(n_{11} + n_{12}) + b_3n_9 + b_4n_4) \\
 &\quad + (1 - \phi)\alpha_o(1 - \tau_o)(b_5(n_6 + n_7) + b_6(n_2 + n_3)),
 \end{aligned}$$

$$\begin{aligned}
 m_5 &= (1 - \phi)\alpha_o((1 - \tau_d)b_4 + b_1y_2)n_1 \\
 &\quad + (1 - \phi)\alpha_o((1 - \tau_d)b_5 + (1 - \tau_o)b_4 + b_3y_1)n_2 \\
 &\quad + (1 - \phi)\alpha_o((1 - \tau_o)b_5 + b_2y_1)n_8 \\
 &\quad + (1 - \phi)\alpha_o((1 - \tau_d)b_5 + (1 - \tau_o)b_4 + b_3y_2)n_3 \\
 &\quad + (1 - \phi)\alpha_o((1 - \tau_d)b_2 + (1 - \tau_o)b_3)(n_6 + n_7) \\
 &\quad + (1 - \phi)\alpha_o(1 - \tau_o)b_2n_{17} \\
 &\quad + (1 - \phi)\alpha_o((1 - \tau_d)b_3 + (1 - \tau_o)b_1)n_4, \\
 m_6 &= (1 - \phi)\alpha_o((1 - \tau_o)b_5 + b_2y_2)n_9 \\
 &\quad + (1 - \phi)\alpha_o((1 - \tau_d)b_6 + b_5y_2)n_4 \\
 &\quad + (1 - \phi)\alpha_o((1 - \tau_o)(b_2n_{19} - n_5) + b_6y_2n_1), \\
 m_7 &= (1 - \phi)\alpha_o((1 - \tau_d)b_6 + b_4y_2)n_4 \\
 &\quad + (1 - \phi)\alpha_o((1 - \tau_o)b_6 + b_5y_2)n_7 \\
 &\quad + (1 - \phi)\alpha_o((1 - \tau_d)b_5 + (1 - \tau_o)b_4 + b_3y_2)n_9 \\
 &\quad + (1 - \phi)\alpha_o(((1 - \tau_d)b_5 + (1 - \tau_o)b_4 + b_3y_2)n_9) \\
 &\quad + (1 - \phi)\alpha_o((1 - \tau_d)b_2 + (1 - \tau_o)b_3)n_{19} \\
 &\quad + (1 - \phi)\alpha_o((1 - \tau_o)b_5 + b_2y_2)n_{12} \\
 &\quad + (1 - \phi)\alpha_o((1 - \tau_o)b_5 + b_2y_1)n_{11} \\
 &\quad + (1 - \phi)\alpha_o(1 - \tau_o)b_2(n_{21} + n_{22}), \\
 m_8 &= (1 - \phi)\alpha_o(((1 - \tau_d)b_5 + (1 - \tau_o)b_4 + b_3y_2)n_7) \\
 &\quad + (1 - \phi)\alpha_o(1 - \tau_o)b_2n_{25} + \\
 &\quad + (1 - \phi)\alpha_o((1 - \tau_d)b_2 + (1 - \tau_o)b_3)(n_{11} + n_{12}) \\
 &\quad + (1 - \phi)\alpha_o(((1 - \tau_d)b_3 + (1 - \tau_o)b_1)n_9) \\
 &\quad + (1 - \phi)\alpha_o((1 - \tau_o)b_5 + b_2y_1)n_{17} \\
 &\quad + (1 - \phi)\alpha_o((1 - \tau_o)b_6 + b_5y_1)n_8 \\
 &\quad + (1 - \phi)\alpha_o((1 - \tau_d)b_5 + (1 - \tau_o)b_4 + b_3y_1)n_6 \\
 &\quad + (1 - \phi)\alpha_o((1 - \tau_d)b_4 + b_1y_2)n_4 \\
 &\quad + (1 - \phi)\alpha_o((1 - \tau_d)b_6 + b_4y_1)n_2 \\
 &\quad + (1 - \phi)\alpha_o((1 - \tau_d)b_6 + b_4y_2)n_3, \\
 m_9 &= (1 - \phi)\alpha_o((1 - \tau_d)b_4 + b_1y_1)n_2 \\
 &\quad + (1 - \phi)\alpha_o((1 - \tau_d)b_4 + b_1y_2)n_3 \\
 &\quad + (1 - \phi)\alpha_o((1 - \tau_d)b_3 + (1 - \tau_o)b_1)(n_6 + n_7) \\
 &\quad + (1 - \phi)\alpha_o((1 - \tau_d)b_2 + (1 - \tau_o)b_3)n_{17} \\
 &\quad + (1 - \phi)\alpha_o((1 - \tau_d)b_5 + (1 - \tau_o)b_4 + b_3y_1)n_8 \\
 &\quad + (1 - \phi)\alpha_o(1 - \tau_d)b_1n_4, \\
 m_{10} &= (1 - \phi)\alpha_o(((1 - \tau_o)b_6 + b_5y_2)n_9) \\
 &\quad + (1 - \phi)\alpha_o((1 - \tau_o)b_5 + b_2y_2)n_{19} \\
 &\quad + (1 - \phi)\alpha_o(1 - \tau_o)(b_2n_{27} + n_{10}) + y_2(b_6n_4 - n_5),
 \end{aligned}$$

$$\begin{aligned}
 m_{11} = & (1 - \phi)\alpha_o b_6 y_1 n_6 \\
 & + (1 - \phi)\alpha_o ((1 - \tau_d)b_5 + (1 - \tau_o)b_4 + b_3 y_2)n_{19} \\
 & + (1 - \phi)\alpha_o ((1 - \tau_o)b_6 + b_5 y_1)n_{11} \\
 & + (1 - \phi)\alpha_o ((1 - \tau_o)b_6 + b_5 y_2)n_{12} \\
 & + (1 - \phi)\alpha_o ((1 - \tau_d)b_2 + (1 - \tau_o)b_3)n_{27} \\
 & + (1 - \phi)\alpha_o ((1 - \tau_o)b_5 + b_2 y_1)n_{21} \\
 & + (1 - \phi)\alpha_o ((1 - \tau_o)b_5 + b_2 y_2)n_{22} \\
 & + (1 - \phi)\alpha_o ((1 - \tau_o)(b_2(n_{30} + n_{31}) + n_{14} + n_{15})) \\
 & + (1 - \phi)\alpha_o (b_6 y_2 n_{17} + ((1 - \tau_d)b_6 + b_4 y_2)n_9) \\
 & + (1 - \phi)\alpha_o (1 - \tau_d)n_{10},
 \end{aligned}$$

$$\begin{aligned}
 m_{12} = & (1 - \phi)\alpha_o ((1 - \tau_d)b_5 + (1 - \tau_o)b_4 + b_3 y_1)n_{11} \\
 & + (1 - \phi)\alpha_o (((1 - \tau_d)b_5 + (1 - \tau_o)b_4)) \\
 & + (1 - \phi)\alpha_o ((1 - \tau_d)b_2 + (1 - \tau_o)b_3)(n_{21} + n_{22}) \\
 & + (1 - \phi)\alpha_o ((1 - \tau_d)b_3 + (1 - \tau_o)b_1)n_{19} \\
 & + (1 - \phi)\alpha_o ((1 - \tau_d)b_2 + (1 - \tau_o)b_3)(n_{21} + n_{22}) \\
 & + (1 - \phi)\alpha_o ((1 - \tau_d)b_3 + (1 - \tau_o)b_1)n_{19} \\
 & + (1 - \phi)\alpha_o ((1 - \tau_o)b_6 + b_5 y_1)n_{17} \\
 & + (1 - \phi)\alpha_o ((1 - \tau_d)b_6 + b_4 y_1)n_6 \\
 & + (1 - \phi)\alpha_o ((1 - \tau_d)b_6 + b_4 y_2)n_7 \\
 & + (1 - \phi)\alpha_o ((1 - \tau_d)b_4 + b_1 y_2)n_9 \\
 & + (1 - \phi)\alpha_o ((1 - \tau_o)b_5 + b_2 y_1)n_{25} \\
 & + (1 - \phi)\alpha_o ((1 - \tau_o)(b_2 n_{29} + n_{18}) + b_6 y_1 n_8),
 \end{aligned}$$

$$\begin{aligned}
 m_{13} = & (1 - \phi)\alpha_o ((1 - \tau_d)b_5 + (1 - \tau_o)b_4 + b_3 y_1)n_{17} \\
 & + (1 - \phi)\alpha_o ((1 - \tau_d)b_4 + b_1 y_1)n_6 \\
 & + (1 - \phi)\alpha_o ((1 - \tau_d)b_4 + b_1 y_2)n_7 \\
 & + (1 - \phi)\alpha_o ((1 - \tau_d)b_2 + (1 - \tau_o)b_3)n_{25} \\
 & + (1 - \phi)\alpha_o ((1 - \tau_d)b_6 + b_4 y_1)n_8 \\
 & + (1 - \phi)\alpha_o ((1 - \tau_d)b_1 n_9 + (1 - \tau_d)b_3(n_{11} + n_{12})) \\
 & + (1 - \phi)\alpha_o (1 - \tau_o)b_1(n_{11} + n_{12}),
 \end{aligned}$$

$$\begin{aligned}
 m_{14} = & (1 - \phi)\alpha_o (1 - \tau_d)b_1(n_6 + n_7) \\
 & + (1 - \phi)\alpha_o ((1 - \tau_d)b_4 + b_1 y_1)n_8 \\
 & + (1 - \phi)\alpha_o ((1 - \tau_d)b_3 + (1 - \tau_o)b_1)n_{17},
 \end{aligned}$$

$$\begin{aligned}
 m_{15} = & (1 - \phi)\alpha_o ((1 - \tau_o)b_6 + b_5 y_2)n_{19} \\
 & + (1 - \phi)\alpha_o ((1 - \tau_o)b_5 + b_2 y_2)n_{27} \\
 & + (1 - \phi)\alpha_o (1 - \tau_o)(b_2 n_{33} + n_{20}) \\
 & + (1 - \phi)\alpha_o y_2(b_6 n_9 + n_{10}),
 \end{aligned}$$

$$\begin{aligned}
 m_{16} = & (1 - \phi)\alpha_o ((1 - \tau_d)b_5 + (1 - \tau_o)b_4 + b_3 y_2)n_{27} \\
 & + (1 - \phi)\alpha_o ((1 - \tau_d)b_2 + (1 - \tau_o)b_3)n_{33} \\
 & + (1 - \phi)\alpha_o (1 - \tau_d)n_{20} \\
 & + (1 - \phi)\alpha_o ((1 - \tau_d)b_6 + b_4 y_2)n_{19} \\
 & + (1 - \phi)\alpha_o ((1 - \tau_o)b_6 + b_5 y_1)n_{21} \\
 & + (1 - \phi)\alpha_o ((1 - \tau_o)b_6 + b_5 y_2)n_{22} \\
 & + (1 - \phi)\alpha_o (1 - \tau_o)(n_{23} + n_{24}) \\
 & + (1 - \phi)\alpha_o (((1 - \tau_o)b_5 + b_2 y_1)n_{30} - n_{16}) \\
 & + (1 - \phi)\alpha_o (((1 - \tau_o)b_5 + b_2 y_2)n_{31} + y_1 n_{14}) \\
 & + (1 - \phi)\alpha_o (b_6(y_1 n_{11} + y_2 n_{12}) + y_2 n_{15}),
 \end{aligned}$$

$$\begin{aligned}
 m_{17} = & (1 - \phi)\alpha_o (((1 - \tau_d)b_5 + (1 - \tau_o)b_4 + b_3 y_2)n_{22}) \\
 & + (1 - \phi)\alpha_o ((1 - \tau_d)b_2 + (1 - \tau_o)b_3)(n_{30} + n_{31}) \\
 & + (1 - \phi)\alpha_o (b_6 y_1 n_{17} + (1 - \tau_o)n_{26} - y_1 n_{18}) \\
 & + (1 - \phi)\alpha_o (1 - \tau_d)(n_{14} + n_{15}) \\
 & + (1 - \phi)\alpha_o ((1 - \tau_d)b_6 + b_4 y_1)n_{11} \\
 & + (1 - \phi)\alpha_o ((1 - \tau_d)b_6 + b_4 y_2)n_{12} \\
 & + (1 - \phi)\alpha_o ((1 - \tau_d)b_5 + (1 - \tau_o)b_4 + b_3 y_1)n_{21} \\
 & + (1 - \phi)\alpha_o ((1 - \tau_d)b_4 + b_1 y_2)n_{19} \\
 & + (1 - \phi)\alpha_o ((1 - \tau_o)b_6 + b_5 y_1)n_{25} \\
 & + (1 - \phi)\alpha_o (((1 - \tau_d)b_3 + (1 - \tau_o)b_1)n_{27}) \\
 & + (1 - \phi)\alpha_o ((1 - \tau_o)b_5 + b_2 y_1)n_{29},
 \end{aligned}$$

$$\begin{aligned}
 m_{18} = & (1 - \phi)\alpha_o ((1 - \tau_d)b_1 n_{19}) \\
 & + (1 - \phi)\alpha_o (((1 - \tau_d)b_5 + (1 - \tau_o)b_4 + b_3 y_1)n_{25}) \\
 & + (1 - \phi)\alpha_o ((1 - \tau_d)b_3 + (1 - \tau_o)b_1)(n_{21} + n_{22}) \\
 & - (1 - \phi)\alpha_o (1 - \tau_d)n_{18} \\
 & + (1 - \phi)\alpha_o (((1 - \tau_d)b_2 + (1 - \tau_o)b_3)n_{29}) \\
 & + (1 - \phi)\alpha_o (((1 - \tau_d)b_4 + b_1 y_1)n_{11} +) \\
 & + (1 - \phi)\alpha_o ((1 - \tau_d)b_4 + b_1 y_2)n_{12} \\
 & + (1 - \phi)\alpha_o ((1 - \tau_d)b_{16} + b_4 y_1)n_{17},
 \end{aligned}$$

$$\begin{aligned}
 m_{19} = & (1 - \phi)\alpha_o ((1 - \tau_d)b_3 + (1 - \tau_o)b_1)n_{25} \\
 & + (1 - \phi)\alpha_o ((1 - \tau_d)b_4 + b_1 y_1)n_{17} \\
 & + (1 - \phi)\alpha_o (1 - \tau_d)b_1(n_{11} + n_{12}),
 \end{aligned}$$

$$\begin{aligned}
 m_{20} = & (1 - \phi)\alpha_o (b_6 y_2 n_{19} + y_2 n_{20}) \\
 & + (1 - \phi)\alpha_o ((1 - \tau_o)b_6 + b_5 y_2)n_{27} \\
 & + (1 - \phi)\alpha_o (1 - \tau_o)n_{28} \\
 & + (1 - \phi)\alpha_o ((1 - \tau_o)b_5 + b_2 y_2)n_{33},
 \end{aligned}$$

$$\begin{aligned}
 m_{21} &= (1 - \phi)\alpha_o(b_6(y_1n_{21} + y_2n_{22}) + y_1n_{23} + y_2n_{24}) \\
 &\quad + (1 - \phi)\alpha_o((1 - \tau_d)b_6 + b_4y_2)n_{27} \\
 &\quad + (1 - \phi)\alpha_o((1 - \tau_o)b_6 + b_5y_1)n_{30} \\
 &\quad + (1 - \phi)\alpha_o((1 - \tau_o)b_6 + b_5y_2)n_{31} \\
 &\quad + (1 - \phi)\alpha_o((1 - \tau_o)n_{32} + (1 - \tau_d)n_{28}) \\
 &\quad + (1 - \phi)\alpha_o(((1 - \tau_d)b_5 + (1 - \tau_o)b_4 + b_3y_2)n_{33}), \\
 m_{22} &= (1 - \phi)\alpha_o((1 - \tau_d)b_6 + b_4y_1)n_{21} \\
 &\quad + (1 - \phi)\alpha_o(((1 - \tau_d)b_5 + (1 - \tau_o)b_4 + b_3y_1)n_{30}) \\
 &\quad + (1 - \phi)\alpha_o(((1 - \tau_d)b_5 + (1 - \tau_o)b_4 + b_3y_2)n_{31}) \\
 &\quad + (1 - \phi)\alpha_ob_6y_1n_{25} + (1 - \phi)\alpha_o(1 - \tau_o)n_{13} \\
 &\quad + (1 - \phi)\alpha_o(((1 - \tau_d)b_3 + (1 - \tau_o)b_1)n_{33}) \\
 &\quad + (1 - \phi)\alpha_o((1 - \tau_d)b_4 + b_1y_2)n_{27} \\
 &\quad + (1 - \phi)\alpha_o((1 - \tau_o)b_6 + b_5y_1)n_{29} \\
 &\quad + (1 - \phi)\alpha_o(1 - \tau_d)(n_{23} + n_{24}) \\
 &\quad + (1 - \phi)\alpha_o(((1 - \tau_d)b_6 + b_4y_2)n_{22} + y_1n_{26}), \\
 m_{23} &= (1 - \phi)\alpha_o((1 - \tau_d)b_4 + b_1y_1)n_{21} \\
 &\quad + (1 - \phi)\alpha_o(((1 - \tau_d)b_5 + (1 - \tau_o)b_4 + b_3y_1)n_{29}) \\
 &\quad + (1 - \phi)\alpha_o(((1 - \tau_d)b_3 + (1 - \tau_o)b_1)(n_{30} + n_{31})) \\
 &\quad + (1 - \phi)\alpha_o(1 - \tau_d)n_{26} \\
 &\quad + (1 - \phi)\alpha_o((1 - \tau_d)b_4 + b_1y_2)n_{22} \\
 &\quad + (1 - \phi)\alpha_o((1 - \tau_d)b_6 + b_4y_1)n_{25} \\
 &\quad + (1 - \phi)\alpha_o((1 - \tau_d)b_1n_{27}),
 \end{aligned}$$

$$\begin{aligned}
 m_{24} &= (1 - \phi)\alpha_o((1 - \tau_d)b_3 + (1 - \tau_o)b_1)n_{29} \\
 &\quad + (1 - \phi)\alpha_o(1 - \tau_d)b_1(n_{21} + n_{22}) \\
 &\quad + (1 - \phi)\alpha_o((1 - \tau_d)b_4 + b_1y_1)n_{25}, \\
 m_{25} &= (1 - \phi)\alpha_o(((1 - \tau_o)b_6 + b_5y_2)n_{33} + b_6y_2n_{27}) \\
 &\quad + (1 - \phi)\alpha_o(y_2n_{28} - (1 - \tau_o)n_{34}), \\
 m_{26} &= (1 - \phi)\alpha_o y_1 n_{32} \\
 &\quad + (1 - \phi)\alpha_o(b_6(y_1n_{30} + y_2n_{31}) - (1 - \tau_d)n_{34}) \\
 &\quad + (1 - \phi)\alpha_o((1 - \tau_d)b_6 + b_4y_2)n_{33}, \\
 m_{27} &= (1 - \phi)\alpha_o y_1 (b_6 n_{29} + n_{13}) \\
 &\quad + (1 - \phi)\alpha_o((1 - \tau_d)b_6 + b_4y_1)n_{30} \\
 &\quad + (1 - \phi)\alpha_o((1 - \tau_d)b_6 + b_4y_2)n_{31} \\
 &\quad + (1 - \phi)\alpha_o((1 - \tau_d)n_{32} + ((1 - \tau_d)b_4 + b_1y_2)n_{33}), \\
 m_{28} &= (1 - \phi)\alpha_o((1 - \tau_d)b_6 + b_4y_1)n_{29} \\
 &\quad + (1 - \phi)\alpha_o((1 - \tau_d)b_4 + b_1y_1)n_{30} \\
 &\quad + (1 - \phi)\alpha_o(((1 - \tau_d)b_4 + b_1y_2)n_{31} + (1 - \tau_d)n_{13}) \\
 &\quad + (1 - \phi)\alpha_o(1 - \tau_d)b_1n_{33}, \\
 m_{29} &= (1 - \phi)\alpha_o((1 - \tau_d)b_4 + b_1y_1)n_{29} \\
 &\quad + (1 - \phi)\alpha_o((1 - \tau_d)b_1(n_{30} + n_{31})), \\
 r_1 &= (1 - \phi)\alpha_d K_6 b_2 (1 - \tau_o)(U_4 + U_5), \\
 r_2 &= (1 - \phi)\alpha_d K_6 ((1 - \tau_o)(b_2 U_6 + b_3(U_4 + U_5))) \\
 &\quad + (1 - \phi)\alpha_d K_6 (1 - \tau_d)b_2(U_4 + U_5), \\
 r_3 &= (1 - \phi)\alpha_d K_6 (1 - \tau_o)(b_2(U_1 + U_2) - b_5(U_4 + U_5)) \\
 &\quad - (1 - \phi)\alpha_d K_6 b_2(y_1 U_4 + y_2 U_5), \\
 r_4 &= (1 - \phi)\alpha_d K_6 ((1 - \tau_o)(b_2 U_7 - b_5 U_6) - b_2 y_1 U_6) \\
 &\quad - (1 - \phi)\alpha_d K_6 ((1 - \tau_d)b_5 + (1 - \tau_o)b_4)(U_4 + U_5) \\
 &\quad - (1 - \phi)\alpha_d K_6 (b_3(y_1 U_4 + y_2 U_5)) \\
 &\quad + (1 - \phi)\alpha_d K_6 (((1 - \tau_d)b_2 + (1 - \tau_o)b_3)(U_1 + U_2)), \\
 r_5 &= (1 - \phi)\alpha_d K_6 ((1 - \tau_d)b_3 + (1 - \tau_o)b_1)(U_4 + U_5) \\
 &\quad + (1 - \phi)\alpha_d K_6 (((1 - \tau_d)b_2 + (1 - \tau_o)b_3)U_6), \\
 r_6 &= (1 - \phi)\alpha_d K_6 ((1 - \tau_o)b_5 + b_2 y_1)U_1 \\
 &\quad + (1 - \phi)\alpha_d K_6 ((1 - \tau_o)b_5 + b_2 y_2)U_2 \\
 &\quad + (1 - \phi)\alpha_d K_6 b_2 (1 - \tau_o)(U_9 + U_{10}) \\
 &\quad - (1 - \phi)\alpha_d K_6 (1 - \tau_o)b_6(U_4 + U_5) \\
 &\quad - (1 - \phi)\alpha_d K_6 b_5(y_1 U_4 + y_2 U_5),
 \end{aligned}$$

$$\begin{aligned}
 r_7 &= (1 - \phi)\alpha_d K_6 ((1 - \tau_d)b_5 + (1 - \tau_o)b_4)(U_1 + U_2) \\
 &\quad + (1 - \phi)\alpha_d K_6 (b_3(y_1 U_1 + y_2 U_2) - b_4(y_1 U_4 + y_2 U_5)) \\
 &\quad - (1 - \phi)\alpha_d K_6 b_6 (1 - \tau_d)(U_4 + U_5) \\
 &\quad - (1 - \phi)\alpha_d K_6 ((1 - \tau_o)b_6 + b_5 y_1) U_6 \\
 &\quad + (1 - \phi)\alpha_d K_6 ((1 - \tau_o)b_5 + b_2 y_1) U_7 \\
 &\quad + (1 - \phi)\alpha_d K_6 (1 - \tau_o) b_2 U_{13} \\
 &\quad + (1 - \phi)\alpha_d K_6 ((1 - \tau_d)b_2 + (1 - \tau_o)b_3)(U_9 + U_{10}), \\
 r_8 &= (1 - \phi)\alpha_d K_6 ((1 - \tau_d)b_2 + (1 - \tau_o)b_3) U_7 \\
 &\quad + (1 - \phi)\alpha_d K_6 ((1 - \tau_d)b_3 + (1 - \tau_o)b_1)(U_1 + U_2) \\
 &\quad - (1 - \phi)\alpha_d K_6 ((1 - \tau_d)b_5 + (1 - \tau_o)b_4 + b_3 y_1) U_6 \\
 &\quad - (1 - \phi)\alpha_d K_6 (1 - \tau_d) b_4 (U_4 + U_5) \\
 &\quad - (1 - \phi)\alpha_d K_6 b_1 (y_1 U_4 + y_2 U_5), \\
 r_9 &= (1 - \phi)\alpha_d K_6 ((1 - \tau_d)(b_1(U_4 + U_5) + b_3 U_6)) \\
 &\quad + (1 - \phi)\alpha_d K_6 (1 - \tau_o) b_1 U_6, \\
 r_{10} &= (1 - \phi)\alpha_d K_6 (1 - \tau_o) b_6 (U_1 + U_2) \\
 &\quad + (1 - \phi)\alpha_d K_6 (b_5(y_1 U_1 + y_2 U_2) - (1 - \tau_o) U_3) \\
 &\quad + (1 - \phi)\alpha_d K_6 (1 - \tau_o) b_5 (U_9 + U_{10}) \\
 &\quad + (1 - \phi)\alpha_d K_6 b_2 (y_1 U_9 + y_2 U_{10}) \\
 &\quad + (1 - \phi)\alpha_d K_6 (1 - \tau_o) b_2 (U_{16} + U_{17}) \\
 &\quad - (1 - \phi)\alpha_d K_6 b_6 (y_1 U_4 + y_2 U_5), \\
 r_{11} &= (1 - \phi)\alpha_d K_6 (1 - \tau_d)(b_6(U_1 + U_2) - U_3) \\
 &\quad + (1 - \phi)\alpha_d K_6 (1 - \tau_d) b_4 (y_1 U_1 + y_2 U_2) \\
 &\quad + (1 - \phi)\alpha_d K_6 ((1 - \tau_o) b_2 U_{19} - b_6 y_1 U_6) \\
 &\quad + (1 - \phi)\alpha_d K_6 ((1 - \tau_d) b_5 + (1 - \tau_o) b_4)(U_9 + U_{10}) \\
 &\quad + (1 - \phi)\alpha_d K_6 b_3 (y_1 U_9 + y_2 U_{10}) \\
 &\quad + (1 - \phi)\alpha_d K_6 ((1 - \tau_o) b_5 + b_2 y_1) U_{13} \\
 &\quad + (1 - \phi)\alpha_d K_6 ((1 - \tau_o)(b_6 U_7 - U_8) + b_5 y_1 U_7) \\
 &\quad + (1 - \phi)\alpha_d K_6 ((1 - \tau_d) b_2 + (1 - \tau_o) b_3)(U_{16} + U_{17}), \\
 r_{12} &= (1 - \phi)\alpha_d K_6 (1 - \tau_d) b_4 (U_1 + U_2) \\
 &\quad + (1 - \phi)\alpha_d K_6 b_1 (y_1 U_1 + y_2 U_2) \\
 &\quad + (1 - \phi)\alpha_d K_6 ((1 - \tau_d) b_5 + (1 - \tau_o) b_4 + b_3 y_1) U_7 \\
 &\quad + (1 - \phi)\alpha_d K_6 ((1 - \tau_d) b_3 + (1 - \tau_o) b_1)(U_9 + U_{10}) \\
 &\quad + (1 - \phi)\alpha_d K_6 ((1 - \tau_d) b_2 + (1 - \tau_o) b_3) U_{13} \\
 &\quad - (1 - \phi)\alpha_d K_6 ((1 - \tau_d) b_6 + b_4 y_1) U_6, \\
 r_{13} &= (1 - \phi)\alpha_d K_6 (1 - \tau_d) b_1 (U_1 + U_2) \\
 &\quad - (1 - \phi)\alpha_d K_6 ((1 - \tau_d) b_4 + b_1 y_1) U_6 \\
 &\quad + (1 - \phi)\alpha_d K_6 ((1 - \tau_d) b_3 + (1 - \tau_o) b_1) U_7, \\
 r_{14} &= (1 - \phi)\alpha_d K_6 (1 - \tau_d) b_1 U_6, \\
 r_{15} &= (1 - \phi)\alpha_d K_6 b_1 (y_1 U_1 + y_2 U_2) \\
 &\quad + (1 - \phi)\alpha_d K_6 ((1 - \tau_o) b_2 U_{21} - y_1 U_3) \\
 &\quad + (1 - \phi)\alpha_d K_6 (1 - \tau_o) b_6 (U_9 + U_{10}) \\
 &\quad + (1 - \phi)\alpha_d K_6 b_5 (y_1 U_9 + y_2 U_{10}) \\
 &\quad + (1 - \phi)\alpha_d K_6 (1 - \tau_o) b_5 (U_{16} + U_{17}) \\
 &\quad + (1 - \phi)\alpha_d K_6 (1 - \tau_o)(U_{11} - U_{12}) \\
 &\quad + (1 - \phi)\alpha_d K_6 (1 - \tau_o) b_5 (U_{16} + U_{17}) \\
 &\quad + (1 - \phi)\alpha_d K_6 b_2 (y_1 U_{16} + y_2 U_{17}), \\
 r_{16} &= (1 - \phi)\alpha_d K_6 ((1 - \tau_d)(b_6(U_9 + U_{10}) + (U_{11} - U_{12}))) \\
 &\quad + (1 - \phi)\alpha_d K_6 (y_1(b_6 U_7 - U_8) + b_4(y_1 U_9 + y_2 U_{10})) \\
 &\quad + (1 - \phi)\alpha_d K_6 ((1 - \tau_d)(b_6 U_{13} + (U_{14} + U_{15}))) \\
 &\quad + (1 - \phi)\alpha_d K_6 ((1 - \tau_d) b_5 + (1 - \tau_o) b_4)(U_{16} - U_{17}) \\
 &\quad + (1 - \phi)\alpha_d K_6 b_3 (y_1 U_{16} + y_2 U_{17}) \\
 &\quad + (1 - \phi)\alpha_d K_6 ((1 - \tau_o) b_5 + b_2 y_1) U_{19} \\
 &\quad + (1 - \phi)\alpha_d K_6 ((1 - \tau_d) b_2 + (1 - \tau_o) b_3) U_{21}, \\
 r_{17} &= (1 - \phi)\alpha_d K_6 ((1 - \tau_d)(b_6 U_7 - U_8) + b_4 y_1 U_7) \\
 &\quad + (1 - \phi)\alpha_d K_6 ((1 - \tau_d) b_2 + (1 - \tau_o) b_3) U_{19} \\
 &\quad + (1 - \phi)\alpha_d K_6 ((1 - \tau_d) b_5 + (1 - \tau_o) b_4 + b_3 y_1) U_{13} \\
 &\quad + (1 - \phi)\alpha_d K_6 (1 - \tau_d) b_4 (U_9 + U_{10}) \\
 &\quad + (1 - \phi)\alpha_d K_6 b_1 (y_1 U_9 + y_2 U_{10}) \\
 &\quad + (1 - \phi)\alpha_d K_6 ((1 - \tau_d) b_3 + (1 - \tau_o) b_1)(U_{16} + U_{17}), \\
 r_{18} &= (1 - \phi)\alpha_d K_6 (1 - \tau_d)(b_4 U_7 + b_1(U_9 + U_{10}) + b_3 U_{13}) \\
 &\quad + (1 - \phi)\alpha_d K_6 (b_1 y_1 U_7 + (1 - \tau_o) b_1 U_{13}), \\
 r_{19} &= (1 - \phi)\alpha_d K_6 (1 - \tau_d) b_1 U_7,
 \end{aligned}$$

$$\begin{aligned}
 r_{20} &= (1 - \phi)\alpha_d K_6 b_6 (y_1 U_9 + y_2 U_{10}) \\
 &\quad + (1 - \phi)\alpha_d K_6 (y_2 U_{11} - y_1 U_{12}) \\
 &\quad + (1 - \phi)\alpha_d K_6 (1 - \tau_d) (b_6 (U_{16} + U_{17}) + U_{18}) \\
 &\quad + (1 - \phi)\alpha_d K_6 b_5 (y_1 U_{16} + y_2 U_{17}) \\
 &\quad + (1 - \phi)\alpha_d K_6 ((1 - \tau_o) b_5 + b_2 y_1) U_{21}, \\
 r_{21} &= (1 - \phi)\alpha_d K_6 (1 - \tau_d) (b_6 (U_{16} + U_{17}) + U_{18}) \\
 &\quad + (1 - \phi)\alpha_d K_6 b_4 (y_1 U_{16} + y_2 U_{17}) \\
 &\quad + (1 - \phi)\alpha_d K_6 (y_1 U_{13} + (U_{14} - U_{15})) \\
 &\quad + (1 - \phi)\alpha_d K_6 (1 - \tau_o) (b_6 U_{19} + U_{20}) \\
 &\quad + (1 - \phi)\alpha_d K_6 (b_5 y_1 U_{19} + b_3 y_1) U_{21} \\
 &\quad + (1 - \phi)\alpha_d K_6 ((1 - \tau_d) b_5 + (1 - \tau_o) b_4) U_{21}, \\
 r_{22} &= (1 - \phi)\alpha_d K_6 (1 - \tau_d) (b_6 U_{13} + (U_{14} + U_{15})) \\
 &\quad + (1 - \phi)\alpha_d K_6 b_4 y_1 U_{13} \\
 &\quad + (1 - \phi)\alpha_d K_6 ((1 - \tau_d) b_3 + (1 - \tau_o) b_1) U_{21} \\
 &\quad + (1 - \phi)\alpha_d K_6 (1 - \tau_d) b_4 (U_{16} + U_{17}) \\
 &\quad + (1 - \phi)\alpha_d K_6 (b_1 (y_1 U_{16} + y_2 U_{17}) + b_3 y_1) U_{19} \\
 &\quad + (1 - \phi)\alpha_d K_6 ((1 - \tau_d) b_5 + (1 - \tau_o) b_4) U_{19}, \\
 r_{23} &= (1 - \phi)\alpha_d K_6 ((1 - \tau_d) b_4 + b_1 y_1) U_{13} \\
 &\quad + (1 - \phi)\alpha_d K_6 (1 - \tau_d) b_1 (U_{16} + U_{17}) \\
 &\quad + (1 - \phi)\alpha_d K_6 ((1 - \tau_d) b_3 + (1 - \tau_o) b_1) U_{19}, \\
 r_{24} &= (1 - \phi)\alpha_d K_6 (1 - \tau_d) b_1 U_{13}, \\
 r_{25} &= (1 - \phi)\alpha_d K_6 (b_6 (y_1 U_{16} + y_2 U_{17}) + y_2 U_{18}) \\
 &\quad + (1 - \phi)\alpha_d K_6 ((1 - \tau_o) b_6 + b_5 y_1) U_{21}, \\
 r_{26} &= (1 - \phi)\alpha_d K_6 y_1 (b_6 U_{19} + U_{20}) \\
 &\quad + (1 - \phi)\alpha_d K_6 + ((1 - \tau_d) b_6 + b_4 y_1) U_{21}, \\
 r_{27} &= (1 - \phi)\alpha_d K_6 y_1 (b_4 U_{19} + b_1 U_{21}) \\
 &\quad + (1 - \phi)\alpha_d K_6 (1 - \tau_d) (b_6 U_{19} + U_{20} + b_4 U_{21}), \\
 r_{28} &= (1 - \phi)\alpha_d K_6 ((1 - \tau_d) (b_1 U_{21} + b_4 U_{19}) + b_1 y_1 U_{19}), \\
 r_{29} &= (1 - \phi)\alpha_d K_6 (1 - \tau_d) b_1 U_{19}, \\
 r_{30} &= (1 - \phi)\alpha_d K_6 b_6 y_1 U_{21},
 \end{aligned}$$

and

$$\begin{aligned}
 b_1 &= (1 - \tau_d) (K_2 K_3 K_4 - \omega \sigma_d K_3), \\
 b_2 &= (1 - \tau_o) (K_2 K_3 K_4 - \omega \sigma_o K_2), \\
 b_3 &= (1 - \tau_d) (K_2 K_3 K_4 - \omega \sigma_o K_2) \\
 &\quad + (1 - \tau_o) (K_2 K_3 K_4 - \omega \sigma_o K_3), \\
 b_4 &= (\mu + (1 - \tau_d) K_1) K_2 K_3 K_4 \\
 &\quad - (\mu + (1 - \tau_d) \psi) \omega \sigma_d K_3, \\
 b_5 &= (\mu + (1 - \tau_o) K_1) K_2 K_3 K_4 \\
 &\quad - (\mu + (1 - \tau_o) \psi) \omega \sigma_o K_2, \\
 b_6 &= \mu K_1 K_2 K_3 K_4, \\
 n_1 &= \zeta (\epsilon_3 a_{14} - \epsilon_2 e_{14} e_{19}) - e_{27} a_1, \\
 n_2 &= \zeta (\epsilon_3 a_{15} - \epsilon_2 e_{15} e_{19}) - e_{28} a_5, \\
 n_3 &= \zeta (\epsilon_3 a_{16} - \epsilon_1 e_{14} e_{19}) - e_{27} a_2, \\
 n_4 &= \zeta (\epsilon_3 a_{17} + \epsilon_2 a_8) + K_5 (\epsilon_3 a_{14} - \epsilon_2 e_{14} e_{19}) - e_{29} a_1 \\
 &\quad + e_{27} a_3, \\
 n_5 &= e_{10} e_{22} e_{27}, \\
 n_6 &= \zeta (\epsilon_3 a_{18} + \epsilon_2 a_9) \\
 &\quad + K_5 (\epsilon_3 a_{15} - \epsilon_2 e_{15} e_{19}) - e_{10} e_{22} e_{28} + e_{28} a_3, \\
 n_7 &= \zeta (\epsilon_3 a_{19} + \epsilon_1 a_8) + K_5 \epsilon_3 a_{16} - e_{29} a_2 - e_{11} e_{22} e_{27} \\
 &\quad + e_{27} a_4, \\
 n_8 &= \zeta (\epsilon_3 a_{20} - \epsilon_1 e_{15} e_{19}) - e_{28} a_2, \\
 n_9 &= \zeta (\epsilon_3 a_{21} + \epsilon_2 a_{10}) + K_5 (\epsilon_3 a_{17} + \epsilon_2 a_8) + e_{29} a_3 \\
 &\quad + e_{27} a_5, \\
 n_{10} &= \zeta \epsilon_2 e_1 - e_{12} e_{22} e_{27}, \\
 n_{11} &= \zeta (\epsilon_3 a_{22} + \epsilon_2 a_{11}) + K_5 (\epsilon_3 a_{18} + \epsilon_2 a_9) + e_{28} a_5, \\
 n_{12} &= \zeta (\epsilon_3 a_{23} + \epsilon_1 a_{10}) + \\
 &\quad K_5 \epsilon_3 a_{19} + e_{29} a_4 + e_{27} a_6, \\
 n_{13} &= \zeta \epsilon_1 e_4, \\
 n_{14} &= \zeta \epsilon_2 e_2 - e_{12} e_{22} e_{28}, \\
 n_{15} &= \zeta \epsilon_1 e_1 - e_{11} e_{22} e_{29}, \\
 n_{16} &= e_{13} e_{22} e_{27}, \\
 n_{17} &= \zeta (\epsilon_3 a_{24} + \epsilon_1 a_9) + K_5 \epsilon_3 a_{20} + e_{28} a_4, \\
 n_{18} &= e_{11} e_{22} e_{28}, \\
 n_{19} &= K_5 (\epsilon_3 a_{21} + \epsilon_2 a_{10}) + \zeta \epsilon_2 e_{16} e_{20} + e_{27} a_7 + e_{29} a_5, \\
 n_{20} &= K_5 \epsilon_2 e_1 + \zeta \epsilon_2 e_3 - e_{12} e_{22} e_{29}, \\
 n_{21} &= \zeta (\epsilon_3 (e_4 e_9 + a_{25}) + \epsilon_2 e_{17} e_{20}) + K_5 (\epsilon_3 a_{22} \\
 &\quad + \epsilon_2 a_{11}) + e_7 e_{28},
 \end{aligned}$$

$$\begin{aligned}
 n_{22} &= \zeta \varepsilon_1 e_{16} e_{20} + K_5 \varepsilon_3 a_{23} + e_8 e_{20} e_{27} + e_{29} a_6, \\
 n_{23} &= K_5 \varepsilon_2 e_2 + \zeta \varepsilon_2 e_4, \\
 n_{24} &= \zeta \varepsilon_1 e_3 - e_{13} e_{22} e_{29}, \\
 n_{25} &= e_{28} a_6 + \zeta \varepsilon_1 a_{11} + K_5 \varepsilon_3 a_{24}, \\
 n_{26} &= \zeta \varepsilon_1 e_2 - e_{13} e_{22} e_{28}, \\
 n_{27} &= K_5 (\varepsilon_3 e_3 e_9 - \varepsilon_2 e_{16} e_{20}) + e_9 e_{20} e_{27} + e_{29} a_7, \\
 n_{28} &= K_5 \varepsilon_2 e_3, \\
 n_{29} &= \zeta \varepsilon_1 e_{17} e_{20} + e_8 e_{20} e_{28}, \\
 n_{30} &= K_5 (\varepsilon_3 (e_4 e_9 + a_{25}) + \varepsilon_2 e_{17} e_{20}) + e_9 e_{20} e_{28}, \\
 n_{31} &= e_8 e_{20} e_{29}, n_{32} = K_5 \varepsilon_2 e_4, \\
 n_{33} &= e_9 e_{20} e_{29}, n_{34} = e_{10} e_{22} e_{29}, \\
 a_1 &= e_5 e_{19} + e_{10} e_{21}, a_2 = e_6 e_{19} + e_{11} e_{21}, \\
 a_3 &= e_5 e_{18} - e_7 e_{19} - e_{12} e_{21}, \\
 a_4 &= e_6 e_{18} - e_8 e_{19} - e_{13} e_{21}, \\
 a_5 &= e_7 e_{18} + e_5 e_{20} - e_9 e_{19}, a_6 = e_8 e_{18} + e_6 e_{20}, \\
 a_7 &= e_9 e_{18} + e_7 e_{20}, a_8 = e_{14} e_{18} - e_{16} e_{19}, \\
 a_9 &= e_{15} e_{18} - e_{17} e_{19}, a_{10} = e_{16} e_{18} + e_{14} e_{20}, \\
 a_{11} &= e_{17} e_{18} + e_{15} e_{20}, a_{14} = e_1 e_5 + e_{10} e_{14}, \\
 a_{15} &= e_2 e_5 + e_{10} e_{15}, a_{16} = e_1 e_6 + e_{11} e_{14}, \\
 a_{17} &= e_1 e_7 + e_3 e_5 + e_{10} e_{16} + e_{12} e_{14}, \\
 a_{18} &= e_2 e_7 + e_4 e_5 + e_{10} e_{17} + e_{12} e_{15}, \\
 a_{19} &= e_1 e_8 + e_3 e_6 + e_{11} e_{16} + e_{13} e_{14}, \\
 a_{20} &= e_2 e_6 + e_{11} e_{15}, \\
 a_{21} &= e_1 e_9 + e_3 e_7 + e_{12} e_{16},
 \end{aligned}$$

$$\begin{aligned}
 a_{22} &= e_2 e_9 + e_4 e_7 + e_{12} e_{17}, \\
 a_{23} &= e_3 e_8 + e_{13} e_{16}, \\
 a_{24} &= e_2 e_8 + e_4 e_6 + e_{11} e_{17} + e_{13} e_{15}, \\
 a_{25} &= e_4 e_8 + e_{13} e_{17}, \\
 U_1 &= e_{30} (e_5 e_{18} - e_7 e_{19} - e_{12} e_{21}), \\
 U_2 &= \varepsilon_1 (e_{14} e_{18} - e_{16} e_{19}), U_3 = e_{10} e_{22} e_{30}, \\
 U_4 &= e_{30} (e_5 e_{19} + e_{10} e_{21}), U_5 = \varepsilon_1 e_{14} e_{19}, \\
 U_6 &= e_{30} (e_6 e_{19} + e_{11} e_{21}) + \varepsilon_1 e_{15} e_{19}, \\
 U_7 &= e_{30} (e_6 e_{18} - e_8 e_{19} - e_{13} e_{21}) \\
 &\quad + \varepsilon_1 (e_{15} e_{18} - e_{17} e_{19}), \\
 U_8 &= e_{11} e_{22} e_{30}, U_9 = e_{30} (e_7 e_{18} - e_9 e_{19} + e_5 e_{20}), \\
 U_{10} &= \varepsilon_1 (e_{16} e_{18} + e_{14} e_{20}), U_{11} = \varepsilon_1 e_1, \\
 U_{12} &= e_{12} e_{22} e_{30}, \\
 U_{13} &= e_{30} (e_8 e_{18} + e_6 e_{20}) + \varepsilon_1 (e_{17} e_{18} + e_{15} e_{20}), \\
 U_{14} &= \varepsilon_1 e_2, U_{15} = e_{13} e_{22} e_{30}, \\
 U_{16} &= e_{30} (e_9 e_{18} + e_7 e_{20}), \\
 U_{17} &= \varepsilon_1 e_{16} e_{20}, U_{18} = \varepsilon_1 e_3, \\
 U_{19} &= (e_8 e_{20} e_{30} + \varepsilon_1 e_{17} e_{20}), \\
 U_{20} &= \varepsilon_1 e_4, U_{21} = e_9 e_{20} e_{30}.
 \end{aligned}$$

The structure of the polynomial $\mathcal{W}(\lambda_d^{**}, \lambda_o^{**})$ in (42) is suggestive of the phenomenon of backward bifurcation.

Acknowledgements This research was supported by grants from the Ministry of Science and ICT, Republic of Korea (No. 2021M3E5E3081425) and Phuket Rajabhat University, Thailand.

Data availability The data that underpins the conclusions of this study are provided within the article. The parameter values utilized by the authors are drawn from various sources documented in Table 3, referencing relevant literature.

Declaration

Conflict of interest There are no conflict of interest to declare.

References

- Abioye AI, Peter OJ, Ogunseye HA, Oguntolu FA, Oshinubi K, Ibrahim AA, Khan I (2021) Mathematical model of COVID-19 in Nigeria with optimal control. *Results Phys* 28:104598
- Agwu CO, Omame A, Inyama SC (2023) Analysis of mathematical model of diabetes and tuberculosis co-infection. *Int J Appl Comput Math* 9(3):36
- Alaje AI, Olayiwola MO (2023) A fractional-order mathematical model for examining the spatiotemporal spread of COVID-19 in the presence of vaccine distribution. *Healthc Anal* 4:100230
- Ando H, Murakami M, Ahmed W, Iwamoto R, Okabe S, Kitajima M (2023) Wastewater-based prediction of COVID-19 cases using a highly sensitive SARS-CoV-2 RNA detection method combined with mathematical modeling. *Environ Int* 173:107743

- Anguelov R, Garba SM, Usaini S (2014) Backward bifurcation analysis of epidemiological model with partial immunity. *Comput Math Appl* 68(9):931–940
- Bugalia S, Bajiya VP, Tripathi JP, Li MT, Sun GQ (2020) Mathematical modeling of COVID-19 transmission: the roles of intervention strategies and lockdown. *Math Biosci Eng* 17(5):5961–5986
- Castillo-Chavez C, Song B (2004) Dynamical models of tuberculosis and their applications. *Math Biosci Eng* 1(2):361–404
- Centers for Disease Control and Prevention (CDC) (2021) SARS-CoV-2 variant classifications and definitions. CDC. <https://www.cdc.gov/coronavirus/2019-ncov/variants/variant-classifications.html>. Accessed 12 Nov 2021
- Centers for Disease Control and Prevention (2024) Centers for Disease Control and Prevention (CDC). <https://covid.cdc.gov/covid-data-tracker/#vaccination-trends>
- Chakraborty C, Sharma AR, Bhattacharya M, Mallik B, Nandi SS, Lee SS (2022) Comparative genomics, evolutionary epidemiology, and RBD-hACE2 receptor binding pattern in B.1.1.7 (Alpha) and B.1.617.2 (Delta) related to their pandemic response in UK and India. *Infect Genet Evol* 101:105282
- Chan JFW, Yuan S, Kok KH, To KKW, Chu H, Yang J, Xing F, Liu J, Yip CCY, Poon RWS et al (2020) A familial cluster of pneumonia associated with the 2019 novel coronavirus indicating person-to-person transmission: a study of a family cluster. *Lancet* 395(10223):514–523
- Driessche P, Watmough J (2002) Reproduction numbers and sub-threshold endemic equilibria for compartmental models of disease transmission. *Math Biosci* 180(1–2):29–48
- European Centre for Disease Prevention and Control (ECDC) (2021) Implications of the further emergence and spread of the SARS-CoV-2 B.1.1.529 Variant of Concern (Omicron) for the EU/EEA-First Update. ECDC. <https://www.ecdc.europa.eu/sites/default/files/documents/threat-assessment-covid-19-emergence-sars-cov-2-variant-omicron-december-2021.pdf>. Accessed 2 Dec 2021
- Feng X, Teng Z, Wang K, Zhang F (2014) Backward bifurcation and global stability in an epidemic model with treatment and vaccination. *Discrete Contin Dyn Syst B* 19(4):999–1025
- Ghosh SK, Ghosh S (2023) A mathematical model for COVID-19 considering waning immunity, vaccination and control measures. *Sci Rep* 13(1):3610
- Gilbert M, Pullano G, Pinotti F, Valdano E, Poletto C, Boëlle PY, d’Ortenzio E, Yazdanpanah Y, Eholie SP, Altmann M et al (2020) Preparedness and vulnerability of African countries against importations of COVID-19: a modelling study. *Lancet* 395(10227):871–877
- Goswami MP, Anjali R, Raj A, Puthiyakath HH, Thanvi J (2022) Media during pandemic crisis in India: an analysis of people’s perception during the first wave of COVID-19. *J Creat Commun* 09732586221090750
- Gumel AB (2012) Causes of backward bifurcations in some epidemiological models. *J Math Anal Appl* 395(1):355–365
- Gumel AB, Lubuma JMS, Sharomi O, Terefe YA (2018) Mathematics of a sex-structured model for syphilis transmission dynamics. *Math Methods Appl Sci* 41(18):8488–8513
- Gumel AB, Iboi EA, Ngonghala CN, Elbasha EH (2021) A primer on using mathematics to understand COVID-19 dynamics: modeling, analysis and simulations. *Infect Dis Model* 6:148–168
- Hamilton BE, Martin JA, Osterman MJ (2024) Births: provisional data for 2023. *Natl Vital Stat Rep* 73(1):1–36
- Hassan TS, Elabbasy E, Matouk A, Ramadan RA, Abdulrahman AT, Odinaev I (2022) Routh–Hurwitz stability and quasiperiodic attractors in a fractional-order model for awareness programs: applications to COVID-19 pandemic. *Discret Dyn Nat Soc* 1:1939260
- Hassan MN, Mahmud MS, Nipa KF, Kamrujjaman M (2023) Mathematical modeling and Covid-19 Forecast in Texas, USA: a prediction model analysis and the probability of disease outbreak. *Disaster Med Public Health Prep* 17:e19
- Hellewell J, Abbott S, Gimma A, Bosse NI, Jarvis CI, Russell TW, Munday JD, Kucharski AJ, Edmunds WJ, Sun F et al (2020) Feasibility of controlling COVID-19 outbreaks by isolation of cases and contacts. *Lancet Glob Health* 8(4):e488–e496
- Hethcote HW (2000) The mathematics of infectious diseases. *SIAM Rev* 42(4):599–653
- Iboi EA, Ngonghala CN, Gumel AB (2020) Will an imperfect vaccine curtail the COVID-19 pandemic in the US? *Infect Dis Model* 5:510–524
- Khajanchi S, Sarkar K, Mondal J, Nisar KS, Abdelwahab SF (2021) Mathematical modeling of the COVID-19 pandemic with intervention strategies. *Results Phys* 25:104285
- Khan MA, Atangana A (2022) Mathematical modeling and analysis of COVID-19: a study of new variant Omicron. *Phys A Stat Mech Appl* 599:127452
- Kouidere A, Balatif O, Rachik M (2023) Cost-effectiveness of a mathematical modeling with optimal control approach of spread of COVID-19 pandemic: a case study in Peru. *Chaos Solitons Fractals X* 10:100090
- La Salle JP (1976) The stability of dynamical systems. SIAM, Philadelphia
- Lakshmikantham V, Leela S, Martynyuk AA (1989) Stability analysis of nonlinear systems. Springer, Berlin
- Lauring AS, Tenforde MW, Chappell JD, Gaglani M, Ginde AA, McNeal T, Ghamande S, Douin DJ, Talbot HK, Casey JD et al (2022) Clinical severity of, and effectiveness of mRNA vaccines against, COVID-19 from Omicron, Delta, and Alpha SARS-CoV-2 variants in the United States: prospective observational study. *BMJ* 376:n242
- León UAP, Avila-Vales E, Huang K (2022) Modeling COVID-19 dynamic using a two-strain model with vaccination. *Chaos Solitons Fractals* 157:111927
- Lioffi S, Tsiambas E, Maipas S, Papageorgiou E, Lazaris A, Kavantzias N (2023) Mathematical modeling for Delta and Omicron variant of SARS-CoV-2 transmission dynamics in Greece. *Infect Dis Model* 8(3):794–805
- Logeswari K, Ravichandran C, Nisar KS (2024) Mathematical model for spreading of COVID-19 virus with the Mittag–Leffler kernel. *Numer Methods Partial Differ Equ* 40(1):e22652
- Madhi SA, Kwatra G, Myers JE, Jassat W, Dhar N, Mukendi CK, Nana AJ, Blumberg L, Welch R, Ngorima-Mabheba N et al (2022) Population immunity and Covid-19 severity with omicron variant in South Africa. *N Engl J Med* 386(14):1314–1326
- Martcheva M (2015) An introduction to mathematical epidemiology, vol 61. Springer, Berlin
- Masandawa L, Mirau SS, Mbalawata IS (2021) Mathematical modeling of COVID-19 transmission dynamics between healthcare workers and community. *Results Phys* 29:104731
- Mitchell C, Kribs C (2019) Invasion reproductive numbers for periodic epidemic models. *Infect Dis Model* 4:124–141
- Mohamadou Y, Halidou A, Kapen PT (2020) A review of mathematical modeling, artificial intelligence and datasets used in the study, prediction and management of COVID-19. *Appl Intell* 50(11):3913–3925
- Murphy SL, Kochanek KD, Xu J, E Arias (2021) Mortality in the United States. 2020 NCHS Data Brief 427:1–8
- Nadim SS, Chattopadhyay J (2020) Occurrence of backward bifurcation and prediction of disease transmission with imperfect lockdown: a case study on COVID-19. *Chaos Solitons Fractals* 140:110163
- Naim M, Yaagoub Z, Zeb A, Sadki M, Allali K (2024) Global analysis of a fractional-order viral model with lytic and non-lytic adaptive immunity. *Model Earth Syst Environ* 10(2):1749–1769

- Ndairou F, Area I, Nieto JJ, Torres DF (2020) Mathematical modeling of COVID-19 transmission dynamics with a case study of Wuhan. *Chaos Solitons Fractals* 135:109846
- Ngonghala CN, Iboi E, Eikenberry S, Scotch M, MacIntyre CR, Bonds MH, Gumel AB (2020) Mathematical assessment of the impact of non-pharmaceutical interventions on curtailing the 2019 novel coronavirus. *Math Biosci* 325:108364
- Oguntolu FA, Peter OJ, Yusuf A, Omede BI, Bolarin G, Ayoola T (2024) Mathematical model and analysis of the soil-transmitted helminth infections with optimal control. *Model Earth Syst Environ* 10(1):883–897
- Okuonghae D, Omame A (2020) Analysis of a mathematical model for COVID-19 population dynamics in Lagos, Nigeria. *Chaos Solitons Fractals* 139:110032
- Omame A, Umana R, Okuonghae D, Inyama S (2018) Mathematical analysis of a two-sex human papillomavirus (HPV) model. *Int J Biomath* 11(07):1850092
- Omame A, Okuonghae D, Umana R, Inyama S (2020) Analysis of a Co-Infection Model for HPV/TB. *Appl Math Model* 77:881–901
- Omede BI, Peter OJ, Atokolo W, Bolaji B, Ayoola TA (2023) A mathematical analysis of the two-strain tuberculosis model dynamics with exogenous re-infection. *Healthc Anal* 4:100266
- Omede BI, Odionyenma UB, Ibrahim AA, Bolaji B (2023) Third wave of COVID-19: mathematical model with optimal control strategy for reducing the disease burden in Nigeria. *Int J Dyn Control* 11(1):411–427
- Patel VK, Shirbhate E, Rajak H (2022) Coronavirus reinfections: an outlook on evidences and effects. *Lessons from COVID-19*. Elsevier, pp 19–40
- Paul JN, Mbalawata IS, Mirau SS, Masandawa L (2023) Mathematical modeling of vaccination as a control measure of stress to fight COVID-19 infections. *Chaos Solitons Fractals* 166:112920
- Riyapan P, Shuaib SE, Intarasit A (2021) A mathematical model of COVID-19 pandemic: a case study of Bangkok, Thailand. *Comput Math Methods Med* 1:6664483
- Saha S, Saha AK (2023) Modeling the dynamics of COVID-19 in the presence of Delta and Omicron variants with vaccination and non-pharmaceutical interventions. *Heliyon* 9:7
- Samui P, Mondal J, Khajanchi S (2020) A mathematical model for COVID-19 transmission dynamics with a case study of India. *Chaos Solitons Fractals* 140:110173
- Sepulveda G, Arenas AJ, Gonzalez-Parra G (2023) Mathematical modeling of COVID-19 dynamics under two vaccination doses and delay effects. *Mathematics* 11(2):369
- South African National Institute for Communicable Diseases (NICD) (2021) Network for genomic surveillance in South Africa SARS-CoV-2 sequencing update. NICD. https://www.nicd.ac.za/wp-content/uploads/2022/01/Update-of-SA-sequencing-data-from-GISAID-30-Dec-2021_dash.pdf. Accessed 31 Dec 2021
- World Health Organization (2019) World Health Organization. <https://covid19.who.int/region/amro/country/us>
- Yaagoub Z, Sadki M, Allali K (2024) A generalized fractional hepatitis B virus infection model with both cell-to-cell and virus-to-cell transmissions. *Nonlinear Dyn* 1–27
- Young M, Crook H, Scott J, Edison P (2022) Covid-19: virology, variants, and vaccines. *BMJ Med* 1:1

Publisher's Note Springer Nature remains neutral with regard to jurisdictional claims in published maps and institutional affiliations.

Springer Nature or its licensor (e.g. a society or other partner) holds exclusive rights to this article under a publishing agreement with the author(s) or other rightsholder(s); author self-archiving of the accepted manuscript version of this article is solely governed by the terms of such publishing agreement and applicable law.